

ADDENDUM TO THE USER MANUAL FOR NASGRO ELASTIC-PLASTIC FRACTURE MECHANICS SOFTWARE MODULE

FINAL REPORT
SwRI® Project 18-05756

NASA Contract Number: NAS8-02051
"Proof Test Design and Analysis"

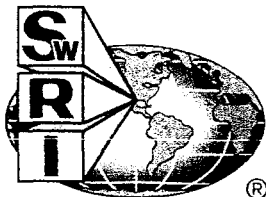
Prepared for

Wayne Gregg
NASA Marshall Space Flight Center
Huntsville, Alabama

Prepared by

Graham Chell and Brian Gardner
Southwest Research Institute
San Antonio, Texas

September 23, 2003



SOUTHWEST RESEARCH INSTITUTE™
SAN ANTONIO
DETROIT
HOUSTON
WASHINGTON

ADDENDUM TO THE USER MANUAL FOR NASGRO ELASTIC-PLASTIC FRACTURE MECHANICS SOFTWARE MODULE

FINAL REPORT
SwRI® Project 18-05756

NASA Contract Number: NAS8-02051
"Proof Test Design and Analysis"

Prepared for

Wayne Gregg
NASA Marshall Space Flight Center
Huntsville, Alabama

Prepared by

Graham Chell and Brian Gardner
Southwest Research Institute
San Antonio, Texas

September 23, 2003

Approved:



Dr. James Lankford, Jr., Director
Materials Engineering Department

Acknowledgements

The authors gratefully acknowledge Wayne Gregg at NASA Marshall Space Flight Center for his understanding and encouragement during the course of this work. Without his strong support the objectives of this work would not have been achieved. Thanks are also due to Patty Soriano who helped prepare all the reports, including this final report.

Table of Contents

	<i>Page</i>
1.0	INTRODUCTION1
2.0	TECHNICAL ISSUES RELATED TO PHASE 2 ENHANCEMENTS.....4
3.0	J SOLUTIONS FOR SURFACE CRACKS IN PLATES SUBJECTED TO ARBITRARY STRESS FIELDS (Crack Model SC02)6
3.1	Implementation of J Solutions for SC02.....6
3.2	Validation of J Solutions for SC028
4.0	J SOLUTIONS FOR AXIAL SURFACE CRACKS IN CYLINDERS SUBJECTED TO ARBITRARY HOOP STRESSES (Crack Model SC04)9
4.1	Implementation of J Solutions for SC04.....9
4.2	Validation of J Solutions for SC0411
5.0	J SOLUTIONS FOR CORNER CRACKS IN PLATES SUBJECTED TO BENDING (Crack Model CC01).....12
5.1	Implementation of J Solutions for CC01 (Bending).....12
5.2	Validation of J Solutions for CC01 (Bending)17
6.0	J SOLUTIONS FOR EMBEDDED CRACKS IN PLATES SUBJECTED TO TENSION AND ARBITRARY STRESSES (Crack Models EC01/EC02)17
6.1	Implementation of J Solutions for EC01/EC0217
6.2	Validation of J Solutions for EC01/EC02.....22
7.0	TECHNICAL ISSUES RELATED TO PHASE 3 ENHANCEMENTS.....25
7.1	Ductile Failure Analysis Routines for 2-DOF Cracks25
7.2	Proof Test Module26
7.3	Tear-Fatigue28
7.4	Multiple Cycle Proof Test Analysis (MCPT)31
8.0	EXAMPLES, VALIDATION, AND PROGRAM ISSUES.....33
8.1	Example Input and Output for Running the EPFM/Proof Test Modules33
8.2	Validation.....33
8.3	Program Issues37
8.3.1	Problems Occurring During Program Execution.....37
8.3.2	CPU Time37
8.3.3	CD Contents.....37

1.0 INTRODUCTION

An elastic-plastic fracture mechanics (EPFM) software module for inclusion in the NASGRO computer program has been developed by Southwest Research Institute under NASA Marshall Space Flight Center Contract (MSFC) NAS8-37828. These modules will hereafter be referred to as the Phase 1 development. The fracture and fatigue assessment capabilities developed in Phase 1 and the theoretical basis of the EPFM approach based on the J-integral, are described in the final report for that contract (R.C. McClung, G. G. Chell, Y.-D. Lee, D. A. Russell, and G. E. Orient., "*Development of a Practical Methodology for Elastic-Plastic and Fully Plastic Fatigue Crack Growth*", August 1998). In particular, the User Manual written in support of the EPFM modules is contained in Appendix K of that report. The reader is referred to Appendix K for further details regarding the J formulations employed in the calculations, the fracture analyses that can be performed, how to run the modules and examples of the input data needed, and validation of the code.

Since the release of the NASGRO EPFM module in 1998, two further enhancements have been made, herein called Phase 2 and Phase 3. In Phase 2, performed under MSFC Contract H-33940D, "*Practical Analytical Tools for Nonlinear Fatigue Crack Growth*," and completed in March 2002, the library of J-integral solutions was improved. In Phase 3, performed under MSFC Contract NAS8-02051, "*Proof Test Design and Analysis*," and completed in September 2003, software modules for implementing proof test methodologies were developed.

The Phase 2 enhancements to the NASGRO EPFM modules included the following:

- (1) Extension of the EPFM solutions for surface cracks (Model SC01) to include surface cracks in rectangular plates subjected to arbitrary uniaxial stressing (Model SC02) and surface cracks on the inside and outside of hollow cylinders subjected to arbitrary non-linear hoop stresses (SC04).
- (2) Extension of the EPFM solutions for centrally embedded cracks subjected to uniform stressing (Model EC01) to cracks subjected to arbitrary non-linear stresses (Model EC02) and improvements in the J solutions for uniform stressing (Models EC01 and EC02).
- (3) Improvements in the accuracies of the EPFM corner crack J solutions for bending (Model CC01).

The improved EPFM solutions developed in Phase 2 have been incorporated into the NASGRO analysis options 5 (J computations), 6 (failure analysis) and 7 (fatigue life analysis).

The Phase 3 enhancements involved significant additions to the EPFM analysis capabilities of NASGRO to facilitate accurate proof test analyses. The proof test methodologies that underpin the proof test modules were developed by SwRI under MSFC Contracts NAS8-37451, "*A Comparison of Single-Cycle Versus Multiple-Cycle Proof Testing Strategies*," and NAS8-39380, "*Guidelines for Proof Test Analysis*." In order to accurately implement these two methodologies, the one degree-of-freedom (1-DOF) ductile failure modules for surface cracks, corner cracks, and embedded cracks developed in Phase 1 were replaced by two degree-of-freedom (2-DOF) modules.

The Phase 3 enhancements to the NASGRO EPFM modules are described below:

- (1) Extension of the Phase 1 EPFM ductile failure module in NASGRO from a 1-DOF assessment (where the severity of surface, corner and embedded cracks is characterized by a single value for the crack-tip driving force, J or K) to a more accurate assessment based on 2-DOF (where the severity of surface, corner and embedded cracks is characterized by two values for the crack-tip driving force, J or K), enabling changes in crack shape during ductile tearing to be more accurately modeled.
- (2) Addition of a proof test module to implement the procedures in *Guidelines for Proof Test Analysis* to facilitate the use of these by practicing engineers. This module leads the engineer step by step through the various stages needed to perform a proof test analysis. The module also incorporates service analysis routines that can be used to determine fatigue crack growth lives, and critical crack and critical load routines.
- (3) Addition of a tear-fatigue crack growth module for ductile materials enabling the behavior of fatigue cracks growing near instability to be quantified. It is well known that near instability, the growth rate of cracks can be greatly accelerated. This routine is used in the multiple cycle proof test routine described in (4).
- (4) Addition of multiple cycle proof test (MCPT) reliability analysis module to implement the procedures described in *A Comparison of Single-Cycle Versus Multiple-Cycle Proof Testing Strategies*. This module includes a probabilistic analysis for taking into account the effect of the distribution in initial crack sizes on the reliability of a fleet of components entering service after MCPT. This module can be exercised to determine the change in service reliability of a MCPT compared with performing no proof test or a single cycle proof test.

The improved EPFM solutions developed in Phase 3 have been incorporated into NASGRO through enhancements to option 6 (2-DOF failure analysis for ductile materials), and the additions of options 8 (single cycle proof test analysis), 9 (tear-fatigue analysis for ductile materials) and 10 (MCPT reliability analysis).

A summary of the current capabilities of the EPFM module and the phase under which they were developed is provided in Table 1. A schematic of the crack models for which EPFM solutions are available is shown in Figure 1.

Table 1. NASGRO EPFM options developed in Phases 1, 2, and 3.

Opt. No.	Analysis Type	Phase 1	Phase 2	Phase 3
		Crack Models and Loading		
5	Elastic-plastic J computation	TC01 - Tension TC02 - Tension Bending EC01 - Tension CC01 - Tension Bending SC01 - Tension Bending	TC01 - Tension TC02 - Tension Bending EC01 - Tension (Improved) EC02 - Arbitrary stress (New) CC01 - Tension Bending (Improved) SC01 - Tension Bending SC02 - Arbitrary stress (New) SC04 - Arbitrary stress (New)	TC01 - Tension TC02 - Tension Bending EC01 - Tension EC02 - Arbitrary stress CC01 - Tension Bending SC01 - Tension Bending SC02 - Arbitrary stress SC04 - Arbitrary stress
6	Elastic-plastic failure analysis	Critical crack 1-DOF Critical load 1-DOF All Phase 1 Models	Critical crack 1-DOF Critical load 1-DOF All Phase 2 Models	Critical crack 2-DOF Critical load 2-DOF All Phase 3 Models
7	Elastic-plastic fatigue life analysis	All Phase 1 Models	All Phase 2 Models	All Phase 3 Models
8	Single cycle proof test analysis			Safe Life Analysis <i>Critical flaw size</i> <i>Fatigue Life</i> Proof Test Analysis <i>Proof load</i> <i>Flaw screening</i> <i>Final crack size</i> All Phase 3 Models
9	Tear-fatigue			Ductile Materials All Phase 3 Models
10	MCPT analysis			Ductile Materials All Phase 3 Models

This Addendum to the User Manual in Appendix K of the final report *Development of a Practical Methodology for Elastic-Plastic and Fully Plastic Fatigue Crack Growth* (hereafter referred to as Appendix K) provides a description of the new analytical developments and software modules resulting from Phases 2 and 3, validation of the software modules, and examples of applying the new modules. Validation of the developments made under Phase 1 is presented in Appendix K.

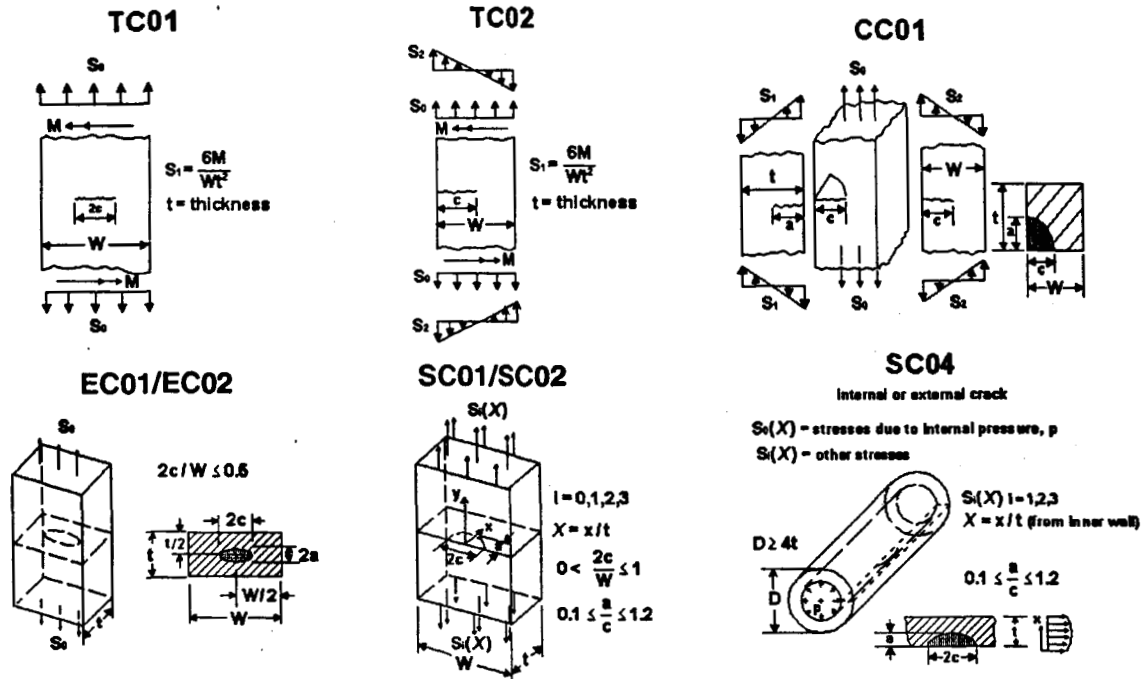


Figure 1. The NASGRO crack models for which EPFM solutions are available.

2.0 TECHNICAL ISSUES RELATED TO PHASE 2 ENHANCEMENTS

The new analyses performed in support of Phase 2 developments consisted of:

- extension of the SC02 solutions to arbitrary stressing,
- addition of EPFM J solutions for axial cracks in cylinders subject to arbitrary hoop stressing (SC04),
- improvement in the accuracy of the J solutions for corner cracks subjected to bending (CC01),
- improvement in the accuracy of the J solutions for embedded cracks subjected to uniform stressing (EC01)
- addition of J solutions for embedded cracks in arbitrary stress fields (EC02).

In the J formulation scheme used in the NASGRO EPFM Module, J is expressed as the sum of elastic, J_e , and plastic, J_p , components, $J = J_e(a_{eff}, \sigma^p + \sigma^s) + J_p(a, \sigma^p)$, where a_{eff} is an effective crack size equal to the original size, a , plus a plastic zone correction, σ signifies the applied stress, and superscripts p and s refer to primary and secondary loads, respectively. The enhancements to the J solutions incorporated in NASGRO during Phase 2 were predominantly related to the plastic component of J, J_p . Therefore, the technical aspects of this Addendum addresses specifically those issues related to the computation of J_p , as $J_e(a_{eff})$ can be determined using linear elastic fracture mechanics principles. In all cases, the reference stress method (RSM), see Appendix K, is used to implement J solutions in the NASGRO EPFM module. In this formulation, it is important to remember that J_p is a function of the primary component of loading, as it corresponds to fully plastic fracture behavior and secondary loads cannot influence this behavior.

In the RSM, the plastic component of J, J_p^{RSM} , is given by an equation of the form

$$J_p^{RSM} = J_e\left(\frac{a}{t}, \frac{a}{c}, \frac{b}{c}\right) \mu V \alpha \left(\frac{P}{P_o^*}\right) \quad (1)$$

for tension loading and

$$J_p^{RSM} = J_e\left(\frac{a}{t}, \frac{a}{c}, \frac{b}{c}\right) \mu V \alpha \left(\frac{M}{M_o^*}\right) \quad (2)$$

for bending, where V is a dimensionless structural parameter and α , σ_o , and n are material properties defining the Ramberg-Osgood equation describing the uniaxial stress-strain behavior (see Appendix K).

The values of V , P_o^* , and M_o^* can be determined from FEA results for h_I using the optimization RSM scheme described in "Development of a Practical Methodology for Elastic-Plastic and Fully Plastic Fatigue Crack Growth". In this optimized RSM approach, values of V and an optimum yield load, P_o^* (or an optimum yield moment, M_o^*) are found such that the RSM reproduces J values derived from finite element analysis (FEA) as accurately as possible. The results of the optimized procedure demonstrate the maximum accuracy that can be obtained using the RSM. However, due to the limited number of FEA J solutions that can be generated, it is not practical to employ the optimized RSM results directly in the NASGRO J module. Instead, a pragmatic approach is followed and the module that uses average values for V and approximate equations for P_o^* and M_o^* based on simple plastic limit load analyses and empirical fits to the actual derived optimized loads. This pragmatic approach is herein called the **hybrid RSM**.

Plastic collapse loads are defined as

$$P_c^* = P_o^* \left(\frac{\sigma_{flow}}{\sigma_o} \right) \quad \lambda < \infty \quad (3a)$$

$$M_c^* = M_o^* \left(\frac{\sigma_{flow}}{\sigma_o} \right) \quad \lambda = 0 \quad (3b)$$

where subscript *c* signifies collapse and the flow stress is defined as

$$\sigma_{flow} = 0.5(\sigma_u + \sigma_y) \quad (4)$$

Failure is predicted when the applied load exceeds the plastic collapse load, irrespective of the applied *J* value.

3.0 J SOLUTIONS FOR SURFACE CRACKS IN PLATES SUBJECTED TO ARBITRARY STRESS FIELDS (Crack Model SC02)

3.1 Implementation of J Solutions for SC02

The SC02 J solutions were implemented in the EPFM module via the hybrid RSM method (see Appendix K). In order to determine the RSM solutions, existing NASGRO stress intensity factor (SIF) solutions for surface cracks in arbitrary stress fields were employed together with net section yield loads derived for surface cracks subjected to combined tension and bending loads. The latter solutions are needed because, in general, arbitrary stress fields when integrated over the load bearing section produce tensile forces and bending moments.

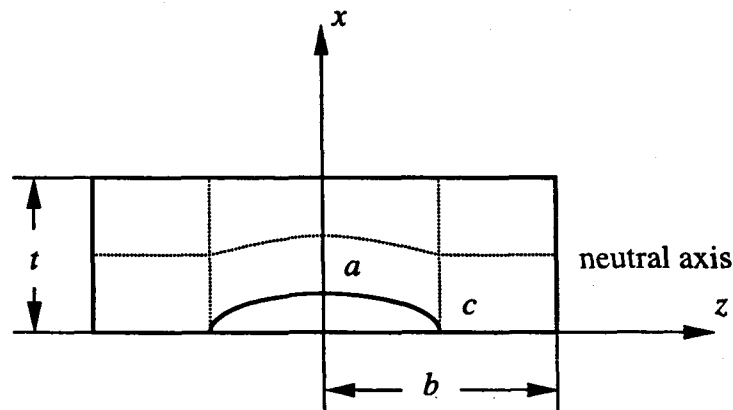


Figure 2. Schematic of SC02 geometry showing location of the neutral axis under combined tension and bending.

The net section yield load for combined tension and bending for model type SC02, characterized by the tensile yield load P_o^* , is derived from a plastic limit analysis assuming a

neutral axis midway across the net section thickness. In reference to the cross section defined in Figure 2, the variation of net section thickness, $t_{net}(z)$, with location z as the plate is traversed is given by

$$t_{net}(z) = \begin{cases} t - a\sqrt{1 - \frac{z^2}{c^2}} & , |z| \leq c \\ t & , |z| > c \end{cases} \quad (5)$$

In this equation, t is the thickness of the plate, a is the depth of the flaw and $2c$ its total surface length. In the case of pure tension, the net section yield load, P_o^* , is derived from the load redistribution due to area reduction and is given by

$$P_o^* = \beta\sigma_o \left(bt - \frac{\pi ac}{2} \right) \quad (6)$$

where $W = \beta b$ is the total length of the plate and σ_o the yield stress. For the SC01/SC02 models $\beta=2$, and for CC01 $\beta=1$. In the case of pure bending, the net section yield moment, M_o^* , can also be determined analytically assuming the form of the neutral axis given in equation (5) as

$$M_o^* = \beta\sigma_o \left[\frac{c}{24} (-3at\pi + 4a^2 + 6t^2) + \frac{t^2}{4} (b - c) \right] \quad (7)$$

In the case of combined tension and bending, a proportionality factor, λ , is introduced defined as

$$\lambda = \frac{M}{Pt} \quad (8)$$

where M is the applied moment and P is the applied tensile load. In the SC02 model, the values for P and M are derived from user specified arbitrary stress distributions by integrating these distributions over the area of the plate.

From plastic limit load theory, the equation for the combined tension and bending yield load, $P_o^*(\lambda)$, can be written as

$$P_o^*(\lambda) = \frac{P_o^*}{2} \left[\left(\left(\frac{\lambda P_o^*}{M_o^*} \right)^2 + 4 \right)^{1/2} - \frac{\lambda P_o^*}{M_o^*} \right] \quad (9)$$

In this equation, $P_o^*(\lambda)$ is a net section tension yield load for combined tension and bend loading. It equals the value of the tensile load that causes net section yielding under proportional loading in the presence of an applied moment related to the tensile load by the proportionality

constant λ given by equation (8). The value of $P_o^*(\lambda)$ reduces to P_o^* and M_o^* in the cases of pure tensile loading and pure bending, respectively. Pure tensile loading is defined by $\lambda=0$, thus

$$P_o^* = P_o^*(\lambda = 0) = \beta\sigma_o \left(2bt - \frac{\pi ac}{2} \right) \quad (10)$$

Pure bending load is defined by $\lambda=\infty$, thus

$$M_o^* = \lambda P_o^*(\lambda = \infty) = \beta\sigma_o \left[\frac{c}{24} (-3at\pi + 4a^2 + 6t^2) + \frac{t^2}{4} (b-c) \right] \quad (11)$$

In the hybrid RSS method, the plastic component of J , J_p^{RSM} , for combined loading is given by the equation

$$J_p^{RSM} = J_p \left(\frac{a}{t}, \frac{a}{c}, \frac{b}{c}, \lambda \right) \mu V(\lambda) \alpha \left(\frac{P}{P_o^* \left(\frac{a}{t}, \frac{a}{c}, \frac{b}{c}, \lambda \right)} \right)^{n-1} \quad (12)$$

where $V(\lambda)$ is a dimensionless structural parameter for the combined loading. Since the value of $V(\lambda)$ was only determined in Phase 1 for the two extreme cases of pure tension, $V(\lambda=0)$, and pure bending, $V(\lambda=\infty)$, its value for combined loading is herein interpolated between these two extreme values using the equation

$$V(\lambda) = V(\lambda = \infty) \left(1 - \exp^{-0.693|\lambda|} \right) + V(\lambda = 0) \exp^{-0.693|\lambda|} \quad (13)$$

The deepest point and surface point values, respectively, of V used in SC01 are 1.0412 and 0.973 for $V(\lambda=\infty)$ and 1.8164 and 1.2561 for $V(\lambda=0)$. These two sets of extreme values for V indicate the maximum inaccuracies in $V(\lambda)$ that could be generated using the interpolation equation given by equation (13).

3.2 Validation of J Solutions for SC02

The SC02 J solutions were implemented for arbitrary stressing by utilizing the existing SC02 SIF routines, adding a routine for determining the applied force and moment corresponding to the arbitrary stress, and introducing a net section yield load solution for combined tension and bending.

The new J solutions were partly validated by applying arbitrary primary loads that simulated uniform stressing and bending and comparing the resulting J values with the values obtained from running the SC01 model for tension and bending. The results are shown in Figure 3 where J values derived from the SC01 model are plotted against J values computed using the new SC02 model solutions. Perfect agreement between the two sets of solutions occurs when the data

points fall on the 1 to 1 line. It can be seen from Figure 3 that excellent agreement obtains between the SC02 and SC01 solutions, indicating that the integration routines used to determine the external forces and moments from the arbitrary stress distribution specified in SC02 and the resulting net section yield solutions are correctly calculated.

Two additional verification tests for SC02 were performed. In the first, a self-equilibrated primary stress of the form $1 - 6\frac{x}{t} + 6\left(\frac{x}{t}\right)^2$ was applied. This form of stress integrates to zero force and moment. The resulting J solutions correctly gave non-zero values for J_e and zero values for J_p . In the second validation exercise, arbitrary stresses were specified that corresponded to combined tension and bending and the resulting J values were compared to the results of manual calculations performed using a spreadsheet. There was exact agreement between the two sets of results (see Appendix 4).

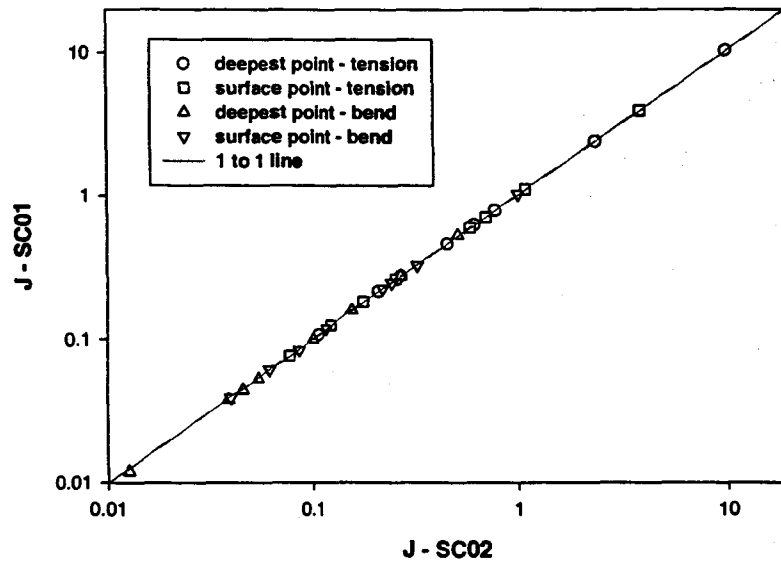


Figure 3. Comparison of J estimations obtained using SC01 and SC02. The arbitrary stress fields used in the SC02 computations were chosen to simulate uniform tension and pure bending, respectively. The deepest point corresponds to the a-tip and the surface point to the c-tip.

4.0 J SOLUTIONS FOR AXIAL SURFACE CRACKS IN CYLINDERS SUBJECTED TO ARBITRARY HOOP STRESSES (Crack Model SC04)

4.1 Implementation of J Solutions for SC04

The SC04 RSM J solutions were implemented in the EPFM module using existing NASGRO SC04 SIF solutions for internal and external axial surface cracks. The net section yield pressure, P_o^* , was taken as equation (B4.9) in *Guidelines for Proof Test Analysis*, which is a modified

form of the equation given by Keifner, Maxey, Eiber, and Duffey in *Failure Stress Levels of Flaws in Pressurized Cylinders* (ASTM STP 536, pp. 461-481). This equation is

$$P_o^* = \frac{\sigma_o t}{R_i} \frac{\left[1 - \frac{a}{t}\right]}{\left[1 - \frac{\left(\frac{a}{t}\right)}{M\left(\rho, \frac{a}{t}\right)}\right]} \quad (14)$$

In this equation, R_m is the mean radius of the cylinder, R_i is the inner radius, and

$$M\left(\rho, \frac{a}{t}\right) = \left(1 + 1.05 \frac{a}{t} \rho^2\right)^{\frac{1}{2}}, \quad \rho = \frac{c}{\sqrt{R_m t}} \quad (15)$$

The RSM for the plastic component of J for the SC04 geometry is

$$J_p^{RSM} = J_e\left(\frac{a}{t}, \frac{a}{c}, \frac{R_m}{t}\right) \mu V \alpha \left(\frac{P}{P_o^*\left(\frac{a}{t}, \rho, \frac{R_i}{t}\right)} \right)^{n-1} \quad (16)$$

where P is the internal pressure, derived by integrating the hoop stress through the wall of the cylinder.

It is important to note that the primary (internal pressure) load can be input in the EPFM module in two ways. In the first, the user specifies the actual pressure and the program internally determines the hoop stress distribution corresponding to that pressure. For external cracks, the derived hoop stress distribution is used in the SIF calculations. For internal cracks, in order to allow for the effects of internal pressure acting on the crack faces, the pressure is added to the derived hoop stress and this combined stress field is employed in the SIF calculations. For both internal and external cracks, the user specified pressure is used in the evaluation of J_p with equation (14) used for P_o^* .

In the second method of defining the applied load, the user directly specifies the hoop stress distribution through the wall. In this case, for external cracks, this stress distribution is used to determine the SIFs and the integrated stress through the wall to determine the internal pressure corresponding to this distribution. For internal cracks, it is assumed that the user specified hoop stress includes a uniform stress component equal to the internal pressure. This stress distribution is used in the SIF calculations to allow for the effects of the internal pressure acting on the crack faces. However, the effects of pressure on the crack faces is not included in the determination of J_p , and equation (14) is used for P_o^* with the pressure P evaluated by integrating the user

specified hoop stress and multiplying the resulting “pressure” by the factor R/R_o in order to obtain the actual pressure, P .

FEA J data is not available for pressurized pipes to allow evaluation of V , so, in lieu of more accurate values, V for the deepest and surface crack positions are both set to 1.

4.2 Validation of J Solutions for SC04

The J solutions predicted by the SC04 model for internal and external surface cracks were validated against the results of manual calculations (see also Appendix 4). Excellent agreement was obtained between the two sets of computations. Comparisons were made when the applied load was specified in terms of an internal pressure and when the load was specified in terms of an arbitrary hoop stress distribution. In addition, internal consistency between the two forms of specifying the applied load was checked for two cylindrical geometries, corresponding to D/t equal to 22 and 102, where D is the outer diameter of the cylinder. In these cases, the arbitrary hoop stress was defined as that printed in the output when the load specification in terms of internal pressure is used. Figures 4 and 5 show the results obtained from this consistency check for internal and external cracks, respectively. It can be seen from the figures that there is excellent agreement between the pressure loaded solutions and the equivalent load defined in terms of an arbitrary hoop stress.

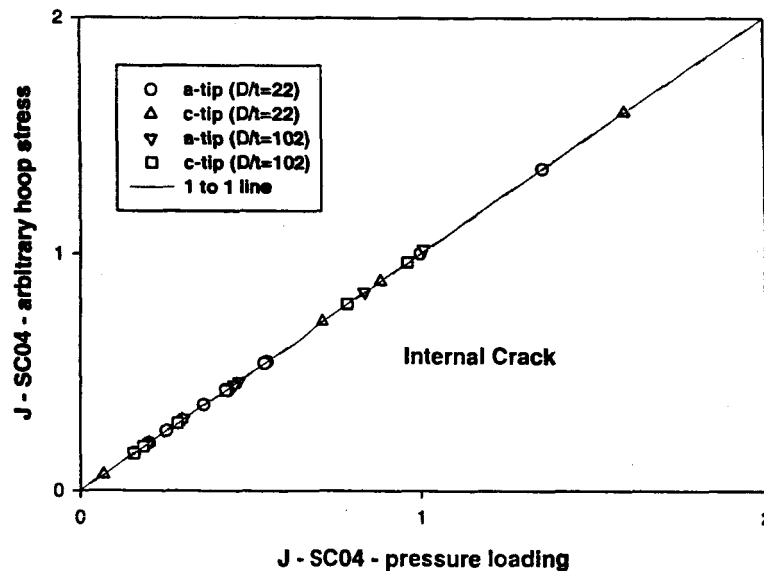


Figure 4. Consistency between J estimations for internal cracks in cylinders (SC04) when the applied primary loading is specified in terms of an internal pressure and a hoop stress distribution corresponding to an internal pressure.

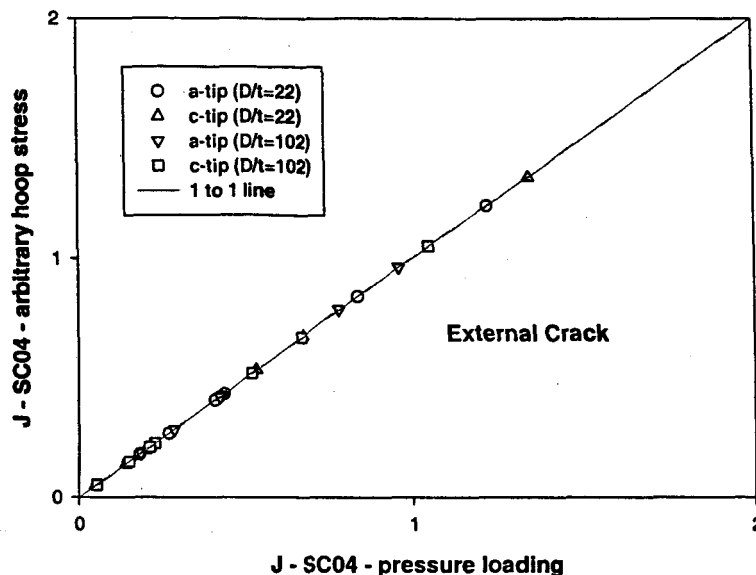


Figure 5. Consistency between J estimations for external cracks in cylinders (SC04) when the applied primary loading is specified in terms of an internal pressure and a hoop stress distribution corresponding to an internal pressure.

5.0 J SOLUTIONS FOR CORNER CRACKS IN PLATES SUBJECTED TO BENDING (Crack Model CC01)

5.1 Implementation of J Solutions for CC01 (Bending)

The current J solutions in NASGRO for corner cracks subjected to bending (CC01) are conservatively based. The accuracy of these solutions was improved by performing elastic-plastic finite element analysis (FEA) to compute J solutions and use the results to reduce the conservatism in the J estimation technique used in the Phase 1 solutions in NASGRO. Only the main results of the FEA are presented in the main text of this Addendum, a more detailed description of the FEA modeling is provided in Appendix 1.

The results of the FEA were used to derive values of h_I calculated as

$$h_I = \frac{J - J_e}{\alpha \sigma_o \epsilon_o t \left(\frac{M}{M_o^*} \right)^{n+1}} \quad (17)$$

Values of h_I were calculated for four different values of the strain-hardening exponent ($n=1, 5, 10, \text{ and } 15$) for each of the geometries in the analysis matrix. (The $n=1$ values correspond to linear elastic solutions with a Poisson ratio equal to the plastic value of 0.5.) The resulting values of h_I and the moment ratio, (M/M_o^*) , at which they were evaluate are presented in Tables

2 through 5. The h_I values were derived from the FEA J values at elliptical angles of 4.5° (c-tip) and 85.5° (a-tip) in order to avoid using the actual free surface values at 0° and 90° that are known to be subject to errors. The values of h_I as a function of elliptical angle are shown graphically in Appendix 1.

Table 2. Model CC01, Corner Crack, Bending Load, $n=1$.

a/t	a/c	$h_I(a)$ at 85.5°	$h_I(c)$ at 4.5°
0.2	0.2	0.7897	0.3100
0.2	0.6	0.5292	0.5477
0.2	1.0	0.3555	0.5621
0.5	0.2	1.1833	0.8753
0.5	0.6	0.4217	1.2060
0.5	1.0	0.2028	1.1263

Table 3. Model CC01, Corner Crack, Bending Load, $n=5$.

a/t	a/c	(M/M_o^*)	$h_I(a)$ at 85.5°	$h_I(c)$ at 4.5°
0.2	0.2	2.145	0.4408	0.1719
0.2	0.6	2.130	0.3613	0.2933
0.2	1.0	2.122	0.2396	0.3367
0.5	0.2	1.943	0.7163	0.4991
0.5	0.6	2.316	0.3014	0.5051
0.5	1.0	2.369	0.1294	0.4846

Table 4. Model CC01, Corner Crack, Bending Load, $n=10$.

a/t	a/c	(M/M_o^*)	$h_I(a)$ at 85.5°	$h_I(c)$ at 4.5°
0.2	0.2	1.540	0.2865	0.1204
0.2	0.6	1.508	0.2568	0.2125
0.2	1.0	1.503	0.1730	0.2403
0.5	0.2	1.505	0.3879	0.3394
0.5	0.6	1.638	0.1809	0.2672
0.5	1.0	1.652	0.08035	0.2488

Table 5. Model CC01, Corner Crack, Bending Load, $n=15$.

a/t	a/c	(M/M_o^*)	$h_I(a)$ at 85.5°	$h_I(c)$ at 4.5°
0.2	0.2	1.353	0.19853	0.08720
0.2	0.6	1.343	0.1843	0.1551
0.2	1.0	1.339	0.1265	0.1755
0.5	0.2	1.380	0.1945	0.1971
0.5	0.6	1.458	0.09734	0.1379
0.5	1.0	1.463	0.04455	0.1279

The optimized yield moments and V values were determined for CC01 under bending using the FEA calculated h_I values for $n=1, 5, 10,$ and 15 . As previously mentioned, the optimized scheme provides the values of V and M_o^* that are independent of strain hardening exponent n and give the best fit between the RSM analytical approach and the FEA results. The results of applying this scheme are shown in Table 6 for the a-tip and c-tip as a function of a/t and a/c .

Table 6. Optimized Yield Moments and V's for CC01 under Bending.

Corner Crack (CC01) Under Bending					
a/t	a/c	a-tip		c-tip	
		Optimized $4M_o^*/t^2W\sigma_o$	V	Optimized $4M_o^*/t^2W\sigma_o$	V
0.2	0.2	1.0068	0.7224	1.0055	0.6310
0.2	0.6	0.9931	0.8745	0.9896	0.6666
0.2	1.0	0.9877	0.8576	0.9879	0.7399
0.5	0.2	0.9607	1.0072	0.9237	0.6641
0.5	0.6	0.9436	1.1279	0.9618	0.7002
0.5	1.0	0.9379	0.9840	0.9658	0.7313
		$V_a^{Average}$	0.9289	$V_c^{Average}$	0.6889
$(V_a^{Average} + V_c^{Average})/2 = 0.8089$					

In Figure 6, the optimized RSM results for h_I ($n>1$) are shown plotted against the values derived from the FEA computations. The data points fall on or near the "1 to 1" line that represents 100% accuracy for the optimized solutions, confirming that in principle the RSM approximation can attain high accuracy. As previously mentioned, the hybrid RSM solutions are employed in NASGRO in order to be able to determine J solutions for a wide range of $a/t, a/c,$ and b/c values. In Phase 1, these hybrid solutions do not use the optimized yield moments but instead use the expression for M_o^* given by equation (7). The values of h_I predicted by the hybrid RSM solution for J are shown plotted against the FEA solutions in Figure 7. In this case, the hybrid RSM solutions consistently over-predict the FEA values, and the accuracy of the solutions is poor. This problem was attributed to the fact that equation (7) is not an accurate estimation for the optimized net section yield moment. With this in mind, studies were performed to obtain a modified form for M_o^* that increased the accuracy of the hybrid RSM solutions. The result of the investigation, the yield moment M_o^{*CC01} , is shown in equation (18) where M_o^* is given by equation (7).

$$M_o^{*CC01} = (1.033 + 0.184 \frac{a}{t})M_o^* \quad (18)$$

The NASGRO EPFM CC01 bend solution for J_p in Phase 3 is taken, therefore, as the hybrid RSM solution given by the equation

$$J_p^{RSM} = J_e \left(\frac{a}{t}, \frac{a}{c}, \frac{b}{c} \right) \mu V \alpha \left(\frac{M}{M_0^{*CC01} \left(\frac{a}{t}, \frac{a}{c}, \frac{a}{t} \right)} \right)^{n-1} \quad (19)$$

where the value of V is 0.8089 (see Table 5), and $\mu=1$. The corresponding hybrid RSM solutions for $h_j(n)$ are given by

$$h_1(n) = \frac{J_e \mu V}{\sigma_o \epsilon_o t \left(\frac{M}{M_0^{*CC01}} \right)^2} \quad (20)$$

The predictions of equation (20) for $n>1$ are compared to the FEA solutions for the a-tip and c-tip obtained from Tables 3 through 5 in Figure 8. It can be seen that there is a significant increase in the accuracy of the hybrid RSM solutions obtained using M_0^{*CC01} compared to those solutions using M_o^* . Indeed, the new solutions are evenly scattered about the 1 to 1 line rather than consistently over-estimating the values of $h_j(n)$.

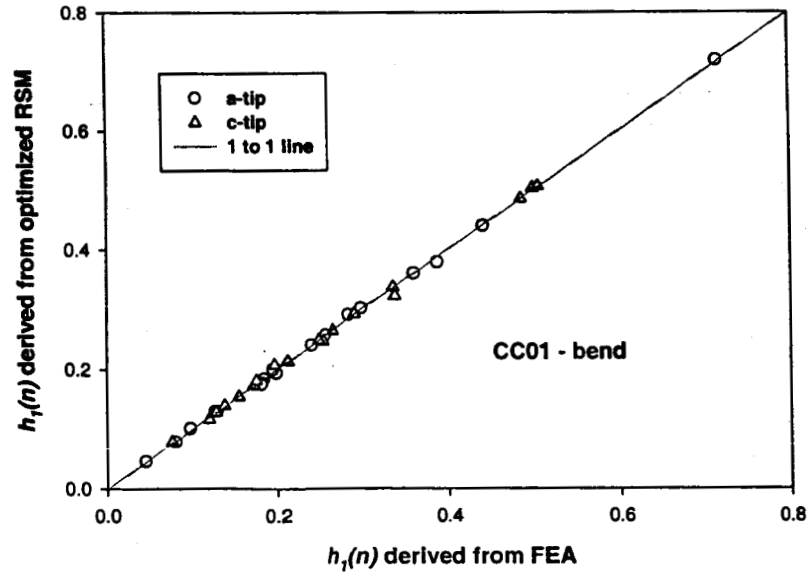


Figure 6. Comparison of $h_j(n>1)$ for CC01 (bending) computed using FEA with the results obtained from applying the RSM using optimized net section yield moments.

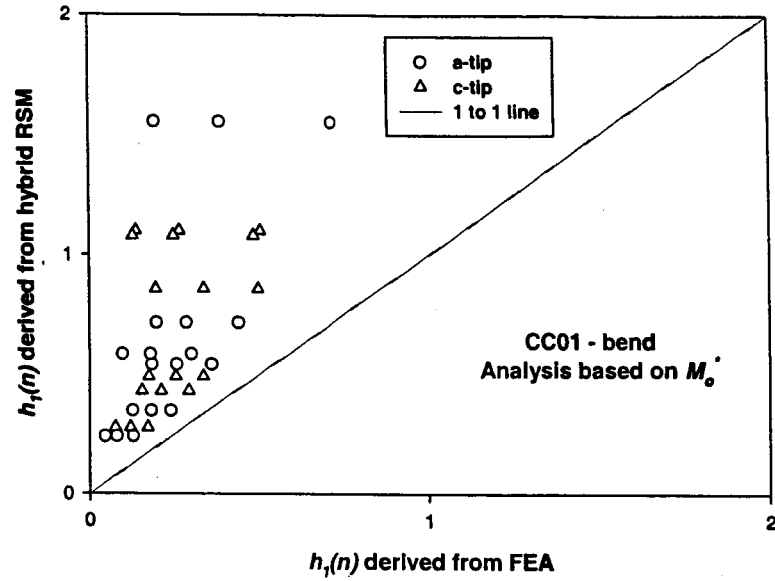


Figure 7. Comparison of $h_1(n>1)$ for CC01(bending) computed using FEA with the results obtained from applying the hybrid RSM using equation (7) for the net section yield moment.

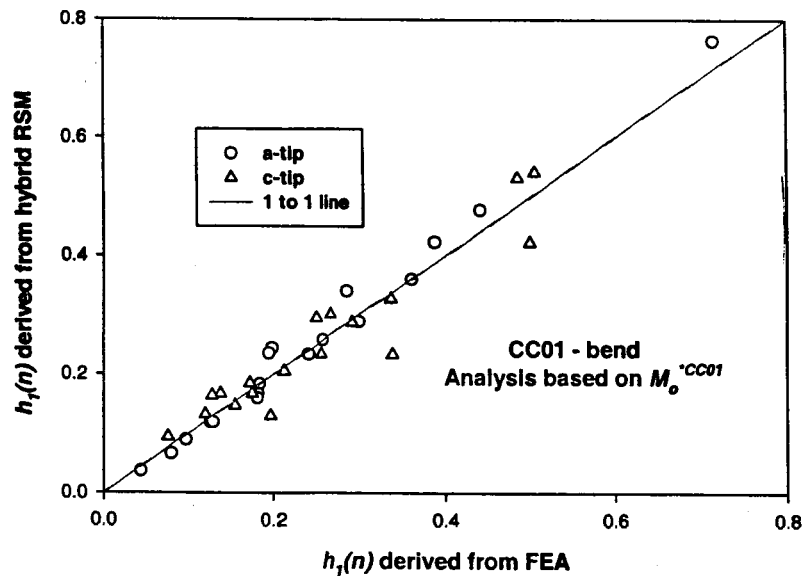


Figure 8. Comparison of $h_1(n>1)$ for CC01 (bending) computed using FEA with the results obtained from applying the hybrid RSM using equation (18) for the net section yield moment.

5.2 Validation of J Solutions for CC01 (Bending)

The CC01 J solutions were implemented for bending using the existing CC01 SIF routines, the net section yield moment given by equation (18) and the average V value of 0.8089 given in Table 6.

Figure 8 provides validation for the new solutions against FEA results in terms of the hybrid RSM and FEA solutions for the h_I functions, defined according to equation (20). This figure demonstrates the kind of accuracy that can be obtained from the RSM solutions. Additional validation was obtained by comparing manual calculations for J_p with J_p values computed using the EPFM module. These computations confirmed that the hybrid RSM solution for J had been accurately implemented in the computer code (see Appendix 4).

6.0 J SOLUTIONS FOR EMBEDDED CRACKS IN PLATES SUBJECTED TO TENSION AND ARBITRARY STRESSES (Crack Models EC01/EC02)

6.1 Implementation of J Solutions for EC01/EC02

The Phase 1 J solutions in NASGRO for embedded cracks subjected to tension (EC01) were considered conservatively based. (However, as will be seen below, this proved not to be the case.) As was done for CC01 in bending, the accuracy of these Phase 1 solutions was improved using the results of FEA to compute J solutions. Only the main results of the FEA are presented in the main text of this Addendum, a more detailed description of the FEA modeling is provided in Appendix 1.

The results of the FEA were used to derive values of h_I calculated as

$$h_I = \frac{J - J_e}{\alpha \sigma_o \epsilon_o \frac{t}{2} \left(\frac{P}{P_o^*} \right)^{n+1}} \quad (21)$$

Values of h_I were calculated for four different values of the strain-hardening exponent ($n=1, 5, 10,$ and 15) and the resulting values of h_I and the load ratios (P/P_o^*) at which they were determined are presented in Tables 7 through 10. The h_I values were derived from the FEA J values at elliptical angles of 4.5° (c-tip) and 85.5° (a-tip) in order to avoid possible errors at 0° and 90° . The values of h_I as a function of elliptical angle are shown graphically in Appendix 1.

Table 7. Embedded Crack, Tension Load, $n=1$.

$2a/t$	a/c	$h_I(a)$ at 85.5°	$h_I(c)$ at 4.5°
0.2	0.2	0.4337	0.09056
0.2	0.6	0.2930	0.1755
0.2	1.0	0.1959	0.1959
0.5	0.2	1.3037	0.2442
0.5	0.6	0.8013	0.4685
0.5	1.0	0.5119	0.5062

Table 8. Embedded Crack, Tension Load, n=5.

$2a/t$	a/c	(P/P_o^*)	$h_I(a)$ at 85.5°	$h_I(c)$ at 4.5°
0.2	0.2	2.134	0.8231	0.1851
0.2	0.6	2.129	0.5299	0.3247
0.2	1.0	2.212	0.3662	0.3654
0.5	0.2	2.354	4.3138	0.7913
0.5	0.6	2.403	1.9887	1.1550
0.5	1.0	2.329	1.1850	1.1319

Table 9. Embedded Crack, Tension Load, n=10.

$2a/t$	a/c	(P/P_o^*)	$h_I(a)$ at 85.5°	$h_I(c)$ at 4.5°
0.2	0.2	1.521	1.0699	0.2376
0.2	0.6	1.458	0.6843	0.4087
0.2	1.0	1.515	0.4755	0.4732
0.5	0.2	1.606	8.8905	1.7439
0.5	0.6	1.619	3.4996	2.0009
0.5	1.0	1.589	1.9506	1.8448

Table 10. Embedded Crack, Tension Load, n=15.

$2a/t$	a/c	(P/P_o^*)	$h_I(a)$ at 85.5°	$h_I(c)$ at 4.5°
0.2	0.2	1.340	1.2678	0.2808
0.2	0.6	1.284	0.8071	0.4765
0.2	1.0	1.333	0.5613	0.5569
0.5	0.2	1.409	14.800	3.1478
0.5	0.6	1.413	5.3330	3.0537
0.5	1.0	1.396	2.8317	2.6808

The optimized yield loads P_o^* and V values were determined for EC01/EC02 using the FEA calculated h_I values for $n=1, 5, 10,$ and 15 . The results of applying this scheme are shown in Table 11 for the a-tip and c-tip as a function of a/t and a/c .

Table 11. Optimized Yield Moments and V's for EC01/EC02 under Tension.

Embedded Crack (EC01/EC02) Under Tension					
2a/t	a/c	a-tip		c-tip	
		Optimized $Po^*/tW\sigma_o$	V	Optimized $Po^*/tW\sigma_o$	V
0.2	0.2	0.9181	1.5916	0.9194	1.7213
0.2	0.6	0.9191	1.5229	0.9226	1.5788
0.2	1.0	0.9181	1.5656	0.9186	1.5660
0.5	0.2	0.7925	1.9930	0.7812	1.8418
0.5	0.6	0.8138	1.6569	0.8156	1.6609
0.5	1.0	0.8237	1.6202	0.8246	1.5714
		$V_a^{Average}$	1.6584	$V_c^{Average}$	1.6567
$(V_a^{Average} + V_c^{Average})/2 = 1.6575$					

In Figure 9, the optimized RSM results for $h_1(n > 1)$ are shown plotted against the values derived from the FEA computations for EC01. The data points fall on or near the "1 to 1" line that represents 100% accuracy for the optimized solutions, yet again confirming that the RSM approximation can attain high accuracy.

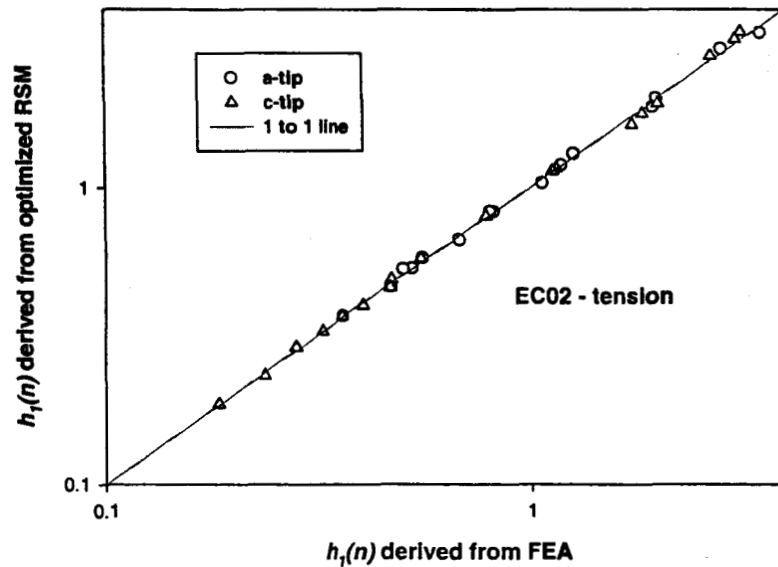


Figure 9. Comparison of $h_1(n > 1)$ for EC01/EC02 computed using FEA with the results obtained from applying the RSM using optimized net section yield loads.

The hybrid RSM J solutions for EC01 in Phase 1 are generated using the equation

$$J_p^{RSM} = J_e(a, c) \mu V \alpha \left(\frac{P}{P_o^*} \right)^{n-1} \quad (22)$$

where P_o^* is related to the reduced load bearing area of the plate and is given by

$$P_o^* = \sigma_o (tW - \pi ac) \quad (23)$$

The values of h_1 corresponding to this hybrid RSM solution for J are shown plotted against the FEA solutions in Figure 10. In this case, the hybrid RSM solutions consistently under-predict the FEA values, and the accuracy of the solutions is poor. This problem is due to the fact that equation (23) provides a poor representation of the optimized net section yield moment.

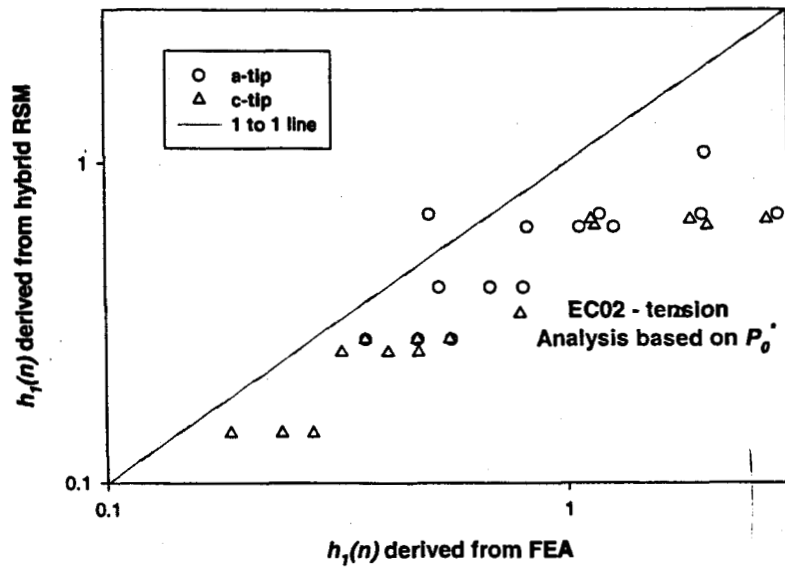


Figure 10. Comparison of $h_1(n > 1)$ for EC01/EC02 computed using FEA with the results obtained from applying the RSM using equation (23) as the net section yield load.

Studies were performed to obtain a modified form for P_o^* that increased the accuracy of the hybrid RSM solutions. Based on this investigation, the Phase 3 NASGRO EPFM EC01 and EC02 tension solutions for J_p are taken as the hybrid RSM solution:

$$J_p^{RSM} = J_e \left(\frac{2a}{t}, \frac{a}{c}, \frac{2c}{W} \right) \mu V \alpha \left(\frac{P}{P_o^{*EC01/EC02} \left(\frac{2a}{t}, \frac{a}{c}, \frac{2c}{W} \right)} \right)^{n-1} \quad (24)$$

In this equation, the value of V is taken as 1.6575 (see Table 11) and $\mu = \frac{1-\nu_p^2}{1-\nu_e^2}$ for both the a-tip and c-tip, where subscripts e and p signify the elastic and plastic values, respectively, of Poisson's ratio. The net section yield load is given by:

$$P_o^{*EC01/EC02} = (1 - 0.4 \frac{2a}{t} \frac{2c}{W}) \left(1 + 0.025 \left[1 + 40 \left(\frac{a}{c} \right)^{1/4} \left(\frac{2a}{t} \frac{2c}{W} \right)^2 \right] \left(4 \frac{2a}{t} \frac{2c}{W} \right)^{1/4} \left(\frac{a}{c} \right)^{1/2} \right) \left(1 - 0.9 \frac{2a}{t} \frac{2c}{W} \right) \left(1 + 0.3102 \frac{2a}{t} \frac{2c}{W} \left(\frac{a}{c} \right)^{0.5 \left(1 - \left[4 \frac{2a}{t} \frac{2c}{W} \right]^{1/2} \right)} \right) P_o^*, a/c \leq 1 \quad (25a)$$

$$P_o^{*EC01/EC02} = (1 - 0.4 \frac{2a}{t} \frac{2c}{W}) \left(1 + 0.025 \left[1 + 40 \left(\frac{c}{a} \right)^{1/4} \left(\frac{2a}{t} \frac{2c}{W} \right)^2 \right] \left(4 \frac{2a}{t} \frac{2c}{W} \right)^{1/4} \left(\frac{c}{a} \right)^{1/2} \right) \left(1 - 0.9 \frac{2a}{t} \frac{2c}{W} \right) \left(1 + 0.3102 \frac{2a}{t} \frac{2c}{W} \left(\frac{c}{a} \right)^{0.5 \left(1 - \left[4 \frac{2a}{t} \frac{2c}{W} \right]^{1/2} \right)} \right) P_o^*, a/c > 1 \quad (25b)$$

where P_o^* is given by equation (23). The hybrid RSM solutions for $h_1(n)$ are given by

$$h_1(n) = \frac{J_e(a,c) \mu V}{\sigma_o \epsilon_o \frac{t}{2} \left(\frac{P}{P_o^{*EC01/EC02}} \right)^2} \quad (26)$$

The predictions of equation (26) for $n > 1$ are compared to the FEA solutions from Tables 8 through 10 for the a-tip and c-tip in Figure 11. The accuracy of the solutions is greatly improved using the modified form for the net section yield load, and the results are now evenly scattered about the 1 to 1 line.

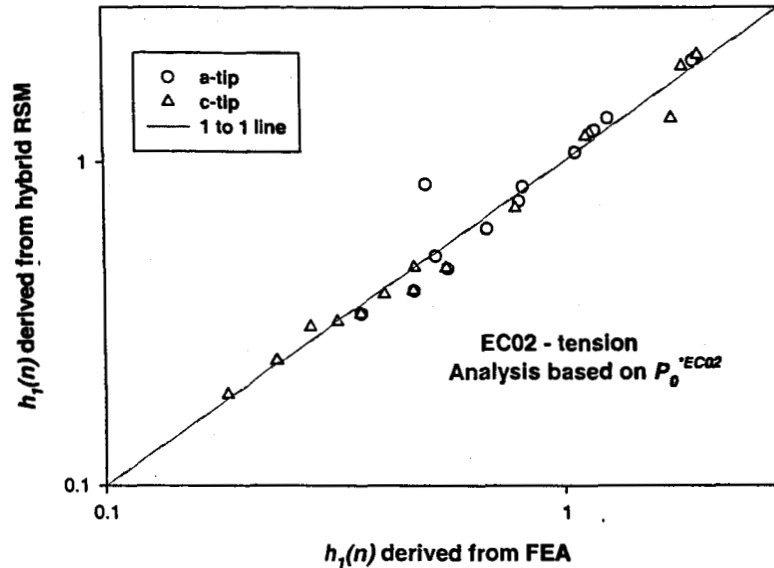


Figure 11. Comparison of $h_I(n>1)$ for EC01/EC02 computed using FEA with the results obtained from applying the RSM using equation (25) as the net section yield load.

In the EC02 model the applied load is not explicitly defined. Instead, the user specifies an arbitrary stress distribution, and the tensile force, P , used in equation (**) is obtained by integrating this stress distribution.

6.2 Validation of J Solutions for EC01/EC02

The new FEA J solutions for embedded cracks subjected to tension loading were used to update the V values and net section yield solutions in the Phase 1 EPFM module, and to implement the new EC02 solutions generated in Phase 2. The SIF solutions employed in EC02 are based on the solutions in KCALC, a program for computing SIFs for cracks in arbitrary stress fields developed and copyrighted by Southwest Research Institute® (SwRI®). This program was used because, unlike the case for SC02, NASGRO did not have the capability of calculating SIFs for embedded cracks subject to arbitrary stress fields. KCALC routines have been validated and are employed in several programs developed by SwRI, such as DARWIN™ (Design Assessment of Reliability With INspection), a software design code, developed for the Federal Aviation Administration (FAA) to help engine manufacturers improve the safety of jet engines used in commercial airliners.

The new J solutions were partly validated by comparing the EC01 and EC02 solutions for uniform stressing. The results are shown in Figure 12 where J values derived from the EC01 model are plotted against J values computed using the new EC02 model solutions. Perfect agreement between the two sets of solutions occurs when the data points fall on the 1 to 1 line. It can be seen from Figure 12 that excellent agreement obtains between the EC02 and EC01 solutions, indicating that the integration routine used to determine the external force from the arbitrary stress distribution specified in EC02 and the resulting net section yield solution is correctly calculated. The small differences between the EC01 and EC02 J values arise because

the NASGRO SIF solution for uniform stressing is used in EC01, whereas, as previously mentioned, the KCALC SIF solution is used in EC02.

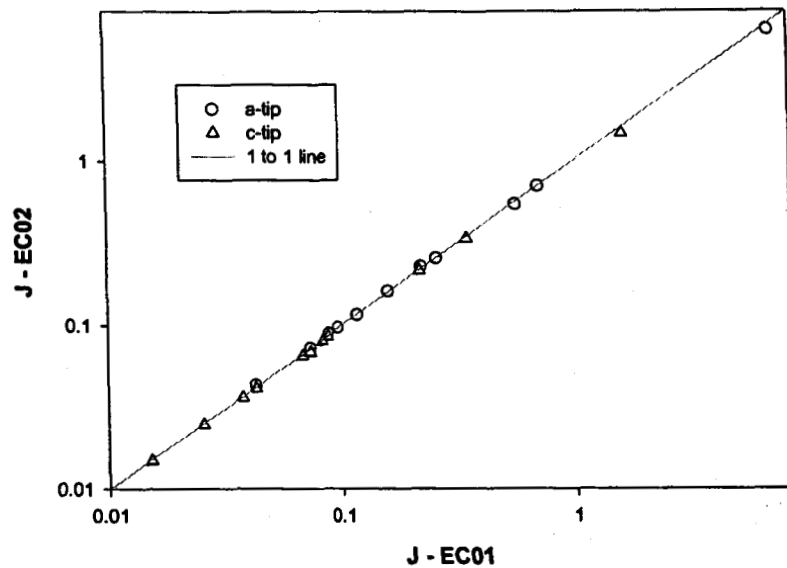


Figure 12. Comparison of J estimations obtained using EC01 and EC02. The arbitrary stress fields used in the EC02 computations were chosen to simulate uniform tension.

An additional verification test for the EC02 model geometry was performed. This was based on an independently developed computer program that employed the KCALC routine and the same net section yield load equations as used in EC02. This independent program was used to generate J values (hereafter referred to as J estimation values) against which the NASGRO EPFM EC02 solutions could be compared. In this comparison, two different load cases were used. The first consisted of a primary load corresponding to a linear stress field of the form $140 - 80 \frac{x}{t}$ ksi. The second load case involved combined primary and secondary loads, with the stress distribution for the primary load given by a uniform stress equal to 100 ksi, and the secondary load corresponding to a self-equilibrated stress of the form $-200 + 1200 \frac{x}{t} - 1200 \left(\frac{x}{t} \right)^2$ ksi. The J values determined using NASGRO for these two load cases are plotted against the J estimation values in Figures 13 and 14. Agreement between the two sets of solutions occurs when the data points fall on the 1 to 1 lines shown in the figures. It can be seen that excellent agreement is obtained between the NASGRO routine solutions and those obtained using the independently developed program.

Additional validation for EC02 J solutions based on manual calculations is provided in Appendix 4.

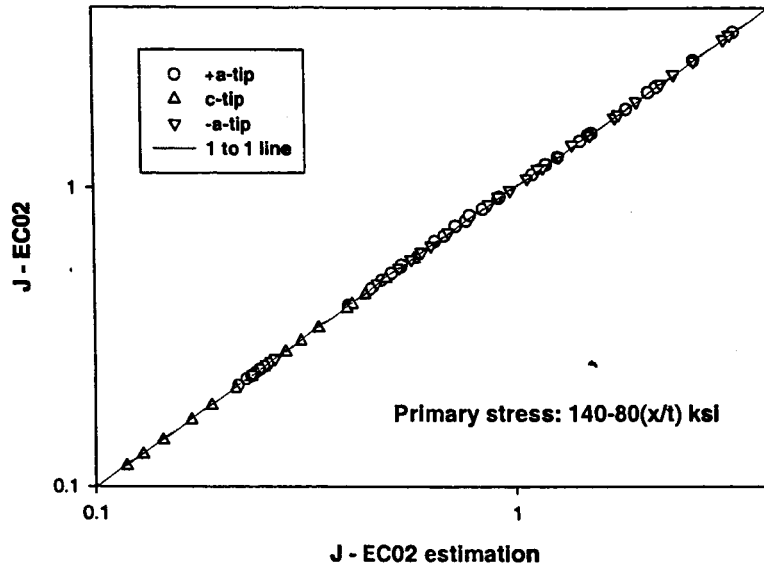


Figure 13. Comparison of EPFM Module J solutions for EC02 with independently derived solutions (J estimates) that used KCALC SIF solutions, and the same V and net section yield loads used in the Module. The primary load is represented by a linear stress distribution.

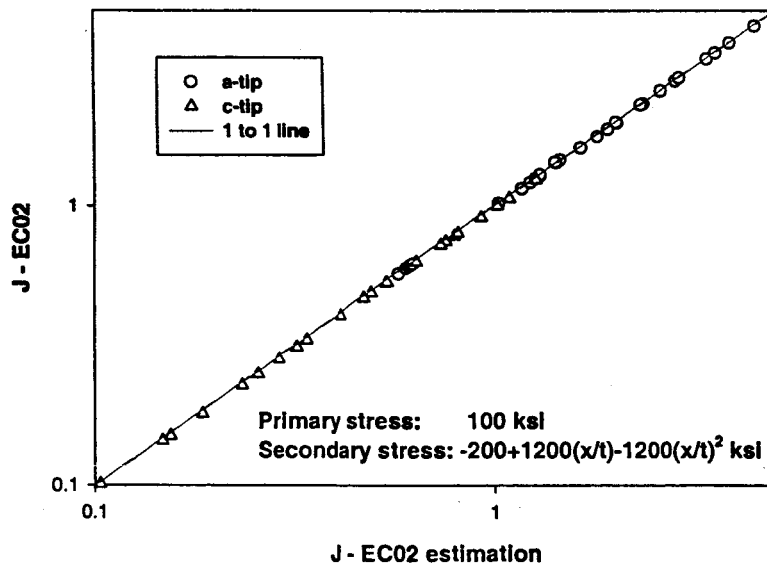


Figure 14. Comparison of EPFM Module J solutions for EC02 with independently derived solutions (J estimates) that used KCALC SIF solutions, and the same V and net section yield loads used in the Module. The primary load corresponds to a uniform stress and the secondary load is a self-equilibrated quadratic stress.

7.0 TECHNICAL ISSUES RELATED TO PHASE 3 ENHANCEMENTS

The major technical issues needed to be overcome to implement the proof test analysis modules were the development of: 2-DOF failure analysis routines for critical load and critical crack analyses; tear-fatigue routines that accurately included 2-DOF interactions between the a-tip and c-tip; and reliability analyses for MCPT analysis.

7.1 Ductile Failure Analysis Routines for 2-DOF Cracks

The development of 2-DOF ductile failure analysis routines for critical crack and critical load analyses is a major advance on the 1-DOF failure routines incorporated into Phase 1 and 2, and is a necessary enhancement in preparation for the introduction of proof test analysis modules in NASGRO.

The conditions for ductile instability at the a-tip for 1-DOF cracks are defined by the equations:

$$J_a(a_i + \Delta a_i, P) = J_R(\Delta a_i) \quad (27)$$

$$\frac{dJ_a}{da} = \frac{dJ_R}{d(\Delta a_i)}$$

where a_i is the initial crack depth before tearing occurs and Δa_i is the amount of tearing at instability. These equations state that instability will occur when the applied J equals J_R and simultaneously the J curve is tangential to the J_R curve.

For 2-DOF cracks, these conditions become:

$$J_a(a_i + \Delta a_i, c_i + \Delta c_i, P) = J_R(\Delta a_i)$$

$$J_c(a_i + \Delta a_i, c_i + \Delta c_i, P) = J_R(\Delta c_i) \quad (28)$$

$$\left(\frac{\partial J_a}{\partial c} \right)_{a,P} \left(\frac{\partial J_c}{\partial a} \right)_{c,P} = \left(\frac{dJ_R}{d(\Delta a_i)} - \left(\frac{\partial J_a}{\partial a} \right)_{c,P} \right) \left(\frac{dJ_R}{d(\Delta c_i)} - \left(\frac{\partial J_c}{\partial c} \right)_{a,P} \right)$$

where a_i and c_i are the initial crack depth and initial half surface length, respectively, and Δc_i is the amount of tearing at the c-tip at instability.

The 2-DOF instability conditions show that instability does not occur when a 1-DOF instability condition occurs at either the a-tip or the c-tip, but that instability is dependent on the conditions at both the a-tip and c-tip and does not correspond to a tangency point, as does the 1-DOF case. Indeed, the instability condition for cracks with 2-DOF states that instability will only occur when both the a-tip and the c-tip are simultaneously unstable.

7.2 Proof Test Module

The proof test module is based on the NASA Final Report, "*Guidelines for Proof Test Analysis*," delivered to MSFC under NASA Contract NAS8-39380. Reference should be made to this document for more details concerning proof test design and analysis. Herein, only a brief summary of the proof test modules developed in Phase 3 is given.

Figure 15 provides an overview of the routines included in the proof test module. Two types of analysis can be performed as part of the proof test procedures: either a **Safe Life Analysis** or a **Proof Test Analysis**. Two options are available if the Safe Life Analysis is selected: either **Critical Flaw Size** or **Fatigue Life**. The purpose of the Safe Life Analysis is to enable the proof test analyst to perform a pre-proof test calculation to determine those regions of a component that may be life limiting. The proof test should be designed to screen out unacceptable flaws in these regions. The life limiting regions may be defined in terms of low fracture tolerance for small cracks or in terms of low fatigue life. High stresses and/or low toughness may give rise to low flaw tolerance, and high cyclic stress ranges and/or environmental factors may give rise to fast crack propagation rates and low fatigue lives.

Three options are currently available if the proof test analysis option is selected: either **Proof Load Analysis** or **Flaw Screening Analysis** or **Final Crack Sizes**. The purpose of the proof load analysis is to determine the proof load necessary to screen out flaws above a specified size. The purpose of the flaw screening analysis is to determine the flaw sizes that are screened out by a specified proof load. The final crack sizes option enables analysts to determine the increase in sizes of specified flaws due to application of the proof load. Although implementation of a proof load analysis or a flaw screening analysis will provide an analyst with information regarding which sizes of flaws will not be present in the component after it has been proof tested, these options will not predict how the population of flaws that survive the proof test has grown due to ductile tearing that did not result in crack instability. The final crack size option is intended to provide this information.



7.3 Tear-Fatigue

Tear-fatigue occurs when load cycling is severe enough to result in simultaneous fatigue crack extension and ductile tearing. The synergy between these two mechanisms of crack propagation results in enhanced crack propagation rates with respect to fatigue crack growth. This point is illustrated in Figure 16 which shows measured crack growth rates plotted against the applied closure corrected cyclic SIF, ΔK_{eff} , for stress ratios, R , of 0.5, 0.1, and -1 . These results demonstrate that the enhanced crack growth rate due to tear-fatigue can be an order of magnitude higher than the predicted fatigue crack growth rate, that tear-fatigue can occur at any R value and, unlike fatigue crack growth, that ΔK_{eff} does not collapse the growth rate in the tear-fatigue regime onto a single curve. A pictorial representation of the tear-fatigue process is shown in Figure 17 and illustrates how the mechanism depends on both fatigue crack growth properties and the J-R curve of the material characterizing the resistance to tearing.

The tear-fatigue methodology is only applicable to ductile materials and is needed to implement the MCPT module in NASGRO. The tear-fatigue methodology is limited to cases of single amplitude loading, which makes it suitable for applying to an MCPT analysis where the proof load is repeatedly applied and removed.

There are two stages to implementing tear-fatigue for 2-DOF flaws. The first stage consists of calculating the amount of ductile tearing that occurs on first application of the proof load. Since the crack tip driving forces at the a-tip and c-tip change as tearing occurs, this stage involves incrementally increasing the applied load up to its maximum value in the fatigue cycle taking into account the resulting incremental changes in the tear lengths at the two tip positions. The second stage consists of actual tear-fatigue as the applied load is cyclically applied, and the a-tip and c-tip incrementally increase in length after each cycle due to fatigue crack growth and ductile tearing.

The two stages can be expressed mathematically the following equations.

Stage 1: First (monotonic) load application

The incremental changes in the tear lengths at the two tips, δa_t and δc_t , due to an incremental change in applied load, δP are given by:

$$\delta a_t = \delta P \frac{J_{a,P}^{a,c}(J_{R,\Delta c_t} - J_{c,c}^{a,P}) + J_{a,c}^{a,P} J_{c,P}^{a,c}}{(J_{R,\Delta a_t} - J_{a,a}^{c,P})(J_{R,\Delta c_t} - J_{c,c}^{a,P}) - J_{a,c}^{a,P} J_{c,a}^{c,P}} \quad (29)$$

$$\delta c_t = \delta P \frac{J_{c,P}^{a,c}(J_{R,\Delta a_t} - J_{a,a}^{c,P}) + J_{c,a}^{c,P} J_{a,P}^{a,c}}{(J_{R,\Delta a_t} - J_{a,a}^{c,P})(J_{R,\Delta c_t} - J_{c,c}^{a,P}) - J_{a,c}^{a,P} J_{c,a}^{c,P}} \quad (30)$$

In these equations, subscript t refers to tear, a and c refer to the a-tip and c-tip, respectively, P to the applied load. Also, the following abbreviations are used:

$$J'_{x,y} = \left(\frac{\partial J_x}{\partial y} \right), \quad (31)$$

$$J_{R,\Delta a_i} = \frac{dJ_R}{d(\Delta a_i)} \quad J_{R,\Delta c_i} = \frac{dJ_R}{d(\Delta c_i)} \quad (32)$$

where Δa_i and Δc_i are the current tear lengths at the a-tip and c-tip, respectively, and J_R is the resistance curve.

Stage 2: Tear-fatigue (cyclic loading)

The incremental changes in crack lengths at the two tips due to a single fatigue cycle are given by:

$$da_f = A(\Delta J_{a,eff})^m \quad (33)$$

$$dc_f = A(\Delta J_{c,eff})^m$$

In these equations, subscript f refers to fatigue, subscript eff to a crack closure corrected quantity, and $\Delta J_{a,eff}$ and $\Delta J_{c,eff}$ are the cyclic changes in J at the a-tip and c-tip, respectively.

The corresponding incremental changes in the tear lengths are assumed to occur at maximum load, P_{max} , in the cycle and are given by:

$$\delta a_i = \frac{(J_{a,a}^{c,P_{max}} \delta a_f + J_{a,c}^{a,P_{max}} \delta c_f)(J_{R,\Delta c_i} - J_{c,c}^{a,P_{max}}) + J_{a,c}^{a,P_{max}} (J_{c,a}^{c,P_{max}} \delta a_f + J_{c,c}^{a,P_{max}} \delta c_f)}{(J_{R,\Delta a_i} - J_{a,a}^{c,P_{max}})(J_{R,\Delta c_i} - J_{c,c}^{a,P_{max}}) - J_{a,c}^{a,P_{max}} J_{c,a}^{c,P_{max}}} \quad (34)$$

$$\delta c_i = \frac{(J_{c,c}^{a,P_{max}} \delta c_f + J_{c,a}^{c,P_{max}} \delta a_f)(J_{R,\Delta a_i} - J_{a,a}^{c,P_{max}}) + J_{c,a}^{c,P_{max}} (J_{a,c}^{a,P_{max}} \delta c_f + J_{a,a}^{c,P_{max}} \delta a_f)}{(J_{R,\Delta a_i} - J_{a,a}^{c,P_{max}})(J_{R,\Delta c_i} - J_{c,c}^{a,P_{max}}) - J_{a,c}^{a,P_{max}} J_{c,a}^{c,P_{max}}} \quad (35)$$

Equations (29), (30), (34), and (35) show that conditions for instability occur when the denominators in these equations become zero, and that these conditions are the same for monotonic loading and cyclic tear-fatigue and for both the a-tip and the c-tip. These instability conditions are precisely those specified in equation (28).

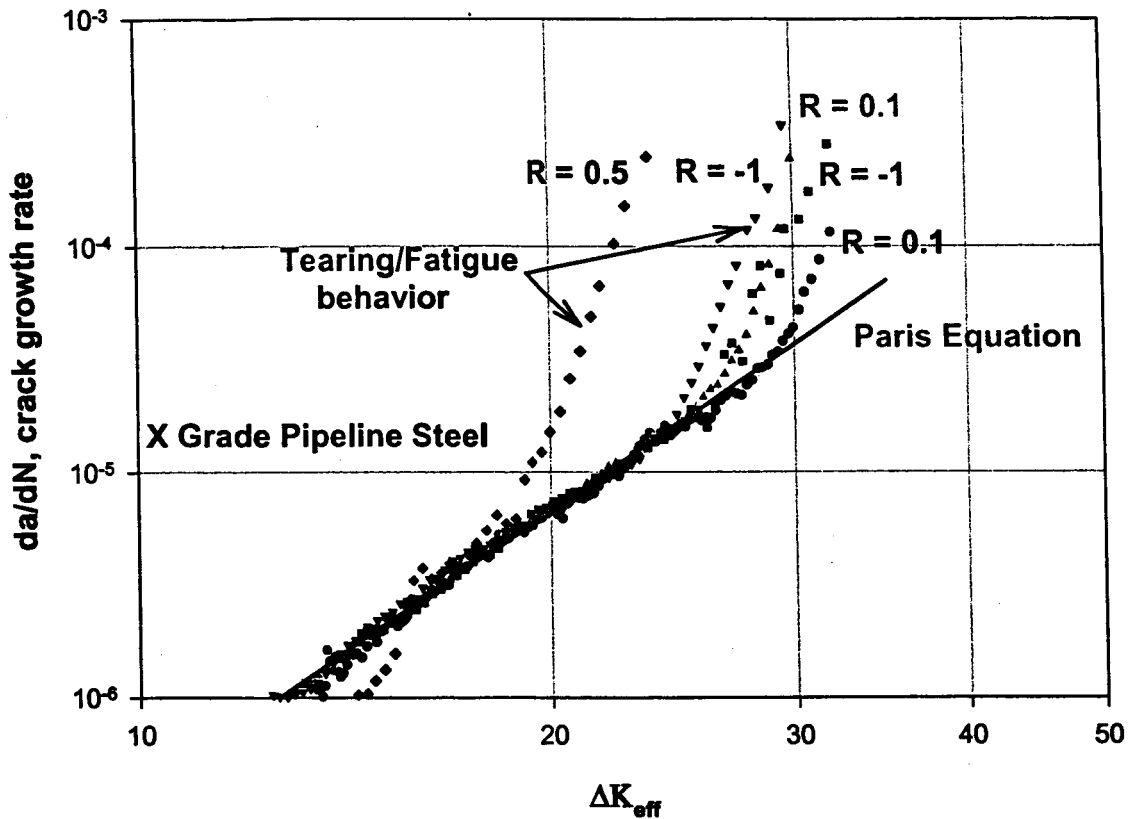
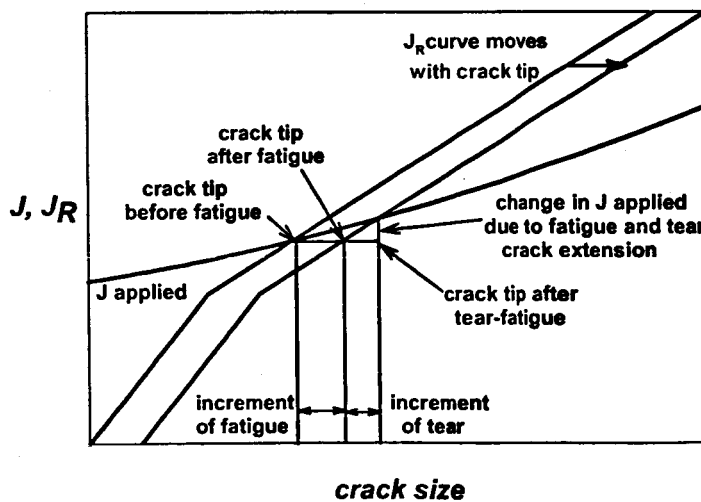


Figure 16. Measured crack growth rate data showing how tear-fatigue accelerates the growth rate with respect to fatigue, illustrated by the Paris equation fit to the data.



- before fatigue cycle the crack is stable and $J=J_R$
- crack advances by fatigue
- resistance curve process zone moves with crack tip
- applied J increases and exceeds resistance ($J>J_R$)
- crack tip tears until stable ($J=J_R$)
- crack advances by fatigue on next cycle etc

Figure 17. Illustration of how the mechanism of tear-fatigue involves synergy between fatigue crack growth and ductile tearing.

7.4 Multiple Cycle Proof Test Analysis (MCPT)

Normally, a component is subjected to a single load cycle during proof testing before entering service. However, for ductile materials, it has been observed that applying multiple load cycles can increase service reliability in some circumstances compared to a single cycle proof test.

According to deterministic proof test analyses, MCPT will cause flaws to extend so a component will enter service with a larger flaw size population than would be the case without MCPT, reducing service reliability. A probabilistic calculation is needed to demonstrate that MCPT can increase service reliability. The argument is based on the fact that MCPT will beneficially change the service reliability by removing those components with large flaws that are service life limiting before they enter service, more than compensating for the potential increase in flaw size population in those components that survive the MCPT.

The methodology employed in the NASGRO MCPT module is based on the work described in the Final Report "A Comparison of Single Cycle Versus Multiple Cycle Proof Test Strategies" performed under Contract NAS8-37451. Consistent with that methodology, there is only one random variable considered in the probabilistic analysis, namely, the initial crack depth.

The MCPT module calculates the following failure probabilities: probability of failure for proof cycles only; probability of failure for proof plus service cycles; and the conditional probability of failure in N_s' service cycles given no failure in N_p' proof cycles.

The reduction of the problem to a single random variable (crack size) allows the probability problem to be reformulated in terms of initial crack size. Therefore, the probability of the number of service cycles being less than or equal to a prescribed number of service cycles is expressed mathematically as

$$P[N_s \leq N_s'] = P[H(a_i) \leq N_s'] = P[a_i \geq H^{-1}(N_s')] = P[a_i \geq a_i^*] \quad (36)$$

where N_s is the number of service cycles at failure, N_s' is a specified number of service cycles, a_i is the initial crack size random variable, $N_s = H(a_i)$ denotes the crack growth function, H^{-1} is the inverse of the crack growth function, and a_i^* is the initial crack size that causes failure on the N_s' service cycle. Similarly, the probability of the number of proof cycles (N_p) being greater than a prescribed number of proof cycles (N_p') is expressed mathematically as

$$P[N_p > N_p'] = P[H(a_i) > N_p'] = P[a_i < H^{-1}(N_p')] = P[a_i < a_i^p] \quad (37)$$

where N_p is the number of proof cycles at failure, N_p' is a prescribed number of proof cycles, a_i^p is the initial crack size which causes failure on the $N_p'+1$ proof cycle. The initial crack sizes for both N_p' proof cycles and N_p' (proof) + N_s' (service) cycles are printed in the output file along with the probabilities defined in equations 1 and 2. The final probability value calculated is the conditional probability of failure in N_s' service cycles given no failure in N_p' proof cycles. Mathematically, the conditional probability is expressed as

$$P \left[(N_s \leq N_s') \mid (N_p > N_p') \right] = \frac{P \left[(N_s \leq N_s') \cap (N_p > N_p') \right]}{P[N_p > N_p']} \quad (38)$$

Because both $P [N_s \leq N_s']$ and $P [N_p > N_p']$ can be represented in terms of the initial crack size distribution a_i , the intersection term in equation (3) can be computed algebraically, once the initial crack sizes a_i^p and a_i^s are known.

An outline of the approach is shown in Figure 18 that illustrates the three stages involved.

The MCPT module currently only has one random variable, the initial flaw size before the proof test. This enables analytical simplifications to be made, avoiding lengthy Monte Carlo calculations.

Stage 3: The probability of the component failing within the specified service lifetime given that it survives the MCPT is the cross-hatched area shown in the figure.

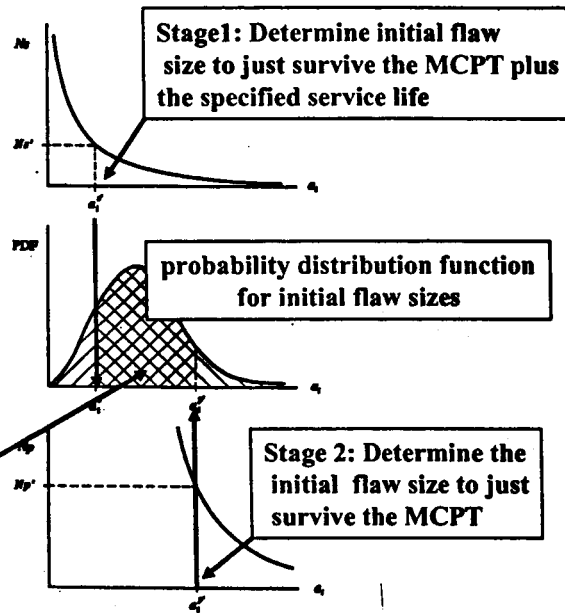


Figure 18. The three stages in the conditional probability calculations in the MCPT module.

The MCPT module can be applied to either 1-degree of freedom (DOF) flaws, or 2-DOF flaws. In the case of the latter, tear-fatigue crack growth is calculated using 2-DOF, based on the monotonic and cyclic crack tip driving forces at the deepest and surface points. The service lifetime calculation begins at the end of the MCPT and uses the final crack size at the end of the proof test as the initial size. The service lifetime calculations are again based on 2-DOF crack growth routines if the problem involves 2-DOF flaws. Note that tear-fatigue crack growth is not allowed for under service conditions as, in general, these will involve variable amplitude loading for which the tear-fatigue routines are not applicable.

The MCPT module calculates the conditional probability of failure for a component for a user specified service lifetime given that the component survives the MCPT. The MCPT is advantageous if this probability is less than the probability of failure determined for a single proof test cycle, or when no proof test is performed.

Although the probabilistic part of the calculations are performed analytically rather than employing Monte Carlo or other numerical methods, never-the-less significant computation time is needed to search and find the initial crack depths that will grow to failure in the user specified proof and service cycles, especially for 2-DOF flaws. Thus, the calculations to evaluate failure probability for a single pair of user specified values for the number of proof cycles and service cycles may take several minutes or more, depending on the speed of the computer used.

8.0 EXAMPLES, VALIDATION, AND PROGRAM ISSUES

8.1 Example Input and Output for Running the EPFM/Proof Test Modules

Examples of the input data needed to run the Modules are presented in Appendix 2. This Appendix contains ten tables listing the data necessary to interactively input data to create the ten example files, Exam1.inp through Exam10.inp, contained on the distribution CD. The data is presented in the order requested by the screen prompts from the Modules. The tables list the name of the input parameter, its value, the units of the parameter, and a brief description of it. The ten examples are summarized in Table 12.

Table 12. Summary of analyses performed in Examples 1 through 10.

Example No.	Option No.	Analysis Type	Crack Model	Loading
1	5	J computation	SC04	primary plus secondary
2	6	critical crack	SC02	primary plus secondary
3	6	critical load	EC02	primary
4	7	fatigue life	CC01	primary and secondary
5	8	pre-proof test critical crack	SC02	primary and secondary
6	8	proof test: flaw screening	SC04	primary
7	8	proof test: proof load	EC02	primary plus secondary
8	8	proof test: final crack size	CC01	primary
9	9	tear-fatigue	SC04	primary plus secondary
10	10	MCPT	SC02	primary

The output files, Exam1.out through Exam10.out, respectively, produced by the example input files are also contained on the distribution CD.

Hard copies of the ten input files and the corresponding output files are given in Appendix 3.

8.2 Validation

The validation of the Modules has been largely directed at ductile failure and fatigue analyses, and, in particular, those analyses that involve tearing and tear-fatigue with 2-DOF. As

mentioned previously, the 2-DOF calculations for ductile materials proved the most difficult to computationally implement.

Appendix 4 lists in tabular form the results of part of the exercise performed to validate the Modules. This exercise complements and provides additional verification material to that already presented in the main part of this Addendum. Appendix 4 presents validation for all the EPFM options (Options 5 through 10). Except for the Option 5 (J calculations), all the analyses used in the validation involved 2-DOF, and except for Option 5 and Option 7 (fatigue lifetime), all the validation analyses addressed ductile fracture behavior.

Appendix 4 presents the results of applying two methods for validating the Modules. In the first, manual spreadsheet calculations were performed to independently evaluate the results of applying the Modules. These validation runs are summarized in Tables A4.1 through A4.6, and Table A4.15 in Appendix 4. The verification runs performed in this exercise are listed in Table 13.

Table 13. List of the manual spreadsheet calculations performed to validate the NASGRO Modules. More details are given in Appendix 4 to which the table numbers refer.

Table Number	Crack Model	Option Number	Description
A4.1	SC04	5 J estimation	Module results for Example 1 in Appendix 2 verified against manual spreadsheet calculations by comparing predicted J_p values.
A4.2	SC02	5 J estimation	Module results verified against manual spreadsheet calculations by comparing predicted J_p values. Primary and secondary loads. Primary stress distribution integrates to a tensile force and zero moment.
A4.3	SC02	5 J estimation	Module results verified against manual spreadsheet calculations by comparing predicted J_p values. Primary stress distribution integrates to a tensile force and moment.
A4.4	CC01	5 J estimation	Module results verified against manual spreadsheet calculations by comparing predicted J_p values. Primary bending load.
A4.5	EC02	5 J estimation	Module results verified against manual spreadsheet calculations by comparing predicted J_p values. Primary and secondary loads.
A4.6	SC02	6 Critical crack size	Module results for Example 2 verified against manual spreadsheet calculations based on running Option 5 to obtain J estimates. Results demonstrate that that the applied J values at the a-tip and c-tip fall on the J-R resistance curve, and the ductile instability criterion is satisfied.
A4.15	SC02	10 MCPT	Module results for Example 10 verified against manual spreadsheet calculations by comparing predicted conditional probability of failure value. The probabilities are evaluated using the initial crack sizes calculated by the module for cracks that would just survive the proof test and service lifetime, respectively.

In the second verification method, self-consistency checks were performed for the Modules by calculating the same result twice using different options and showing that similar results were produced. The results of these internal consistency checks are summarized in Tables A4.7 through A4.14, and Tables A4.16 and A4.17 in Appendix 4. The verification runs performed are listed in Table 14.

Table 14. List of the internal consistency calculations performed to validate the NASGRO Modules. Self-consistency between the Modules is investigated by using two different options to calculate the results for similar problems. More details are given in Appendix 4 to which the table numbers refer.

Table Number	Crack Model	Options Compared		Description
		Option	Option	
7	SC02	6 Critical Crack	6 Critical Load	The critical crack sizes (Option 6) determined in Example 2 are used to specify the initial crack sizes in critical load (Option 6) calculations. Internal consistency is achieved by demonstrating that the critical load equals the applied load used in the critical crack size computations, and the predicted tear lengths are the same.
8	EC02	6 Critical Load	6 Critical Crack	The critical load (Option 6) results calculated in Example 3 are used to specify the applied loads in critical crack size (Option 6) calculations. Internal consistency is achieved by demonstrating that the critical crack sizes equal the initial crack sizes used in the critical load computations, and the predicted tear lengths are the same.
9	CC01	7 Fatigue Life	8 Safe Life: Fatigue Life	Fatigue crack growth behavior predicted in Example 4 using the fatigue life analysis (Option 7) is shown to be consistent with similar behavior predicted by the Safe Life: Fatigue Life analysis (Option 8).
10	SC02	8 Safe Life: Critical Crack Size	6 Critical Load	The critical crack sizes predicted by Example 5 in a Safe Life analysis (Option 8) are used to specify the initial crack sizes in critical load (Option 6) calculations. Internal consistency is achieved by demonstrating that the critical load equals the applied load used in the critical crack size computations, and the predicted tear lengths are the same.
11	SC04	8 Proof Test: Flaw Screening	8 Proof Test: Proof Load	The screened crack sizes predicted in a Proof Test analysis (Option 8) in Example 6 are used to specify the initial crack sizes in a proof load estimate using Proof Test analysis (Option 8). Internal consistency is achieved by

Table Number	Crack Model	Options Compared		Description
		Option	Option	
			6 Critical Load	demonstrating that the proof load needed to screen against the initial crack sizes equals the proof load used in the flaw screening computations, and the predicted tear lengths are the same.
			6 Critical Crack Size	The screened crack sizes predicted in a Proof Test analysis (Option 8) are used to specify the initial crack sizes in a critical load analysis (Option 6). Internal consistency is achieved by demonstrating that the critical load corresponds to the proof load used for flaw screening.
				The screened flaw sizes proof load used in the Proof Test analysis (Option 8) are demonstrated equal to the instability crack sizes calculated using a critical crack analysis (Option 6). used to specify the initial crack sizes in a critical load analysis (Option 6).
12	EC02	8 Proof Test: Proof Load	8 Proof Test: Flaw Screening	In Example 7 the proof load (Option 8) necessary to screen against a specified initial crack size is shown to be consistent with the predicted flaw size screened against when this load is applied as the proof load.
13	CC01	8 Proof Test: Final Crack Size	9 Tear-Fatigue	The final crack size at the end of a Proof Test (Option 8) in Example 8 is demonstrated to be the same as the final crack size at the end of the first load in a Tear-Fatigue (Option 9) analysis.
14	SC04	9 Tear-Fatigue	8 Proof Test: Final Crack Size	The final crack size at the end of the first load application in the Tear-Fatigue (Option 9) analysis of Example 9 is demonstrated to be the same as the final crack size at the end of a Proof Test (Option 8).
16	SC02	10 MCPT	7 Fatigue Life	The calculated initial crack size for a specified service life in a MCPT (Option 10) analysis with no proof test is shown to be consistent with a fatigue life (Option 7) analysis.
17	SC02	10 MCPT	9 Tear-Fatigue	The calculated initial crack size for a specified number of proof test cycles in a MCPT (Option 10) analysis with no service cycles is shown to be consistent with a Tear-Fatigue (Option 9) analysis.

8.3 Program Issues

8.3.1 Problems Occurring During Program Execution

In some instances the search routines employed to solve Option 6, Option 8, and Option 10 analyses may encounter problems. The causes of these problems are usually attributable to one of the following:

1. Limitations on the range of geometrical parameters (a/c , a/t) for which the Phase 1 SIF solutions are valid. If the required solution falls outside of these validity ranges then the search routines in the program will fail.
2. Critical crack size and critical load calculations for ductile materials involving 2-DOF cracks involve evaluating derivatives of J and J_R (for example, see equation (28)). The search routines may encounter problems in finding solutions in these cases because of discontinuities in the derivatives caused by:
 - A. The change in gradient in J_R as the J-R curve transitions from the blunting line to the ductile tearing curve;
 - B. The change in gradient in J_R as the J-R curve transitions from the ductile tearing curve to the saturation value where the gradient becomes zero;
 - C. The transition of J from a continuously varying function of crack size and load to an assumed infinite value when the reference stress equals or exceeds the flow stress defined in equation (3).

However, the user is recommended to check the reasonableness of input data before first assuming that program problems are caused by one of the reasons given above.

8.3.2 CPU Time

In some cases, the number of iterations needed to accurately compute the 2-DOF results for ductile materials is very large due to the sensitivity of the results to growth history. The computations are particularly long if both primary and secondary loads are applied. As a result, in deterministic calculations the computations can take between seconds to tens of seconds to complete. The root finding procedures necessary to implement the MCPT analysis involve even longer computations and, in these cases, CPU times that may extend out to minutes in duration.

8.3.3 CD Contents

The delivered CD contains the following items:

1. An electronic version of this Letter Report.
2. An executable file for running the MSFC Version 6.0 of the NASGRO EPFM and Proof Test Modules.
3. Input files for exercising the executable and the corresponding output files.



APPENDIX 1: Finite Element Analysis of CC01 (Bending) and EC01/EC02 (Tension)

A.1: FEA for CC01 (Bending) Model

Finite element models were created for CC01 geometries. A schematic of the CC01 model is shown in Figure A.1. Each of the CC01 finite element meshes was generated for the present matrix of crack geometries using Patran. The finite element modeling took advantage of appropriate symmetry conditions to reduce the size of the models needed for analysis. Thus, in the case of CC01, symmetry conditions enabled the model size to be reduced to half the size needed to model the full geometry. Consistent with the FEA-based J results used in Appendix K, the ratios $b/c=4$ and $c/h=0.25$ were held constant for all the analyses, where h is the height of the cracked plate. The elements used in the analysis were 20-noded brick elements with reduced integration. The 20-noded brick elements utilized quadratic shape functions for improved accuracy under bending conditions. Additionally, the reduced integration element enabled more accurate representation of the constant volume condition associated with plastic deformation. Each finite element model contained a focused ring of element around the crack front. Crack tip elements were used along the crack front to approximate the $r^{\frac{n}{n+1}}$ strain singularity predicted from analysis. In this configuration, the nodes on the crack front are free to move independently while the mid-side nodes remain at the midpoints. All of the FEA were performed using ABAQUS.

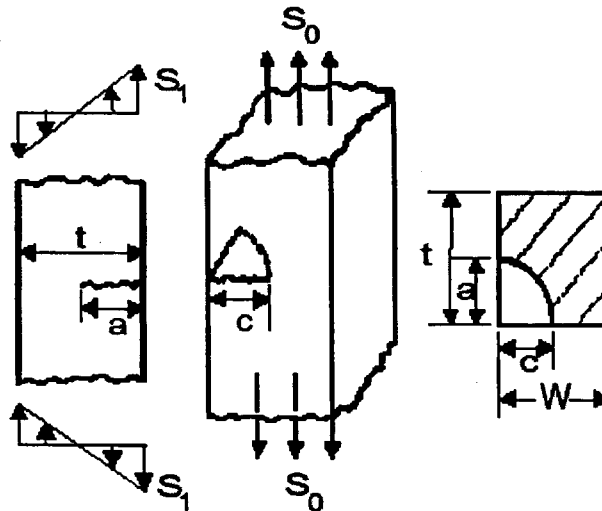


Figure A.1. Schematic of the CC01 crack model modeled using FEA. In the present case, only solutions for bending (S_1) were determined, the tensile load (S_0) was set to zero.

The problem of fully plastic bending in a plate presented some challenges in the development of appropriate finite element models suitable for evaluating the plastic component of J. The first problem encountered was the formation of poorly conditioned deformed elements at high load levels. In the FEA analysis performed to derive the J solutions reported in

Appendix K, the condition for convergence of the fully plastic h_I values appearing in the EPRI formulation for J (see Appendix K) is found by iterating the load value until the elastic J value, J_e , is small compared to the total J value, J , along with proper $(n+1)$ power dependence of J_p on the load value. In the case of bending, this convergence condition proved difficult to attain. Near the crack front, the elements are generally small compared to the specimen dimensions, approximately $10^{-1}a$ for this study. Under the conditions of large plastic strains and high load values required for the condition $J_p/J_e \gg 1$ to obtain, the deformation of the crack tip elements resulted in poorly conditioned elements. It was observed that the remote strain for configurations in which with ratio of $J/J_e = 100$ exceeded 100%. This problem was overcome by performing a convergence study of the fully plastic h_I value as a function of load based on J_p . In this analysis, a finite element model was evaluated for both elastic-plastic and elastic material properties and J_p evaluated as the $J - J_e$.

The second problem encountered was buckling under the applied load value. Initially, the bending moment was applied to the finite element model as a distributed stress along the top surface, using the *DLOAD user subroutine in ABAQUS. Analysis of the deformed shape of the finite element model showed very small crack tip opening displacement (CTOD) that varied little with increasing bending load. This type of deformation behavior is indicative of buckling in the finite element model. This problem was overcome by changing the boundary conditions from applied stress to applied displacement where the z-displacement was prescribed along the top surface of the model and the bending moment was calculated using the nodal force obtained from the analysis.

The accuracy of the finite element models was examined through comparisons with published research. In the review of the published research, it was noted that there is little agreement on the fully plastic results between different authors. One of the problems noted in many of the publications was a lack of information regarding boundary conditions and convergence criteria for the fully plastic analyses.

In the first stage of validating the FEA, the finite element models used in the current study were evaluated under purely linear-elastic material properties so that the results could be compared with the benchmark solutions of Newman & Raju. Excellent agreement was obtained between the current finite element model solutions and the equivalent bend solutions of Newman & Raju.

In the second stage of the validation, it was hoped to compare calculated elastic-plastic J results with similar solutions obtained from the open literature. However, a literature review did not yield any published J results for the fully plastic corner crack in a plate subjected to bending. The closest published results found to a corner crack in bending were those for a surface crack in a plate under bending reported by Yagawa et al. in *Three-dimensional Fully Plastic Solutions for Semi-elliptical Surface Cracks* (Int. J of Press. Ves. and Piping, Vol. 53, pp. 457-510). As is evident from Figure 2, adding a symmetry boundary condition to the face with a normal in the positive x direction can create a surface crack model. In order to compare the present finite element modeling with Yagawa et al., finite element models for the surface crack in a plate geometry were created for two crack geometries: $a/c = 0.2$ and $a/c = 1.0$, both with $a/t = 0.5$. Significant variation was noted between the solutions of Yagawa et al. and the current finite

element model, especially for the elongated ($a/c = 0.2$) crack configuration. In this case, the values of the crack tip parameters f_1 (deep crack tip, a) and f_2 (surface crack tip, c) calculated by Yagawa et al differed by 100% and 10%, respectively, from the values generated in this study.

Several different finite element models for the elongated crack configuration were created to verify the current solution. In addition to solution verification, the finite element study was also used to investigate the influence of mesh density and boundary conditions on the solution. A boundary condition of particular concern was the top surface. Yagawa et al. state "...axial nodal displacements along the top surface were constrained to deform linearly along the top surface so that it remains plane during deformation." In the current analysis, the axial nodal displacements were constrained to be linear along the thickness yet the results for fully plastic h_1 convergence yielded non-planar top surface deformations. This was caused by warping, a phenomenon that can accompany bending deformation and is more pronounced in those models with small thickness to width ratios. The results of this finite element study showed the mesh density in the z -direction has a small influence on f_1 (approximately 10%), but a much larger influence on f_2 (approximately 25%). The increased influence on f_2 is directly attributable to warping.

In another set of calculations, the finite element models were constrained to reduce the amount of warping. The results for these cases showed an approximate 50% reduction in the calculated value of f_1 . As a result, the values of f_1 and f_2 calculated under constrained warping conditions now showed acceptable agreement with the results of Yagawa et al. Therefore, the difference between the current analysis results and those of Yagawa was demonstrated to be due to warping. In addition, the agreement with the results of Yagawa et al under similar boundary conditions validated the finite element modeling employed for the surface crack and hence, by implication, also the corner crack, since the surface and corner crack models only differed through applied boundary conditions.

The finite element models employed for CC01 geometry calculations allowed for the natural deformation of the specimen to occur under load controlled bending. Thus, it was not considered necessary to inhibit warping in these models.

A review of FEA based J solutions in the literature revealed that there is no consistent or well defined method employed to define fully plastic J behavior. In the present case, the FEA model solutions were considered converged when successive values of h_1 were within 1% for a constant displacement step of 0.0625 units (1.563% nominal strain), where

$$h_1 \equiv \frac{J}{\alpha \sigma_o \epsilon_o t \left(\frac{M}{M_o^*} \right)^{n+1}}, \quad J = J_e + J_p \quad (A1.1)$$

and M_o^* is given by equation (7). At this point in the computations, J_p was significantly larger than J_e , and near fully plastic attained. As the loading on the finite element model produced

nominal strains exceeding 25%, a divergence in the h_I value were observed in some models. This divergence can be attributed to poorly conditioned deformed elements. Therefore, the finite element models were analyzed for convergence between 6.25% and 12.5% nominal strain.

After the convergence load was determined, a second FEA was performed to determine J_e at this load value. The value of h_I was then calculated as

$$h_I = \frac{J - J_e}{\alpha \sigma_o \epsilon_o t \left(\frac{M}{M_o} \right)^{n+1}} \tag{A1.2}$$

The values of h_I as a function of elliptical angle are shown graphically in Figures A1.2 through A1.7.

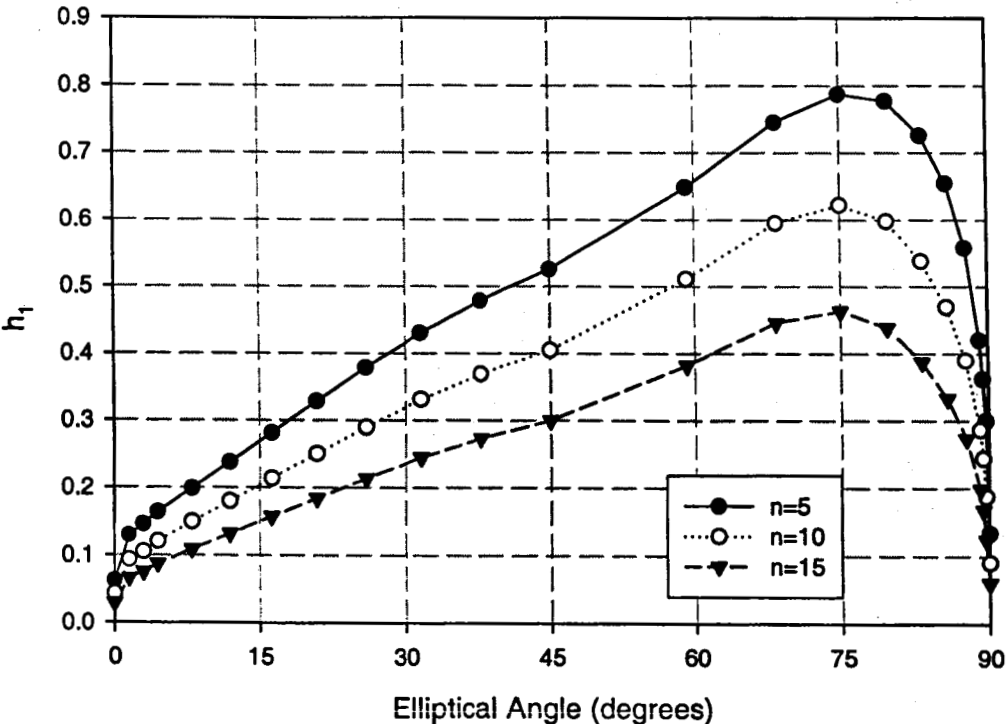


Figure A1.2. Variation of h_I with elliptical angle for CC01 subjected to bending, $a/t=0.2$, $a/c=0.2$.

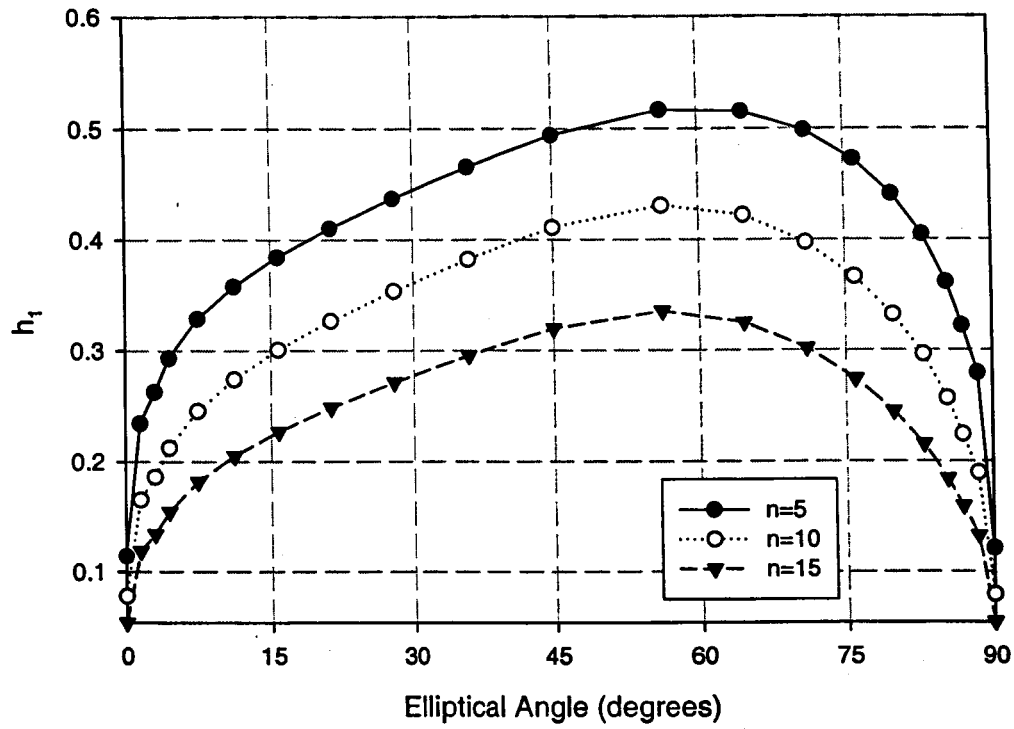


Figure A1.3. Variation of h_1 with elliptical angle for CC01 subjected to bending, $a/t=0.2$, $a/c=0.6$.

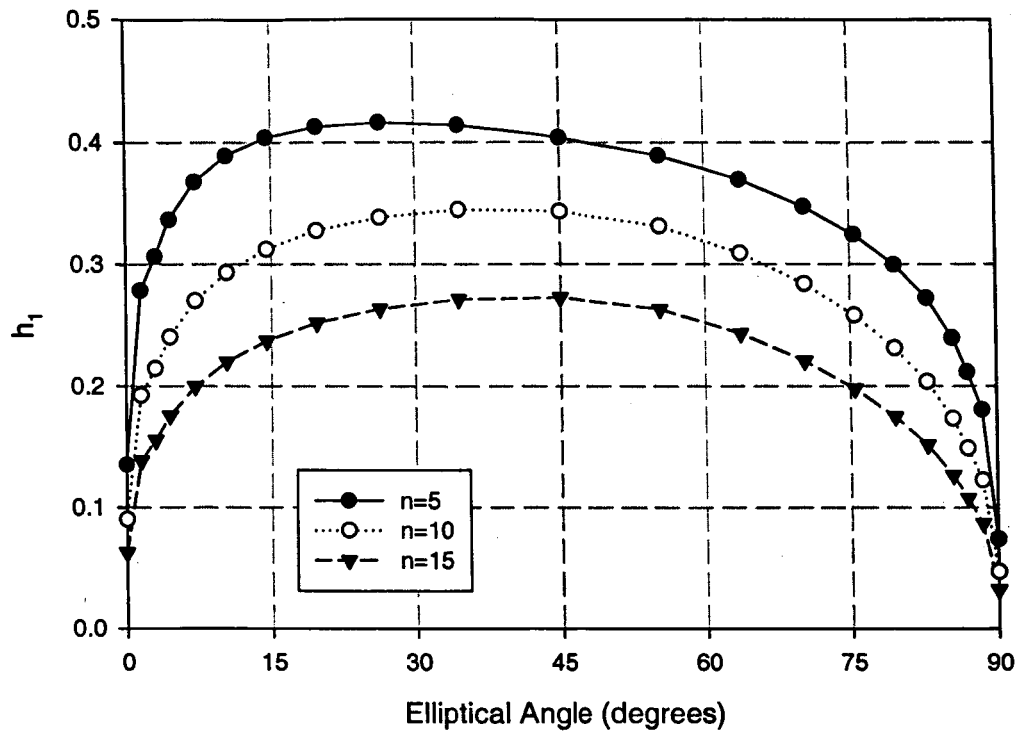


Figure A1.4. Variation of h_1 with elliptical angle for CC01 subjected to bending, $a/t=0.2$, $a/c=1.0$.

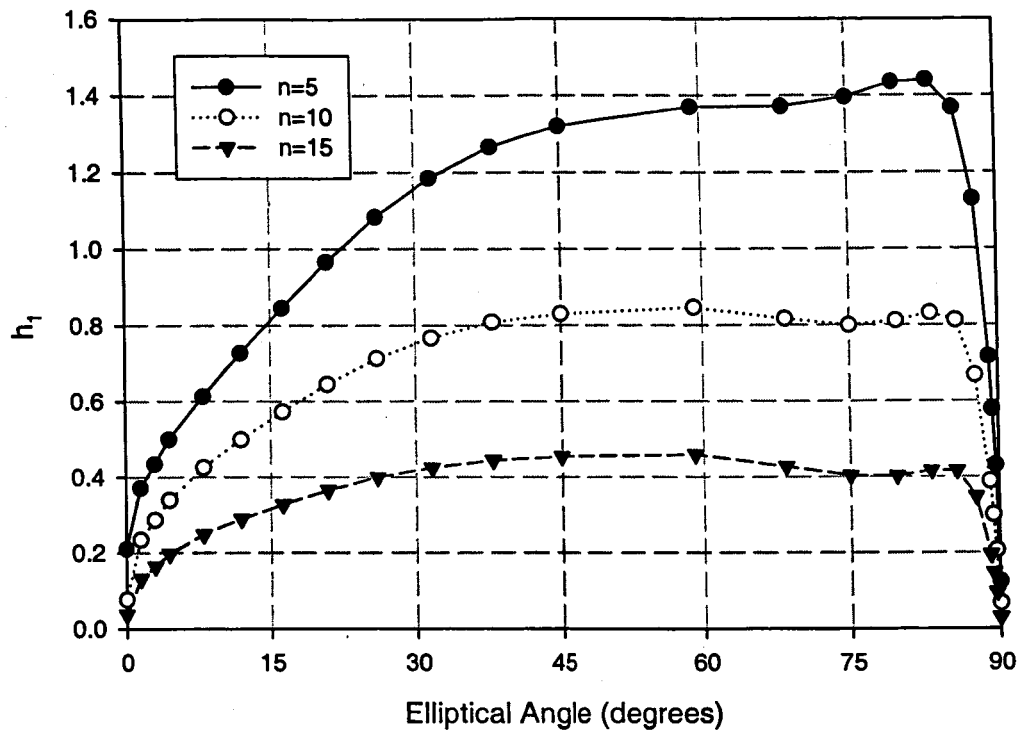


Figure A1.5. Variation of h_1 with elliptical angle for CC01 subjected to bending, $a/t=0.5$, $a/c=0.2$.

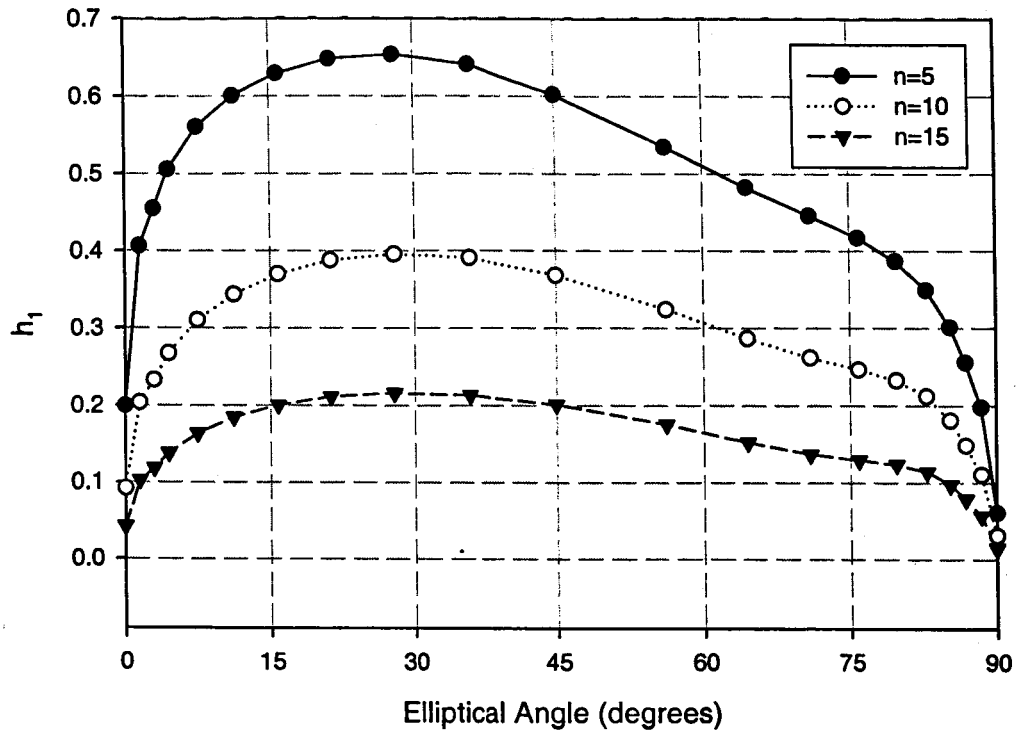


Figure A1.6. Variation of h_1 with elliptical angle for CC01 subjected to bending, $a/t=0.5$, $a/c=0.6$.

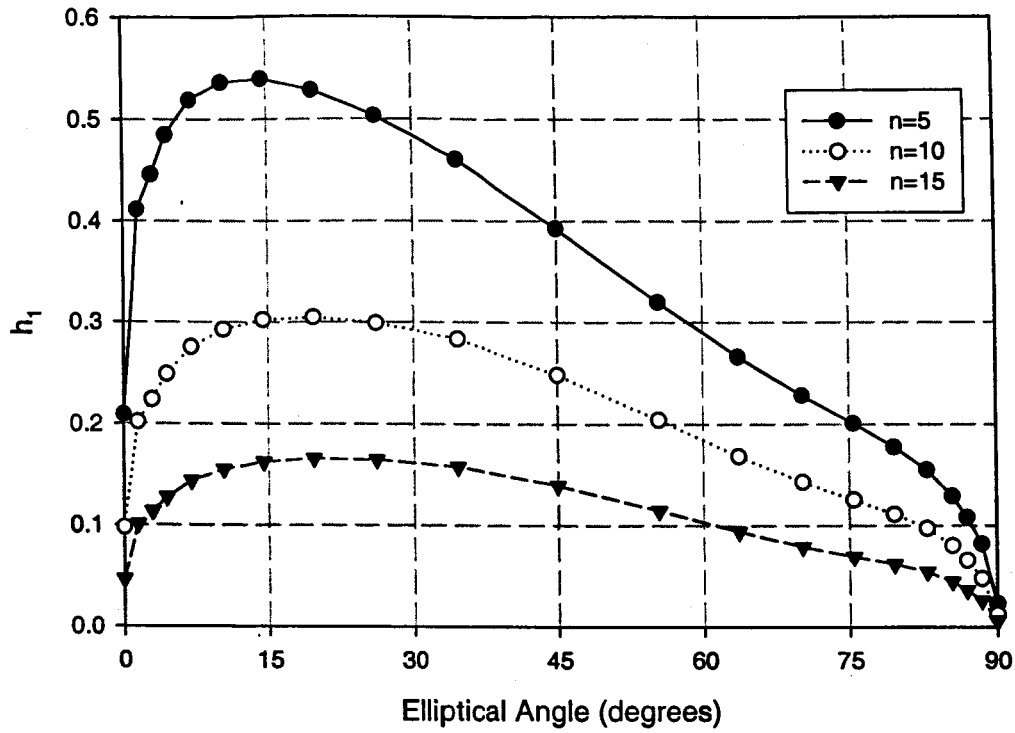


Figure A1.7. Variation of h_1 with elliptical angle for CC01 subjected to bending, $a/t=0.5$, $a/c=1.0$.

FEA for EC01/EC02 (Tension) Models

In the case of the EC01/EC02 finite element model, the crack front is contained within the plate and there is no intersection of the crack front with a free surface. Figure A1.8 is a schematic of the embedded crack geometry.

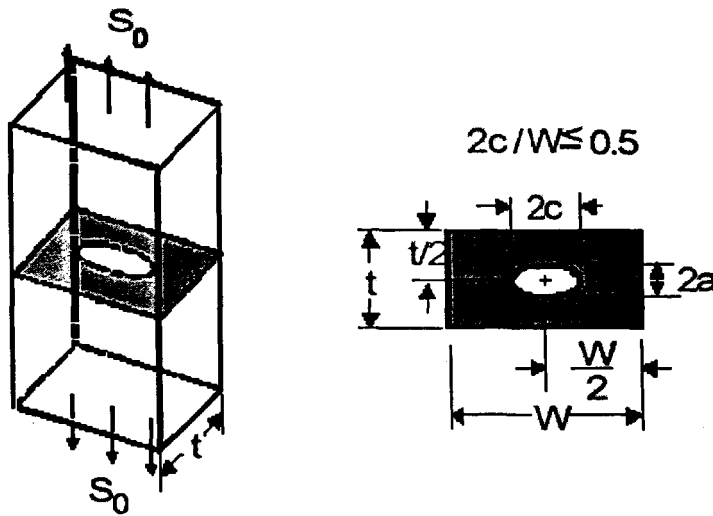


Figure A1.8. EC02 crack model.

Symmetry allowed the geometry to be reduced to one eighth its size in the finite element modeling. In the FEA modeling, the ratios $b/c=4$ and $c/h=0.25$ were held constant for all the analyses, where $b=w/2$. As for the CC01 modeling, 20-noded brick elements with reduced integration were used with a focused ring of elements around the crack front and crack tip elements that approximated the $r^{-\frac{n}{n+1}}$ strain singularity at the tip.

After the convergence load was determined following similar procedures to those for the CC01 modeling, a second FEA was performed to determine J_e at this load value. The value of h_I was then calculated as

$$h_I = \frac{J - J_e}{\alpha \sigma_o \epsilon_o \frac{t}{2} \left(\frac{P}{P_o^*} \right)^{n+1}} \quad (\text{A.3})$$

The computed values of h_I as a function of elliptical angle are shown graphically in Figures A1.9 through A1.14.

Embedded Crack ($a/c = 0.2$, $a/t = 0.2$)

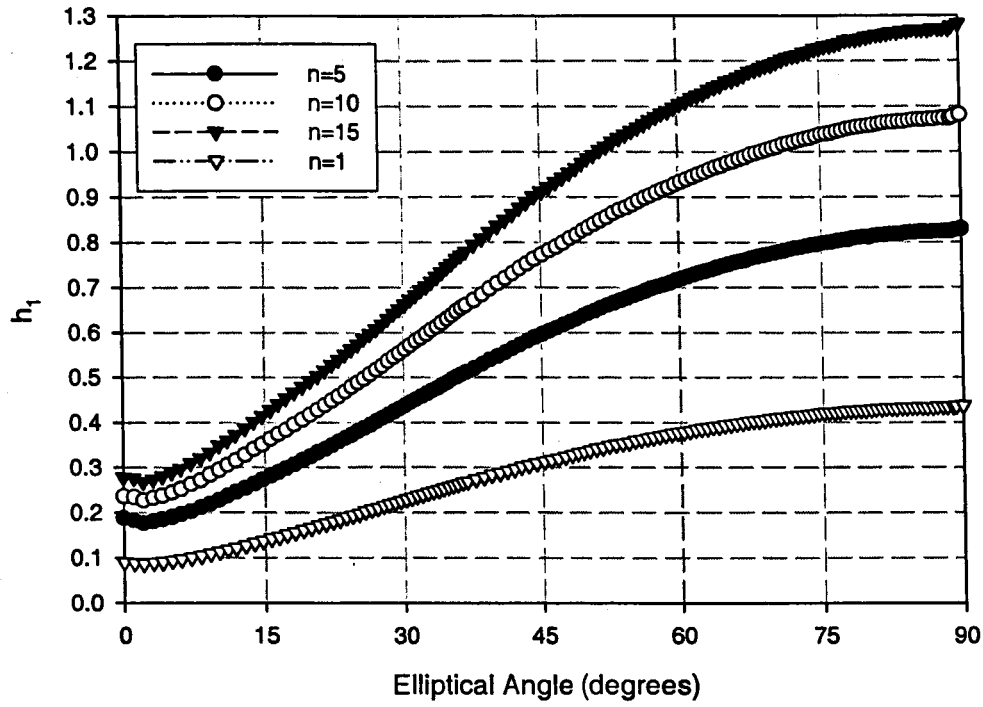


Figure A1.9. Variation of h_1 with elliptical angle for EC01 subjected to tension, $a/t=0.2$, $a/c=0.2$.

Embedded Crack ($a/c = 0.2$, $a/t = 0.5$)

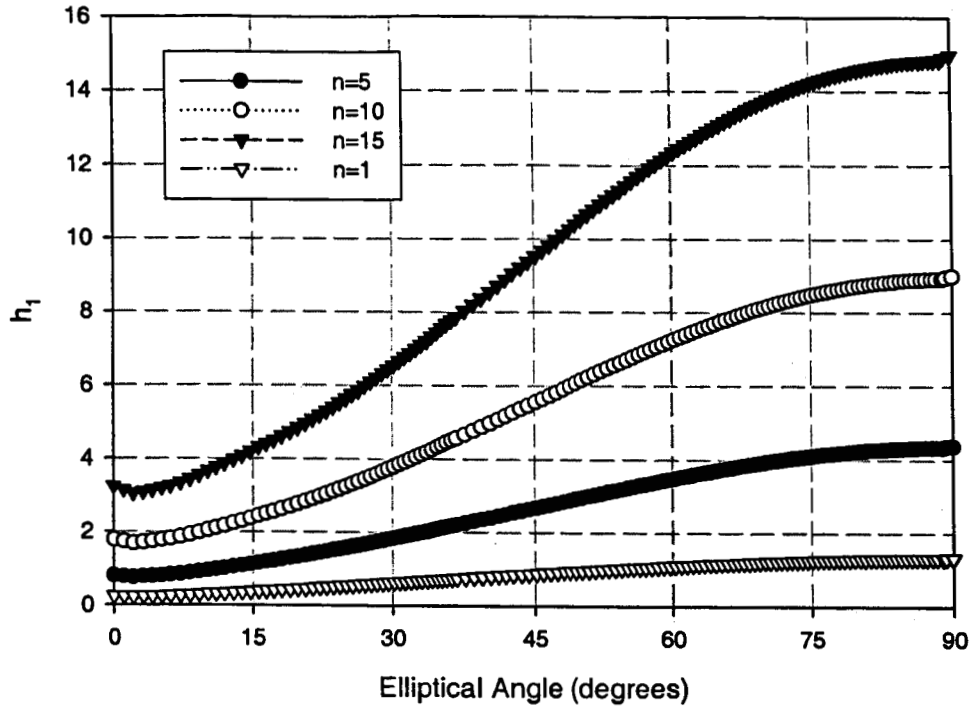


Figure A1.10. Variation of h_1 with elliptical angle for EC01 subjected to tension, $a/t=0.5$, $a/c=0.2$.

Embedded Crack ($a/c = 0.6$, $a/t = 0.2$)

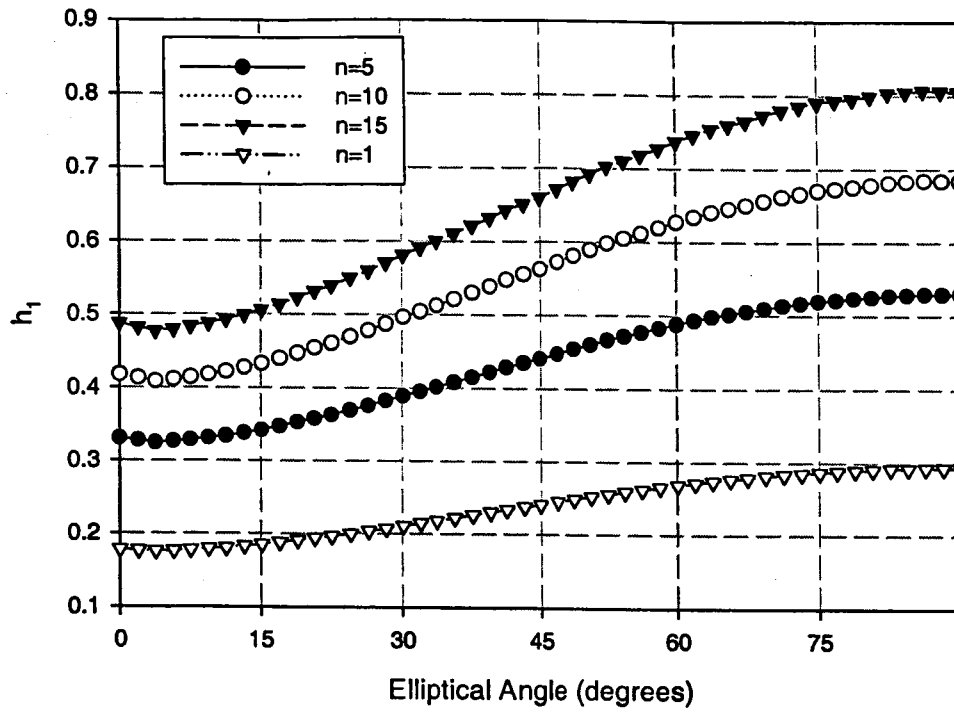


Figure A1.11. Variation of h_1 with elliptical angle for EC01 subjected to tension, $a/t=0.2$, $a/c=0.6$.

Embedded Crack ($a/c = 0.6$, $a/t = 0.5$)

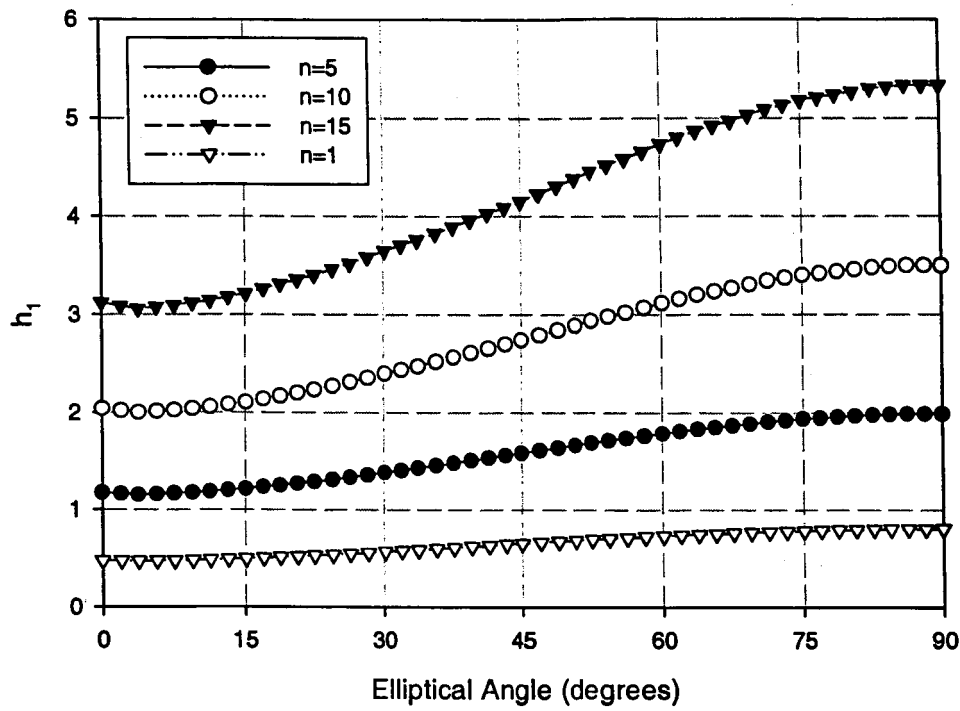


Figure A1.12. Variation of h_j with elliptical angle for EC01 subjected to tension, $a/t=0.5$, $a/c=0.6$.

Embedded Crack ($a/c = 1.0$, $a/t = 0.2$)

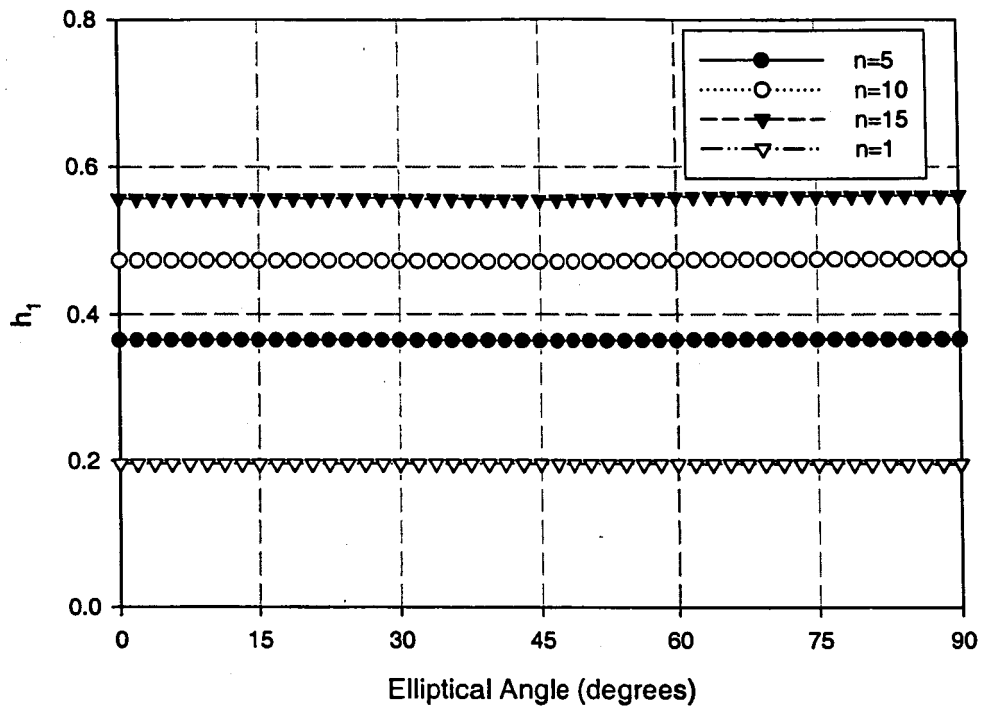


Figure A1.13. Variation of h_1 with elliptical angle for EC01 subjected to tension, $a/t=0.2$, $a/c=1.0$.

Embedded Crack ($a/c = 1.0$, $a/t = 0.5$)

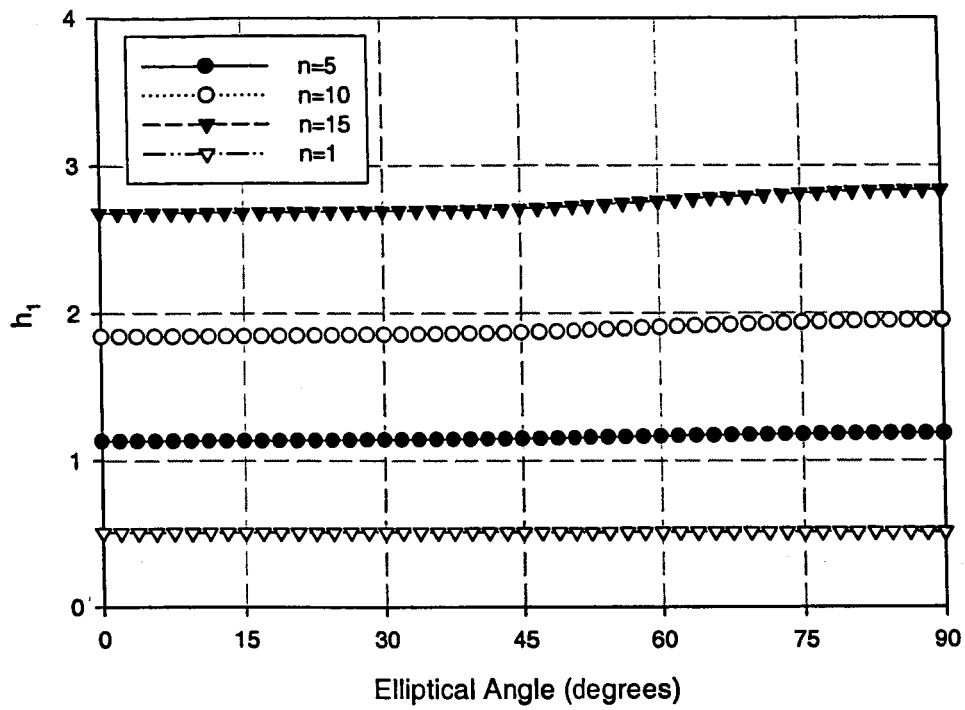


Figure A1.14. Variation of h_I with elliptical angle for EC01 subjected to tension, $a/t=0.5$, $a/c=1.0$.

APPENDIX 2: EXAMPLE INPUT DATA

This Appendix contains ten tables listing the data necessary to interactively input data to create the ten example files, Exam1.inp through Exam10.inp, contained on the distribution CD. The corresponding output files, Exam1.out through Exam10.out, respectively, are also contained on the distribution CD. Hard copies of the ten input and output files are given in Appendix 3.

EXAMPLE 1: ELASTIC-PLASTIC J COMPUTATION

Session Data			
<i>Parameter</i>	<i>Value</i>	<i>Unit</i>	<i>Description</i>
Option	5		elastic-plastic J computation
Type of Session	1		interactive input while creating a batch file
Input File Name	Example1.inp		batch file to be created
Output File Name	Example1.out		output file for printed results
Type of units	1		U.S. customary units
Crack Geometry			
<i>Parameter</i>	<i>Value</i>	<i>Unit</i>	<i>Description</i>
Model Type	SC		surface crack
Crack Type	4		axial crack in cylinder subject to arbitrary hoop stressing
Thickness	0.25	inches	cylinder thickness
Diameter	6	inches	outer diameter of cylinder
Crack location	i		internal crack
Material: Tensile Properties			
<i>Parameter</i>	<i>Value</i>	<i>Unit</i>	<i>Description</i>
Elastic Modulus	30000	ksi	Young's modulus
Poisson's Ratio	0.3		elastic Poisson ratio
Alpha	1		coefficient in Ramberg-Osgood equation
Sigma0	100	ksi	yield stress in Ramberg-Osgood equation
N	10		exponent in Ramberg-Osgood equation
Yield Stress	100	ksi	material 0.2% yield stress
Ultimate Stress	150	ksi	ultimate strength

Applied Loading			
<i>Parameter</i>	<i>Value</i>	<i>Unit</i>	<i>Description</i>
Loading Condition	2		primary and secondary Load
Number of Stresses	1		number of stress distributions to be specified
<i>Primary Load</i>			
Specify Unit Pressure?	Y		primary load will be specified as internal pressure
Pressure	10	ksi	internal pressure
<i>Secondary Load</i>			
X/t	0		normalized distance
Stress	80	ksi	stress value
X/t	0.25		normalized distance
Stress	60	ksi	stress value
X/t	0.5		normalized distance
Stress	30	ksi	stress value
X/t	0.75		normalized distance
Stress	0	ksi	stress value
X/t	1		normalized distance
Stress	-40	ksi	stress value
X/t	-1		End Input
Crack Sizes			
<i>Parameter</i>	<i>Value</i>	<i>Unit</i>	<i>Description</i>
Interactively Input?	1		manually specify crack sizes
A	0.05	inches	crack depth
C	0.05	inches	half crack surface length
A	0.05	inches	crack depth
C	0.1	inches	half crack surface length
A	0.05	inches	crack depth
C	0.15	inches	half crack surface length
A	0.1	inches	crack depth
C	0.1	inches	half crack surface length
A	0.1	inches	crack depth
C	0.15	inches	half crack surface length
A	0.15	inches	crack depth
C	0.15	inches	half crack surface length
A	-1		End Input
Post Analysis Data			
Print	P		print results to output file
Master Menu?	0		return to master menu
Quit?	1		quit and save batch files
Option	0		Terminate Session

EXAMPLE 2: ELASTIC-PLASTIC FAILURE ANALYSIS: CRITICAL CRACK

Session Data			
<i>Parameter</i>	<i>Value</i>	<i>Unit</i>	<i>Description</i>
Option	6		elastic-plastic failure analysis
Type of Session	1		interactive input while creating a batch file
Input File Name	Example2.inp		batch file to be created
Output File Name	Example2.out		output file for printed results
Type of units	1		U.S. customary units
Crack Geometry			
<i>Parameter</i>	<i>Value</i>	<i>Unit</i>	<i>Description</i>
Model Type	SC		Surface crack
Crack Type	2		crack in finite width plate subject to arbitrary stressing
Thickness	1	inches	plate thickness
Width	5	inches	plate width
Material: Tensile Properties			
<i>Parameter</i>	<i>Value</i>	<i>Unit</i>	<i>Description</i>
Elastic Modulus	30000	ksi	Young's modulus
Poisson's Ratio	0.3		elastic Poisson ratio
Alpha	1		coefficient in Ramberg-Osgood equation
Sigma0	100	ksi	yield stress in Ramberg-Osgood equation
n	10		exponent in Ramberg-Osgood Equation
Yield Stress	100	ksi	material 0.2% Yield Stress
Ultimate Stress	200	ksi	ultimate strength
Crack Shape			
<i>Parameter</i>	<i>Value</i>	<i>Unit</i>	<i>Description</i>
Constant Aspect Ratio?	1		crack has constant aspect ratio as opposed to constant surface length
Apect Ratio	0.35		value of a/c

Analysis Type			
Parameter	Value	Unit	Description
Critical Crack	1		perform critical crack calculation as opposed to critical load
Ductile	2		Perform ductile analysis as opposed to brittle analysis
Material Toughness Properties			
Parameter	Value	Unit	Description
Toughness, J_{mat}	0.25	ksi-inch	Toughness expressed in terms of the J-integral
Resistance Curve	1		The J-R curve is expressed as a quadratic form in the tear length
Dj0	0.245	ksi-inch	First coefficient of quadratic equation for J_R
Dj1	30	ksi	Coefficient of linear J-R term
Dj2	-50	ksi inch ⁻¹	Coefficient of quadratic J-R term
da _{max}	0.3	inches	Saturation tear length, the value of J_R is constant for tear lengths that exceed this value
Applied Loading			
Parameter	Value	Unit	Description
Interactively input load?	1		The loads will be specified manually
Loading Condition	2		Primary and Secondary Load
Number of Stresses	1		Number of Stress Distributions to be Specified
Primary Load			
x/t	0		Normalized Distance
Stress	120	ksi	Stress Value
x/t	1		Normalized Distance
Stress	120	ksi	Stress Value
x/t	-1		End Input
Secondary Load			
x/t	0		Normalized Distance
Stress	100	ksi	Stress Value
x/t	1		Normalized Distance
Stress	50	ksi	Stress Value
x/t	-1		End Input

<i>Primary Load Factor</i>			
Load factor	1		The load will be factored by this quantity
Session Data			
stop	0		End Input Data
Post Analysis Data			
Print	P		Print Results to Output File
Master Menu?	0		Return to Master Menu
Quit?	1		Quit and Save Batch Files
Option	0		Terminate Session

EXAMPLE 3: ELASTIC-PLASTIC FAILURE ANALYSIS: CRITICAL LOAD

Session Data			
<i>Parameter</i>	<i>Value</i>	<i>Unit</i>	<i>Description</i>
Option	6		elastic-plastic failure analysis
Type of Session	1		interactive input while creating a batch file
Input File Name	Example3.inp		batch file to be created
Output File Name	Example3.out		output file for printed results
Type of units	2		Metric units
Crack Geometry			
<i>Parameter</i>	<i>Value</i>	<i>Unit</i>	<i>Description</i>
Model Type	EC		embedded crack
Crack Type	2		crack in finite width plate subject to arbitrary stressing
Thickness	0.05	meters	plate thickness
Width	0.15	meters	plate width
Material: Tensile Properties			
<i>Parameter</i>	<i>Value</i>	<i>Unit</i>	<i>Description</i>
Elastic Modulus	210000	MPa	Young's modulus
Poisson's Ratio	0.3		elastic Poisson ratio
Alpha	1.5		coefficient in Ramberg-Osgood equation
Sigma0	400	MPa	yield stress in Ramberg-Osgood equation
n	15		exponent in Ramberg-Osgood Equation
Yield Stress	400	Mpa	material 0.2% Yield Stress
Ultimate Stress	600	MPa	ultimate strength
Crack Shape			
<i>Parameter</i>	<i>Value</i>	<i>Unit</i>	<i>Description</i>
Constant Aspect Ratio?	1		crack has constant aspect ratio as opposed to constant surface length
Apect Ratio	0.25		value of a/c

Analysis Type			
Parameter	Value	Unit	Description
Critical Loads	2		perform critical load calculation as opposed to critical crack
Ductile	2		Perform ductile analysis as opposed to brittle analysis
Material Toughness Properties			
<i>Parameter</i>	<i>Value</i>	<i>Unit</i>	<i>Description</i>
Toughness, J_{mat}	0.05	MPa-meter	Toughness expressed in terms of the J-integral
Resistance Curve	2		The J-R curve is expressed as the tear length raised to a power
Dj1	5.0	MPa-meter	coefficient of power law equation for J_R
Dj2	0.5	MPa	exponent of power law for J-R term
da_{max}	0.004	meters	Saturation tear length, the value of J_R is constant for tear lengths that exceed this value
Loading Condition			
<i>Parameter</i>	<i>Value</i>	<i>Unit</i>	<i>Description</i>
Loading Condition	0		Primary load only
Number of Stresses	1		Number of Stress Distributions to be Specified
x/t	0		Normalized Distance
Stress	400	MPa	Stress Value
x/t	1		Normalized Distance
Stress	400	MPa	Stress Value
x/t	-1		End Input
Crack Sizes			
<i>Parameter</i>	<i>Value</i>	<i>Unit</i>	<i>Description</i>
Interactively Input?	1		manually specify crack sizes
A	0.003	meters	crack depth
A	0.004	meters	half crack surface length
A	0.005	meters	crack depth
a	-1		End input
Session Data			
stop	0		End Input Data

Post Analysis Data			
Print	P		Print Results to Output File
Master Menu?	0		Return to Master Menu
Quit?	1		Quit and Save Batch Files
Option	0		Terminate Session

EXAMPLE 4: ELASTIC-PLASTIC FATIGUE LIFE ANALYSIS

Session Data			
<i>Parameter</i>	<i>Value</i>	<i>Unit</i>	<i>Description</i>
Option	7		elastic-plastic failure analysis
Type of Session	1		interactive input while creating a batch file
Input File Name	Example4.inp		batch file to be created
Output File Name	Example4.out		output file for printed results
Type of units	1		U.S. customary units
Crack Geometry			
<i>Parameter</i>	<i>Value</i>	<i>Unit</i>	<i>Description</i>
Model Type	CC		Corner crack
Crack Type	1		crack in finite width plate
Tension	1		Tension as opposed to bending
Thickness	2	inches	plate thickness
Width	2	inches	plate width
Material: Tensile Properties			
<i>Parameter</i>	<i>Value</i>	<i>Unit</i>	<i>Description</i>
Elastic Modulus	30000	ksi	Young's modulus
Poisson's Ratio	0.3		elastic Poisson ratio
Alpha	1		coefficient in Ramberg-Osgood equation
Sigma0	100	ksi	yield stress in Ramberg-Osgood equation
n	10		exponent in Ramberg-Osgood Equation
Yield Stress	100	ksi	material 0.2% Yield Stress
Ultimate Stress	300	ksi	ultimate strength
Service Load Spectrum (Schedule)			
<i>Block Case Definition: Case #1: Maximum Load Data</i>			
Maximum Load Type	2		Primary and Secondary load
<i>Primary Maximum Load</i>			
Tensile stress	80	ksi	Primary tensile stress at maximum load

<i>Secondary Maximum Load</i>			
x/t	0		Normalized Distance
Stress	50	ksi	Stress Value
x/t	1		Normalized Distance
Stress	50	ksi	Stress Value
x/t	-1		End Input
<i>Block Case Definition: Case #1: Minimum Load Data</i>			
Minimum Load Type	2		Primary and Secondary load
<i>Primary Minimum Load</i>			
Tensile stress	0	ksi	Primary tensile stress at maximum load
<i>Secondary Minimum Load</i>			
x/t	0		Normalized Distance
Stress	50	ksi	Stress Value
x/t	1		Normalized Distance
Stress	50	ksi	Stress Value
x/t	-1		End Input
<i>Cycles</i>			
Number of cycles	2		Number of times maximum and minimum loads for Case # 1 are applied
<i>Block Case Definition: Case #2: Maximum Load</i>			
Maximum Load Type	2		Primary and Secondary load
<i>Primary Maximum Load</i>			
Tensile stress	50	ksi	Primary tensile stress at maximum load
<i>Secondary Maximum Load</i>			
x/t	0		Normalized Distance
Stress	50	ksi	Stress Value
x/t	1		Normalized Distance
Stress	50	ksi	Stress Value
x/t	-1		End Input
<i>Block Case Definition: Case #2: Maximum Load</i>			
Minimum Load Type	2		Primary and Secondary load
<i>Primary Minimum Load</i>			
Tensile stress	0	ksi	Primary tensile stress at maximum load

<i>Secondary Minimum Load</i>			
x/t	0		Normalized Distance
Stress	50	ksi	Stress Value
x/t	1		Normalized Distance
Stress	50	ksi	Stress Value
x/t	-1		End Input
<i>Cycles</i>			
Number of cycles	1		Number of times maximum and minimum loads for Case # 2 are applied
<i>Block Case Definition: Case #3: Maximum Load</i>			
Maximum Load Type	-1		Terminate Block Case Input
<i>Load Spectrum (Schedule)</i>			
Block Case #	1		Block Case number or ID
Times applied	2		Number of times Block Case 1 is applied
Block Case #	2		Block Case number or ID
Times applied	1		Number of times Block Case 2 is applied
Block Case #	-1		End load spectrum input
<i>Material Properties</i>			
<i>Parameter</i>	<i>Value</i>	<i>Unit</i>	<i>Description</i>
Toughness, J_{mat}	0.5	ksi-inch	Toughness expressed in terms of the J-integral
Fatigue coefficient	$1e^{-9}$	Chosen so crack growth rate is in inches/cycle	Coefficient in Paris equation
Fatigue exponent	4		Exponent in Paris equation
U_0	1		Crack closure term appropriate to Paris equation test data
Alp (a-tip)	1		Constraint factor for a-tip (used in crack closure evaluation)
Alp (c-tip)	1		Constraint factor for c-tip (used in crack closure evaluation)
<i>Initial Crack Size</i>			
<i>Parameter</i>	<i>Value</i>	<i>Unit</i>	<i>Description</i>
a	0.05	inches	Crack depth at a-tip
c	0.1	inches	Crack depth at c-tip

Schedule and Print Data			
Maximum number of schedules	100		The fatigue calculations will terminate after the load schedule has been applied this number of times if failure has not occurred first
Print interval	10		Results will be printed to the output file after the schedule has been applied this number of times
Post Analysis Data			
Print	P		Print Results to Output File
Master Menu?	0		Return to Master Menu
Quit?	1		Quit and Save Batch Files
Option	0		Terminate Session

**EXAMPLE 5: PROOF TEST PROCEDURE: PRE-PROOF TEST ANALYSIS:
CRITICAL CRACK**

Session Data			
<i>Parameter</i>	<i>Value</i>	<i>Unit</i>	<i>Description</i>
Option	8		elastic-plastic failure analysis
Type of Session	1		interactive input while creating a batch file
Input File Name	Example5.inp		batch file to be created
Output File Name	Example5.out		output file for printed results
Type of units	1		U.S. customary units
Proof Test Analysis Type	1		Perform Pre-Proof Test Safe Life Analysis as opposed to Proof Test Analysis
Pre-Proof Analysis Type	1		Perform Critical Flaw Size calculation as opposed to Fatigue Life calculation.
Crack Geometry			
<i>Parameter</i>	<i>Value</i>	<i>Unit</i>	<i>Description</i>
Model Type	SC		Surface crack
Crack Type	2		crack in finite width plate subject to arbitrary stressing
Thickness	1	inches	plate thickness
Width	5	inches	plate width
Material: Tensile Properties			
<i>Parameter</i>	<i>Value</i>	<i>Unit</i>	<i>Description</i>
Elastic Modulus	30000	ksi	Young's modulus
Poisson's Ratio	0.3		elastic Poisson ratio
Alpha	1		coefficient in Ramberg-Osgood equation
Sigma0	100	ksi	yield stress in Ramberg-Osgood equation
n	10		exponent in Ramberg-Osgood Equation
Yield Stress	100	ksi	material 0.2% Yield Stress
Ultimate Stress	300	ksi	ultimate strength

Crack Shape			
<i>Parameter</i>	<i>Value</i>	<i>Unit</i>	<i>Description</i>
Constant Aspect Ratio?	1		crack has constant aspect ratio as opposed to constant surface length
Apect Ratio	0.6		value of a/c
Analysis Type			
<i>Parameter</i>	<i>Value</i>	<i>Unit</i>	<i>Description</i>
Ductile	2		Perform ductile analysis as opposed to brittle analysis
Material Toughness Properties			
<i>Parameter</i>	<i>Value</i>	<i>Unit</i>	<i>Description</i>
Toughness, J_{mat}	0.25	ksi-inch	Toughness expressed in terms of the J-integral
Resistance Curve	1		The J-R curve is expressed as a quadratic form in the tear length
Dj0	0.245	ksi-inch	First coefficient of quadratic equation for J_R
Dj1	30	ksi	Coefficient of linear J-R term
Dj2	-50	ksi inch ⁻¹	Coefficient of quadratic J-R term
da _{max}	0.3	inches	Saturation tear length, the value of J_R is constant for tear lengths that exceed this value
Applied Service Loading			
<i>Parameter</i>	<i>Value</i>	<i>Unit</i>	<i>Description</i>
Manually input load?	1		The loads will be specified manually
Loading Condition	2		Primary and Secondary Load
Primary Service Load			
x/t	0		Normalized Distance
Stress	110	ksi	Stress Value
x/t	1		Normalized Distance
Stress	120	ksi	Stress Value
x/t	-1		End Input
Secondary Service Load			
x/t	0		Normalized Distance
Stress	100	ksi	Stress Value
x/t	1		Normalized Distance
Stress	50	ksi	Stress Value
x/t	-1		End Input

<i>Primary Load Factor</i>			
Service Load factor	1		The service primary load will be factored by this quantity
Post Analysis Data			
Print	P		Print Results to Output File
Master Menu?	0		Return to Master Menu
Quit?	1		Quit and Save Batch Files
Option	0		Terminate Session

EXAMPLE 6: PROOF TEST PROCEDURE: FLAW SCREENING

Session Data			
<i>Parameter</i>	<i>Value</i>	<i>Unit</i>	<i>Description</i>
Option	8		elastic-plastic failure analysis
Type of Session	1		interactive input while creating a batch file
Input File Name	Example6.inp		batch file to be created
Output File Name	Example6.out		output file for printed results
Type of units	2		Metric units
Proof Test Analysis Type	2		Perform Proof Test Analysis as opposed to Pre-Proof Test Safe Life Analysis
Flaw Screening	2		Perform Flaw Screening Analysis as opposed to Proof Load Analysis or Final Crack Size Analysis
Crack Geometry			
<i>Parameter</i>	<i>Value</i>	<i>Unit</i>	<i>Description</i>
Model Type	SC		Surface crack
Crack Type	4		crack in cylinder subject to arbitrary hoop stressing
Thickness	0.084	meters	cylinder thickness
Diameter	1.183	meters	Outer diameter of cylinder
External	e		Crack is on the outside of the cylinder
Material: Tensile Properties			
<i>Parameter</i>	<i>Value</i>	<i>Unit</i>	<i>Description</i>
Elastic Modulus	210000	MPa	Young's modulus
Poisson's Ratio	0.3		elastic Poisson ratio
Alpha	1.677		coefficient in Ramberg-Osgood equation
Sigma0	556	MPa	yield stress in Ramberg-Osgood equation
n	17.7		exponent in Ramberg-Osgood Equation
Yield Stress	556	MPa	material 0.2% Yield Stress
Ultimate Stress	900	MPa	ultimate strength

Crack Shape			
<i>Parameter</i>	<i>Value</i>	<i>Unit</i>	<i>Description</i>
Apect Ratio	0.61		value of a/c
Analysis Type			
<i>Parameter</i>	<i>Value</i>	<i>Unit</i>	<i>Description</i>
Ductile	2		Perform ductile analysis as opposed to brittle analysis
Material Toughness Properties			
<i>Parameter</i>	<i>Value</i>	<i>Unit</i>	<i>Description</i>
Toughness, J_{mat}	0.433	MPa-meter	Toughness expressed in terms of the J-integral
Resistance Curve	1		The J-R curve is expressed as a quadratic form in the tear length
Dj0	0.361	MPa-meter	First coefficient of quadratic equation for J_R
Dj1	503.3	MPa	Coefficient of linear J-R term
Dj2	-2325	MPa meter ⁻¹	Coefficient of quadratic J-R term
da_{max}	0.005	meter	Saturation tear length, the value of J_R is constant for tear lengths that exceed this value
Applied Proof Loading			
<i>Parameter</i>	<i>Value</i>	<i>Unit</i>	<i>Description</i>
Manually input load?	1		The loads will be specified manually
Loading Condition	1		Primary Load
Primary Load			
Specify Unit Pressure?	Y		primary load will be specified as internal pressure
Pressure	80.45	MPa	internal pressure
Proof Load Factor	1		The proof load is scaled by this factor
Post Analysis Data			
Print	P		Print Results to Output File
Master Menu?	0		Return to Master Menu
Quit?	1		Quit and Save Batch Files
Option	0		Terminate Session

EXAMPLE 7: PROOF TEST PROCEDURE: PROOF LOAD

Session Data			
<i>Parameter</i>	<i>Value</i>	<i>Unit</i>	<i>Description</i>
Option	8		elastic-plastic failure analysis
Type of Session	1		interactive input while creating a batch file
Input File Name	Example7.inp		batch file to be created
Output File Name	Example7.out		output file for printed results
Type of units	1		U.S. Customary units
Proof Test Analysis Type	2		Perform Proof Test Analysis as opposed to Pre-Proof Test Safe Life Analysis
Proof Load	1		Perform Proof Load Analysis as opposed to Flaw Screening Analysis or Final Crack Size Analysis
Crack Geometry			
<i>Parameter</i>	<i>Value</i>	<i>Unit</i>	<i>Description</i>
Model Type	EC		Embedded crack
Crack Type	2		Embedded crack in plate subject to arbitrary stressing
Thickness	0.5	inches	plate thickness
Width	6	meters	Plate width
Material: Tensile Properties			
<i>Parameter</i>	<i>Value</i>	<i>Unit</i>	<i>Description</i>
Elastic Modulus	30000	ksi	Young's modulus
Poisson's Ratio	0.3		elastic Poisson ratio
Alpha	1		coefficient in Ramberg-Osgood equation
Sigma0	80	ksi	yield stress in Ramberg-Osgood equation
n	25		exponent in Ramberg-Osgood Equation
Yield Stress	80	ksi	material 0.2% Yield Stress
Ultimate Stress	120	ksi	ultimate strength
Crack Shape			
<i>Parameter</i>	<i>Value</i>	<i>Unit</i>	<i>Description</i>
Apect Ratio	0.25		value of a/c

Analysis Type			
Parameter	Value	Unit	Description
Ductile	2		Perform ductile analysis as opposed to brittle analysis
Material Toughness Properties			
Parameter	Value	Unit	Description
Toughness, J_{mat}	0.2	ksi-inch	Toughness expressed in terms of the J-integral
Resistance Curve	2		The J-R curve is expressed as the tear length raised to a power
Dj1	5	Ksi-inch ^{1-DJ2}	Coefficient of linear J-R term
Dj2	0.5		Coefficient of quadratic J-R term
da _{max}	0.1	inches	Saturation tear length, the value of J_R is constant for tear lengths that exceed this value
Applied Proof Loading			
Parameter	Value	Unit	Description
Loading Condition	1		Primary and Secondary Loads present during proof testing
Primary Proof Load			
X/t	0		Normalized distance
stress	60	Ksi	Stress value
X/t	0.2		Normalized distance
stress	55	Ksi	Stress value
X/t	0.4		Normalized distance
stress	52	Ksi	Stress value
X/t	0.6		Normalized distance
stress	50	Ksi	Stress value
X/t	0.8		Normalized distance
stress	49	Ksi	Stress value
X/t	1		Normalized distance
stress	47	Ksi	Stress value
X/t	-1		End input
Secondary Proof Load			
X/t	0		Normalized distance
stress	90	ksi	Stress value
X/t	1		Normalized distance
stress	0	ksi	Stress value
X/t	-1		End input

Crack Sizes			
Interactively input?	1		Manually input initial crack sizes
Crack size, a	0.025	inches	Half length of crack at a-tip
Crack size, a	0.03	inches	Half length of crack at a-tip
Crack size, a	0.035	inches	Half length of crack at a-tip
Crack size, a	0.04	inches	Half length of crack at a-tip
Crack size, a	0.045	inches	Half length of crack at a-tip
Crack size, a	0.05	inches	Half length of crack at a-tip
Crack size, a	-1		End input
Post Analysis Data			
Print	P		Print Results to Output File
Master Menu?	0		Return to Master Menu
Quit?	1		Quit and Save Batch Files
Option	0		Terminate Session

EXAMPLE 8: PROOF TEST PROCEDURE: FINAL CRACK SIZE

Session Data			
<i>Parameter</i>	<i>Value</i>	<i>Unit</i>	<i>Description</i>
Option	8		elastic-plastic failure analysis
Type of Session	1		interactive input while creating a batch file
Input File Name	Example8.inp		batch file to be created
Output File Name	Example8.out		output file for printed results
Type of units	1		U.S. Customaryc units
Proof Test Analysis Type	3		Perform Proof Test Analysis as opposed to Pre-Proof Test Safe Life Analysis
Final Crack Size	3		Perform Final Crack Size Analysis as opposed to Proof Load Analysis or Flaw Screening Analysis
Crack Geometry			
<i>Parameter</i>	<i>Value</i>	<i>Unit</i>	<i>Description</i>
Model Type	CC		Surface crack
Crack Type	1		Corner crack in plate
Bending	2		Bending in the thickness direction as opposed to tension
Thickness	2	inches	plate thickness
Width	2	inches	Plate width
Material: Tensile Properties			
<i>Parameter</i>	<i>Value</i>	<i>Unit</i>	<i>Description</i>
Elastic Modulus	30000	ksi	Young's modulus
Poisson's Ratio	0.3		elastic Poisson ratio
Alpha	1.2		coefficient in Ramberg-Osgood equation
Sigma0	150	ksi	yield stress in Ramberg-Osgood equation
n	20		exponent in Ramberg-Osgood Equation
Yield Stress	150	MPa	material 0.2% Yield Stress
Ultimate Stress	200	MPa	ultimate strength

Crack Shape			
<i>Parameter</i>	<i>Value</i>	<i>Unit</i>	<i>Description</i>
Crack depth, a	0.5	inches	Initial crack depth at the a-tip
Aspect ratio	1		Initial aspect ratio, a/c
Proof Load			
Secondary proof load?	0		No secondary stress is present during the proof test
Bending stress	220	ksi	Primary proof load
Material Toughness Properties			
<i>Parameter</i>	<i>Value</i>	<i>Unit</i>	<i>Description</i>
Resistance Curve	1		The J-R curve is expressed as a quadratic form in the tear length
Dj0	0.145	Ksi-inch	First coefficient of quadratic equation for J _R
Dj1	30	ksi	Coefficient of linear J-R term
Dj2	-50	ksi inch ⁻¹	Coefficient of quadratic J-R term
da _{max}	0.3	inch	Saturation tear length, the value of J _R is constant for tear lengths that exceed this value
Toughness, J _{mat}	0.15	Ksi-inch	Toughness expressed in terms of the J-integral
Post Analysis Data			
Print	P		Print Results to Output File
Master Menu?	0		Return to Master Menu
Quit?	1		Quit and Save Batch Files
Option	0		Terminate Session

EXAMPLE 9: ELASTIC-PLASTIC TEAR-FATIGUE LIFE ANALYSIS

Session Data			
<i>Parameter</i>	<i>Value</i>	<i>Unit</i>	<i>Description</i>
Option	9		elastic-plastic failure analysis
Type of Session	1		interactive input while creating a batch file
Input File Name	Example9.inp		batch file to be created
Output File Name	Example9.out		output file for printed results
Type of units	1		U.S. customary units
Crack Geometry			
<i>Parameter</i>	<i>Value</i>	<i>Unit</i>	
Model Type	SC		Surface crack
Crack Type	4		Axial crack in cylinder
Thickness	0.5	inches	Thickness of cylinder
Diameter	40.	inches	Outer diameter of cylinder
Crack location	e		External crack
Material: Tensile Properties			
<i>Parameter</i>	<i>Value</i>	<i>Unit</i>	<i>Description</i>
Elastic Modulus	30000	ksi	Young's modulus
Poisson's Ratio	0.3		elastic Poisson ratio
Alpha	1		coefficient in Ramberg-Osgood equation
Sigma0	100	ksi	yield stress in Ramberg-Osgood equation
N	10		exponent in Ramberg-Osgood Equation
Yield Stress	100	ksi	material 0.2% Yield Stress
Ultimate Stress	150	ksi	ultimate strength
Crack Size			
Crack depth	0.25		Depth of surface crack
Aspect ratio	0.5		a/c value

Service Load History			
Cycles	100		Number of service cycles
Cyclic load type	1		Primary and Secondary load
<i>Primary Maximum Load</i>			
<i>(Note : Stress distributions are specified with respect to the <u>inner</u> surface of the cylinder for external cracks.)</i>			
Unit pressure?	n		Primary stress distribution is not identical to that due to internal pressure
x/t	0		Normalized Distance
Stress	90	ksi	Stress Value
x/t	1		Normalized Distance
Stress	80	ksi	Stress Value
x/t	-1		End Input
<i>Secondary maximum load</i>			
<i>(Note: Stress distributions are specified with respect to the <u>inner</u> surface of the cylinder for external cracks.)</i>			
x/t	0		Normalized Distance
Stress	-100	ksi	Stress Value
x/t	1		Normalized Distance
Stress	100	ksi	Stress Value
x/t	-1		End Input
<i>Primary Minimum Load</i>			
<i>(Note: Stress distributions are specified with respect to the <u>inner</u> surface of the cylinder for external cracks.)</i>			
Unit pressure?	n		Primary stress distribution is not identical to that due to internal pressure
x/t	0		Normalized distance
Stress	0	ksi	Stress Value
x/t	1		Normalized distance
Stress	0	ksi	Stress Value
x/t	-1		End Input
<i>Secondary minimum load</i>			
<i>(Note: Stress distributions are specified with respect to the <u>inner</u> surface of the cylinder for external cracks.)</i>			
x/t	0		Normalized Distance
Stress	-100	ksi	Stress Value
x/t	1		Normalized distance
stress	100	ksi	Stress value
x/t	-1		End Input

Material Properties			
Parameter	Value	Unit	Description
Resistance Curve	1		The J-R curve is expressed as a quadratic form in the tear length
Dj0	0.2	Ksi-inch	First coefficient of quadratic equation for J_R
Dj1	30	ksi	Coefficient of linear J-R term
Dj2	0	ksi inch ⁻¹	Coefficient of quadratic J-R term
da _{max}	0.2	inch	Saturation tear length, the value of J_R is constant for tear lengths that exceed this value
Toughness, J_{mat}	0.21	Ksi-inch	Toughness expressed in terms of the J-integral
U_0	1		Crack closure term appropriate to Paris equation test data
Alp (a-tip)	1		Constraint factor for a-tip (used in crack closure evaluation)
Alp (c-tip)	1		Constraint factor for c-tip (used in crack closure evaluation)
Fatigue coefficient	1e ⁻¹⁰	Chosen so crack growth rate is in inches/cycle	Coefficient in Paris equation
Fatigue exponent	4		Exponent in Paris equation
Post Analysis Data			
Print	P		Print Results to Output File
Master Menu?	0		Return to Master Menu
Quit?	1		Quit and Save Batch Files
Option	0		Terminate Session

EXAMPLE 10: MULTI-CYCLE PROOF TEST ANALYSIS

Session Data			
<i>Parameter</i>	<i>Value</i>	<i>Unit</i>	<i>Description</i>
Option	10		elastic-plastic failure analysis
Type of Session	1		interactive input while creating a batch file
Input File Name	Example10.inp		batch file to be created
Output File Name	Example10.out		output file for printed results
Type of units	1		U.S. customary units
Crack Geometry			
<i>Parameter</i>	<i>Value</i>	<i>Unit</i>	
Model Type	SC		Surface crack
Crack Type	2		Crack in plate
Thickness	1	inches	plate thickness
Width	10	inches	plate width
Material: Tensile Properties			
<i>Parameter</i>	<i>Value</i>	<i>Unit</i>	<i>Description</i>
Elastic Modulus	30000	ksi	Young's modulus
Poisson's Ratio	0.3		elastic Poisson ratio
Alpha	1		coefficient in Ramberg-Osgood equation
Sigma0	100	ksi	yield stress in Ramberg-Osgood equation
n	5		exponent in Ramberg-Osgood Equation
Yield Stress	100	ksi	material 0.2% Yield Stress
Ultimate Stress	200	ksi	ultimate strength
Crack Size			
Distribution constant	0.15		Constant in the crack size exponential distribution function
Aspect ratio	0.5		a/c value
Proof and Service Load Histories			
Proof cycles	4		Number of times proof load is applied
Cycles	50		Number of service cycles
Cyclic load type	0		Primary load only

<i>Primary Maximum Proof Load</i>			
x/t	0		Normalized Distance
Stress	120	ksi	Stress Value
x/t	1		Normalized Distance
Stress	120	ksi	Stress Value
x/t	-1		End Input
<i>Primary Minimum Proof Load</i>			
x/t	0		Normalized Distance
Stress	0	ksi	Stress Value
x/t	1		Normalized Distance
Stress	0	ksi	Stress Value
x/t	-1		End Input
<i>Service Load History (Schedule)</i>			
Number of load blocks	1		Number of load blocks that constitute the service load history
cycles	2		Number of cycles load block 1 is applied
Load type	0		Primary loads only, no secondary loads
<i>Maximum primary service load</i>			
x/t	0		Normalized distance
Stress	80	ksi	Stress Value
x/t	1		Normalized distance
Stress	80	ksi	Stress Value
x/t	-1		End Input
<i>Minimum primary service load</i>			
x/t	0		Normalized Distance
Stress	0	ksi	Stress Value
x/t	1		Normalized distance
stress	0	ksi	Stress value
x/t	-1		End Input

Material Properties			
<i>Parameter</i>	<i>Value</i>	<i>Unit</i>	<i>Description</i>
Resistance Curve	1		The J-R curve is expressed as a quadratic form in the tear length
Dj0	0.2	Ksi-inch	First coefficient of quadratic equation for J _R
Dj1	20	ksi	Coefficient of linear J-R term
Dj2	0	ksi inch ⁻¹	Coefficient of quadratic J-R term
da _{max}	0.2	inch	Saturation tear length, the value of J _R is constant for tear lengths that exceed this value
Toughness, J _{mat}	0.21	Ksi-inch	Toughness expressed in terms of the J-integral
U ₀	1		Crack closure term appropriate to Paris equation test data
Alp (a-tip)	1		Constraint factor for a-tip (used in crack closure evaluation)
Alp (c-tip)	1		Constraint factor for c-tip (used in crack closure evaluation)
Proof Fatigue coefficient	1e ⁻⁹	Chosen so crack growth rate is in inches/cycle	Coefficient in Paris equation applicable to proof test
Proof Fatigue exponent	4		Exponent in Paris equation applicable to proof test
Service fatigue	0		Service fatigue crack growth properties same as proof test properties
Service Fatigue coefficient	2e ⁻⁹	Chosen so crack growth rate is in inches/cycle	Coefficient in Paris equation applicable to proof test
Service Fatigue exponent	4		Exponent in Paris equation applicable to proof test
Post Analysis Data			
Print	P		Print Results to Output File
Master Menu?	0		Return to Master Menu
Quit?	1		Quit and Save Batch Files
Option	0		Terminate Session

APPENDIX 3: INPUT AND OUTPUT FILES FOR EXAMPLES 1 THROUGH 12

EXAMPLE 1

INPUT FILE: Exam1.inp

```
Exam1.out      Output file name*12
  1      1=US units; 2=SI units
sc      Crack Model Type
  4      Crack Model Number
0.250000E+00   T
0.600000E+01   Outer Diameter
i
0.3000E+05     Elastic Young's modulus
  0.300       Poisson's ratio
  1.000       Alpha
0.1000E+03     Sigma0
  10.000      n
  0.1000E+03 material yield stress
  0.1500E+03 material ultimate stress
  2 1: Primary, 2: Primary+Secondary
  1 # of Stress Dist
y      Internal Pressure (Y/N)
  10.00       Internal Pressure
  0.0000E+00 Non-Dimensional position
  0.8000E+02 Stress value
  0.2500E+00 Non-Dimensional position
  0.6000E+02 Stress value
  0.5000E+00 Non-Dimensional position
  0.3000E+02 Stress value
  0.7500E+00 Non-Dimensional position
  0.0000E+00 Stress value
  0.1000E+01 Non-Dimensional position
  -.4000E+02 Stress value
  -.1000E+01 Non-Dimensional position
  1      1=interactively input, 2=tabulate the data
0.0500E+00    a( 1)
0.0500E+00    c( 1)
0.0500E+00    a( 2)
0.1000E+00    c( 2)
0.0500E+00    a( 3)
0.1500E+00    c( 3)
0.1000E+00    a( 4)
0.1000E+00    c( 4)
0.1000E+00    a( 5)
0.1500E+00    c( 5)
0.1500E+00    a( 6)
0.1500E+00    c( 6)
-.1000E+01    a( 7)
P      P(1st col.): to print
  0      1:to resume, 0: stop
```

OUTPUT FILE: Exam1.out

ELASTIC-PLASTIC J CALCULATION FOR SC04

DATE: 18-SEP-03 TIME: 15:17:22
(computed: NASA/FLAGRO Version 3.00, October 1995.)
Elastic-Plastic Fracture Module (EPFM) V.x.xx, Aug. 2002
U.S. customary units [inches, ksi, ksi sqrt(in)]

Input Filename = exam1.inp
Output Filename = Exam1.out

Cylinder Thickness, t = 0.2500
Outer Diameter, D = 6.0000

Crack Type = INTERNAL

Material Yield Stress = 100.00

Material Ultimate Stress = 150.00

Data for the Nonlinear Material Behavior:

Sig0 = 0.1000E+03
E = 0.3000E+05
nu = 0.3000E+00
alpha = 0.1000E+01
n = 0.1000E+02

Internal Pressure 10.000

PRIMARY LOAD DISTRIBUTION 1:

Norm. x Stress
Stresses at 10 points

Distance x/t (from inner wall)	Stress due to Int. Pressure	Total Stress
0.0000	125.2174	125.2174
0.1111	123.9715	123.9715
0.2222	122.7624	122.7624
0.3333	121.5887	121.5887
0.4444	120.4490	120.4490
0.5556	119.3420	119.3420
0.6667	118.2665	118.2665
0.7778	117.2214	117.2214
0.8889	116.2053	116.2053
1.0000	115.2174	115.2174

SECONDARY LOAD DISTRIBUTION:

Norm. x	Stress
0.00	0.8000E+02
0.25	0.6000E+02
0.50	0.3000E+02
0.75	0.0000E+00
1.00	-.4000E+02



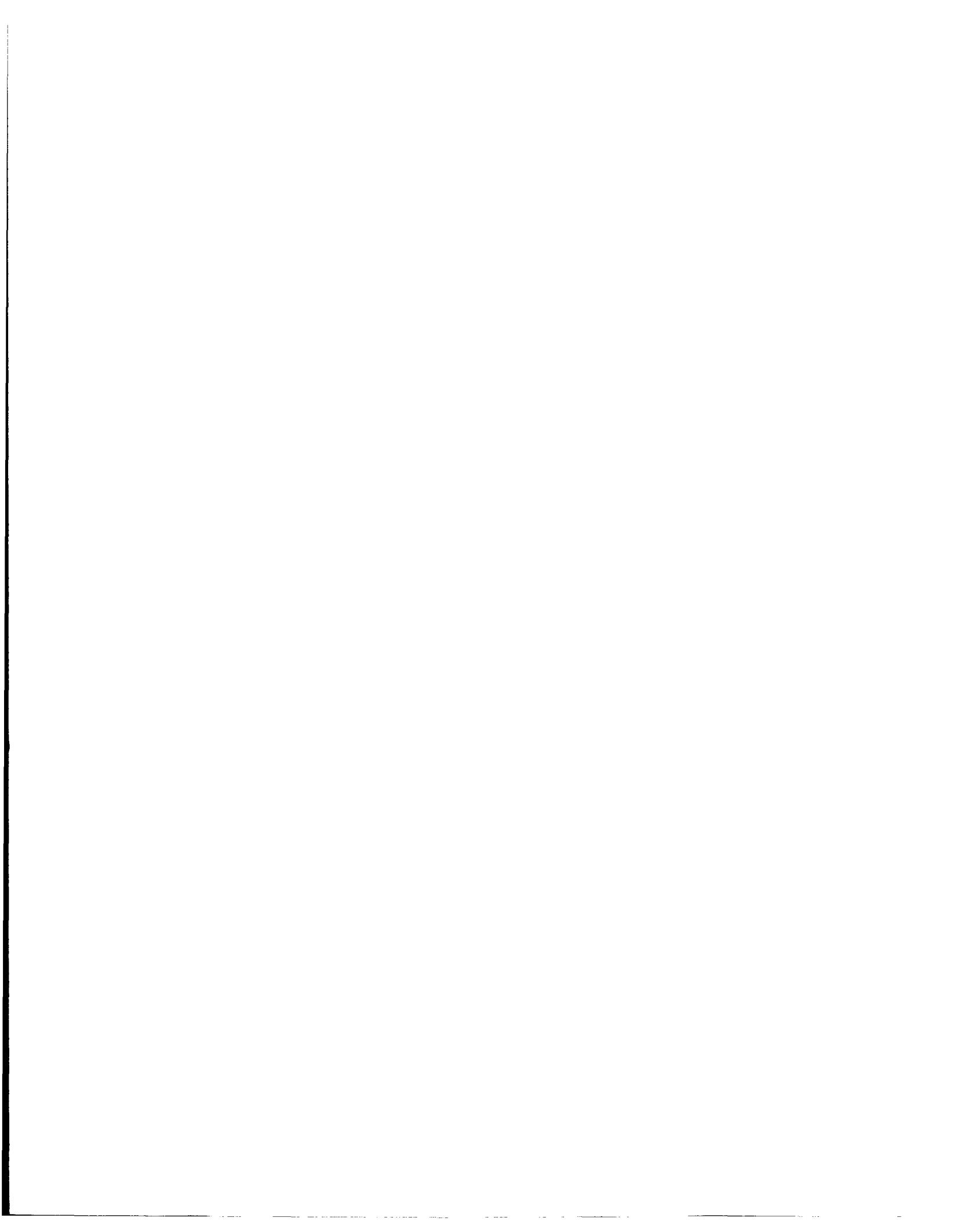
Model Code= SC04

	a	c	Je(a)	Je(c)	Jp(a)	Jp(c)	J(a)
J(c)							
	0.500E-01	0.500E-01	0.104E+00	0.125E+00	0.591E-01	0.102E+00	0.164E+00
	0.227E+00						
	0.500E-01	0.100E+00	0.164E+00	0.127E+00	0.110E+00	0.943E-01	0.274E+00
	0.221E+00						
	0.500E-01	0.150E+00	0.203E+00	0.121E+00	0.136E+00	0.825E-01	0.339E+00
	0.204E+00						
	0.100E+00	0.100E+00	0.189E+00	0.277E+00	0.123E+00	0.223E+00	0.312E+00
	0.500E+00						
	0.100E+00	0.150E+00	0.265E+00	0.298E+00	0.193E+00	0.242E+00	0.458E+00
	0.540E+00						
	0.150E+00	0.150E+00	0.254E+00	0.476E+00	0.211E+00	0.418E+00	0.466E+00
	0.895E+00						

EXAMPLE 2

INPUT FILE: Exam2.inp

```
Exam2.out      Output file name*12
 1      1=US units; 2=SI units
sc      Crack Model Type
2      Crack Model Number
0.1000E+01    Thickness
0.5000E+01    Width
0.3000E+05    Elastic Young's modulus
 0.300      Poisson's ratio
1.000      Alpha
0.1000E+03    Sigma0
10.000      n
0.1000E+03    material yield stress
0.2000E+03    material ultimate stress
 1      1: const. asp. 2: const. length
0.3500E+00    constant aspect ratio
 1      1: crit. crack 2: crit. load
 2      1: brittle, 2: ductile
0.2500E+00    matl toughness
 1      1: quad. 2: power
0.2450E+00    dj0 -- quadratic
0.3000E+02    dj1 -- quadratic
-.5000E+02    dj2 -- quadratic
0.3000E+00    da(max) -- quadratic
1      1= interactively input, 2= create a table
2      1= pri., 2=pri. & sec.
 1 # of Stress Dist
0.0000000000000000E+000    Nondim position
120.0000000000000    Stress value
1.000000000000000    Nondim position
120.0000000000000    Stress value
-1.000000000000000    Nondim position
```



0.0000E+00 Non-Dimensional position
 0.1000E+03 Stress value
 0.1000E+01 Non-Dimensional position
 0.5000E+02 Stress value
 -.1000E+01 Non-Dimensional position
 1.000 Load Factor # 1
 0 1 = input, 0 = stop
 P P(1st col.): to print
 0 1:to resume, 0: stop

OUTPUT FILE: Exam2.out

ELASTIC-PLASTIC ANALYSIS FOR CRITICAL CRACK/LOAD FOR SC02

 DATE: 17-SEP-03 TIME: 16:04:43
 (computed: NASA/FLAGRO Version 3.00, October 1995.)
 Elastic-Plastic Fracture Module (EPFM) V.x.xx, Aug. 2002
 U.S. customary units [inches, ksi, ksi sqrt(in)]

Input Filename = Exam2.inp
 Output Filename = Exam2.out

Plate Thickness, t = 1.0000
 " Width, W = 5.0000

Material Yield Stress = 100.00

Material Ultimate Stress = 200.00

Data for the Nonlinear Material Behavior:

Sig0 = 0.1000E+03
 E = 0.3000E+05
 nu = 0.3000E+00
 alpha = 0.1000E+01
 n = 0.1000E+02

Data for the Elastic Plastic Failure Analysis

DUCTILE ANALYSIS is performed
 Ultimate Tensile Stress (Su) = 0.2000E+03
 Jmat = 0.2500E+00
 Kmat(c) = 0.8660E+02, Kmat(a) = 0.9078E+02
 Search for *CRITICAL CRACK LENGTH*

Constant aspect ratio = 0.3500E+00

Fracture resistance curve(quadratic form):

$J_r = (0.2450E+00) + (0.3000E+02) * x + (-.5000E+02) * x^2$
 da(max) = 0.3000E+00

Model Code= SC02

PRIMARY LOAD DISTRIBUTION 1:

Norm. x	Stress
0.00	0.1200E+03



```

          1.00          0.1200E+03
SECONDARY LOAD DISTRIBUTION:
      Norm. x          Stress
          0.00          0.1000E+03
          1.00          0.5000E+02

```

TABLE OUTPUT (Fixed a/c=0.350E+00):

```

Pri. Load a_init   a_crit   a_inst   da(tear)  P/P0_init P/P0_crit
P/P0_inst
      c_init   c_crit   c_inst   dc(tear)
0.100E+01 0.163E-01 0.111E+00 0.257E+00 0.147E+00 0.120E+01 0.121E+01
0.124E+01

0.467E-01 0.316E+00 0.416E+00 0.101E+00

```

EXAMPLE 3

INPUT FILE: Exam3.inp

```

Exam3.out          Output file name*12
  2      1=US units; 2=SI units
ec      Crack Model Type
  2      Crack Model Number
  0.500E-01      Thickness
  0.150E+00      Width
  0.2100E+06      Elastic Young's modulus
  0.300      Poisson's ratio
  1.500      Alpha
  0.4000E+03      Sigma0
  15.000      n
  0.4000E+03 material yield stress
  0.6000E+03 material ultimate stress
  1      1: const. asp. 2: const. length
  0.2500E+00      constant aspect ratio
  2      1: crit. crack 2: crit. load
  2      1: brittle, 2: ductile
  0.5000E-01      mat1 toughness
  2      1: quad. 2: power
  0.5000E+01      dj1 -- power law
  0.5000E+00      dj2 -- power law
  0.4000E-02      da(max) -- power law
  0      1: with 2nd load, 0: w/o 2nd load
  1 # of Stress Dist
  0.0000000000000000E+000      Nondim position
  400.0000000000000      Stress value
  1.000000000000000      Nondim position
  400.0000000000000      Stress value
  -1.000000000000000      Nondim position
  1      1= interactively input, 2=create a table
  0.3000E-02      a( 1)
  0.4000E-02      a( 2)

```

0.5000E-02 a(3)
-.1000E+01 end of input
0 1 = input, 0 = stop
P P(1st col.): to print
0 1:to resume, 0: stop

OUTPUT FILE: Exam3.out

ELASTIC-PLASTIC ANALYSIS FOR CRITICAL CRACK/LOAD FOR EC02

DATE: 17-SEP-03 TIME: 16:04:02
(computed: NASA/FLAGRO Version 3.00, October 1995.)
Elastic-Plastic Fracture Module (EPFM) V.x.xx, Aug. 2002
SI units [mm, MPa, MPa sqrt(mm)]

Input Filename = Exam3.inp
Output Filename = Exam3.out

Thickness, t = 0.0500
Width, W = 0.1500
X Offset, XD = 0.0000

[Note: Solution accurate if $2c/W < \text{or} = 0.5$]

Material Yield Stress = 400.00

Material Ultimate Stress = 600.00

Data for the Nonlinear Material Behavior:

Sig0 = 0.4000E+03
E = 0.2100E+06
nu = 0.3000E+00
alpha = 0.1500E+01
n = 0.1500E+02

Data for the Elastic Plastic Failure Analysis

DUCTILE ANALYSIS is performed

Ultimate Tensile Stress (Su) = 0.6000E+03

Jmat = 0.5000E-01

Kmat(c) = 0.1074E+03, Kmat(a) = 0.1074E+03

Search for *CRITICAL LOAD*

Constant aspect ratio = 0.2500E+00

Fracture resistance curve (power law):

$J_r = (0.5000E+01) * x^{(0.5000E+00)}$

da(max) = 0.4000E-02

Model Code= EC02

PRIMARY LOAD DISTRIBUTION 1:

Norm. x	Stress
0.00	0.4000E+03
1.00	0.4000E+03

TABLE OUTPUT (Fixed a/c=0.250E+00):

a	P_init	P_inst	da(tear)	dc(tear)	P_init/P0
0.300E-02	0.316E+01	0.336E+01	0.168E-02	0.237E-03	0.107E+01
0.114E+01					
0.400E-02	0.302E+01	0.321E+01	0.150E-02	0.167E-03	0.104E+01
0.110E+01					
0.500E-02	0.288E+01	0.306E+01	0.135E-02	0.128E-03	0.100E+01
0.106E+01					

EXAMPLE 4

INPUT FILE: Exam4.inp

```

Exam4.out          Output file name*12
  1      1=US units; 2=SI units
cc      Crack Model Type
  1      Crack Model Number
  1      1=tension, 2=bending
0.2000E+01      Thickness
0.2000E+01      Width
0.3000E+05      Elastic Young's modulus
  0.300      Poisson's ratio
  1.000      Alpha
0.1000E+03      Sigma0
  10.000      n
  0.1000E+03 material yield stress
  0.3000E+03 material ultimate stress
    2 1: p(max), 2:p+s(max)
0.8000E+02      loading stress
  0.0000E+00 Non-Dimensional position
  0.5000E+02 Stress value
  0.1000E+01 Non-Dimensional position
  0.5000E+02 Stress value
  -.1000E+01 Non-Dimensional position
    2 1: p(min), 2:p+s(min)
0.0000E+00      loading stress
  0.0000E+00 Non-Dimensional position
  0.5000E+02 Stress value
  0.1000E+01 Non-Dimensional position
  0.5000E+02 Stress value
  -.1000E+01 Non-Dimensional position
    2 no. of cycles
    2 1: p(max), 2:p+s(max)
0.9000E+02      loading stress
  0.0000E+00 Non-Dimensional position
  0.5000E+02 Stress value
  0.1000E+01 Non-Dimensional position
  0.5000E+02 Stress value
  -.1000E+01 Non-Dimensional position
    2 1: p(min), 2:p+s(min)
0.0000E+00      loading stress

```

```

0.0000E+00 Non-Dimensional position
0.5000E+02 Stress value
0.1000E+01 Non-Dimensional position
0.5000E+02 Stress value
-.1000E+01 Non-Dimensional position
  1 no. of cycles
-1 terminate input
  1 Block Case ID.
    2 no. of times
  2 Block Case ID.
    1 no. of times
-1 Block Case ID.
0.5000E+00 Jmat
0.1000E-08 C in Paris Law
0.4000E+01 m in Paris Law
0.1000E+01 baseline U0
0.1000E+01 alp_bury
0.1000E+01 alp_surf
0.5000E-01 initial a
0.1000E+00 initial c
    100 max. no. of schedule
    10 print interval
P P(1st col.): to print
0 1:to resume, 0: stop

```

OUTPUT FILE: Exam4.out

ELASTIC-PLASTIC FATIGUE LIFE CALCULATION FOR CC01

DATE: 18-SEP-03 TIME: 13:29:02
(computed: NASA/FLAGRO Version 3.00, October 1995.)
Elastic-Plastic Fracture Module (EPFM) V.x.xxx, Aug. 2002
U.S. customary units [inches, ksi, ksi sqrt(in)]

Input Filename = exam4.inp
Output Filename = Exam4.out

Plate Thickness, t = 2.0000
Plate Width, W = 2.0000

Material Yield Stress = 100.00

Material Ultimate Stress = 300.00

Data for the Nonlinear Material Behavior:

Sig0 = 0.1000E+03
E = 0.3000E+05
nu = 0.3000E+00
alpha = 0.1000E+01
n = 0.1000E+02

Model Code= CC01 under uniform tension

BLOCK CASE DEFINITION:

Blk Cse.	Maximum Load Values		Minimum Load Values,		Cycle
1	Primary Load		Primary Load		2
	i	Si	i	Si	
	0	0.8000E+02	0	0.1000E-09	
	1	0.0000E+00	1	0.0000E+00	
	2	0.0000E+00	2	0.0000E+00	
	3	0.0000E+00	3	0.0000E+00	
	Secondary Load		Secondary Load		
	Norm. x	S(Norm. x)	Norm. x	S(Norm. x)	
	0.0000E+00	0.5000E+02	0.0000E+00	0.5000E+02	
	0.1000E+01	0.5000E+02	0.1000E+01	0.5000E+02	
2	Primary Load		Primary Load		1
	i	Si	i	Si	
	0	0.9000E+02	0	0.1000E-09	
	1	0.0000E+00	1	0.0000E+00	
	2	0.0000E+00	2	0.0000E+00	
	3	0.0000E+00	3	0.0000E+00	
	Secondary Load		Secondary Load		
	Norm. x	S(Norm. x)	Norm. x	S(Norm. x)	
	0.0000E+00	0.5000E+02	0.0000E+00	0.5000E+02	
	0.1000E+01	0.5000E+02	0.1000E+01	0.5000E+02	

DEFINITION OF LOAD SPECTRUM (or SCHEDULE):

Blk. Case ID	No. of Times Applied
1	2
2	1

FATIGUE DATA (da/dN=C*dK^m):

J(mat) = 0.5000E+00
 C = 0.1000E-08
 m = 0.4000E+01
 U0 = 0.1000E+01
 alp (c) = 0.1000E+01
 alp (a) = 0.1000E+01

 a(init) = 0.5000E-01
 c(init) = 0.1000E+00
 Max. No. of Schedules = 100
 Pint interval = 10 schedules

RESULTS OF FATIGUE ANALYSIS:

SCHEDULE	a	c	D_Jeff(a)	D_Jeff(c)	Jmax(a)
10	0.6651E-01	0.1037E+00	0.2474E-01	0.1291E-01	0.1423E+00
0.1074E+00	0.83	0.72			
20	0.8660E-01	0.1113E+00	0.2710E-01	0.1830E-01	0.1644E+00
0.1392E+00	0.81	0.74			
30	0.1115E+00	0.1259E+00	0.3054E-01	0.2497E-01	0.1940E+00
0.1785E+00	0.79	0.76			
40	0.1454E+00	0.1524E+00	0.3671E-01	0.3385E-01	0.2410E+00
0.2332E+00	0.78	0.77			
50	0.1999E+00	0.2025E+00	0.4867E-01	0.4758E-01	0.3272E+00
0.3243E+00	0.78	0.78			

Results: two-D at c tip, $J_{\text{bury}}(\text{max})=0.5054\text{E}+00$,
 $J_{\text{surf}}(\text{max})=0.5046\text{E}+00$

$J(\text{mat})=0.5000\text{E}+00$
with $a=0.2978\text{E}+00$, $c=0.2985\text{E}+00$ after 58-th schedule,
total no. of cycles= 295

EXAMPLE 5

INPUT FILE: Exam5.inp

```
Exam5.out      Output file name*12
  1      1=US units; 2=SI units
  1      Proof Test Procedure
  1      Proof Test - Safe Pre-Proof Life Analysis
sc      Crack Model Type
  2      Crack Model Number
0.1000E+01     Thickness
0.5000E+01     Width
0.3000E+05     Elastic Young's modulus
  0.300      Poisson's ratio
  1.000      Alpha
0.1000E+03     Sigma0
  10.000     n
  0.1000E+03 material yield stress
  0.3000E+03 material ultimate stress
  1      1: const. asp. 2: const. length
0.6000E+00     constant aspect ratio
  2      1: brittle, 2: ductile
0.2500E+00     mat1 toughness
  1      1: quad. 2: power
0.2450E+00     dj0 -- quadratic
0.3000E+02     dj1 -- quadratic
-.5000E+02     dj2 -- quadratic
0.3000E+00     da(max) -- quadratic
  1      1= interactively input, 2= create a table
  2      1= pri., 2=pri. & sec.
  0.0000000000000000E+000      Nondim position
  110.0000000000000      Stress value
  1.000000000000000      Nondim position
  120.0000000000000      Stress value
  -1.000000000000000      Nondim position
0.0000E+00     Non-Dimensional position
0.1000E+03     Stress value
0.1000E+01     Non-Dimensional position
0.5000E+02     Stress value
-.1000E+01     Non-Dimensional position
  1.000 Load Factor # 1
  0      1 = input, 0 = stop
P      P(1st col.): to print
  0      1:to resume, 0: stop
```

OUTPUT FILE: Exam5.out

```
*****
*   SAFE LIFE PRE-PROOF TEST ANALYSIS   *
*****
```

CRITICAL FLAW SIZE

Elastic-Plastic fracture mechanics will be used to determine the maximum tolerable crack size that could just survive service conditions

ELASTIC-PLASTIC PROOF LOAD ANALYSIS FOR SC02

DATE: 17-SEP-03 TIME: 16:08:25
(computed: NASA/FLAGRO Version 3.00, October 1995.)
Elastic-Plastic Fracture Module (EPFM) V.x.xx, Aug. 2002
U.S. customary units [inches, ksi, ksi sqrt(in)]

Input Filename = exam5.inp
Output Filename = Exam5.out

Plate Thickness, t = 1.0000
Width, W = 5.0000

Material Yield Stress = 100.00

Material Ultimate Stress = 300.00

Data for the Nonlinear Material Behavior:

Sig0 = 0.1000E+03
E = 0.3000E+05
nu = 0.3000E+00
alpha = 0.1000E+01
n = 0.1000E+02

Data for the Elastic Plastic Failure Analysis

DUCTILE ANALYSIS is performed
Ultimate Tensile Stress (Su) = 0.3000E+03
Jmat = 0.2500E+00
Kmat(c) = 0.8660E+02, Kmat(a) = 0.9078E+02
Search for *CRITICAL CRACK LENGTH*

Constant aspect ratio = 0.6000E+00

Fracture resistance curve(quadratic form):

$J_r = (0.2450E+00) + (0.3000E+02) * x + (-.5000E+02) * x^2$
da(max) = 0.3000E+00

Model Code= SC02

PRIMARY LOAD DISTRIBUTION 1:

Norm. x	Stress
0.00	0.1100E+03
1.00	0.1200E+03

SECONDARY LOAD DISTRIBUTION:

Norm. x	Stress
0.00	0.1000E+03
1.00	0.5000E+02

TABLE OUTPUT (Fixed a/c=0.600E+00):

```

*****
*****
*           IMPORTANT NOTE           *
*****
*****

```

The Critical Flaw Size for Ductile Materials is the calculated critical crack size and equals the instability crack size minus ductile tearing. A crack with an initial size greater than the critical size will tear to instability under the given service load.

```

ERROR[JSC02]: exceeds plastic collapse load!
a=0.182E+00, c=0.304E+00
p=0.198E+03, pmax=0.197E+03

```

```

ERROR[JSC02]: exceeds plastic collapse load!
a=0.251E+00, c=0.418E+00
p=0.195E+03, pmax=0.193E+03

```

```

ERROR[JSC02]: exceeds plastic collapse load!
a=0.199E+00, c=0.332E+00
p=0.198E+03, pmax=0.196E+03

```

```

ERROR[JSC02]: exceeds plastic collapse load!
a=0.212E+00, c=0.354E+00
p=0.197E+03, pmax=0.195E+03

```

```

ERROR[JSC02]: exceeds plastic collapse load!
a=0.222E+00, c=0.370E+00
p=0.197E+03, pmax=0.195E+03

```

```

ERROR[JSC02]: exceeds plastic collapse load!
a=0.215E+00, c=0.358E+00
p=0.197E+03, pmax=0.195E+03

```

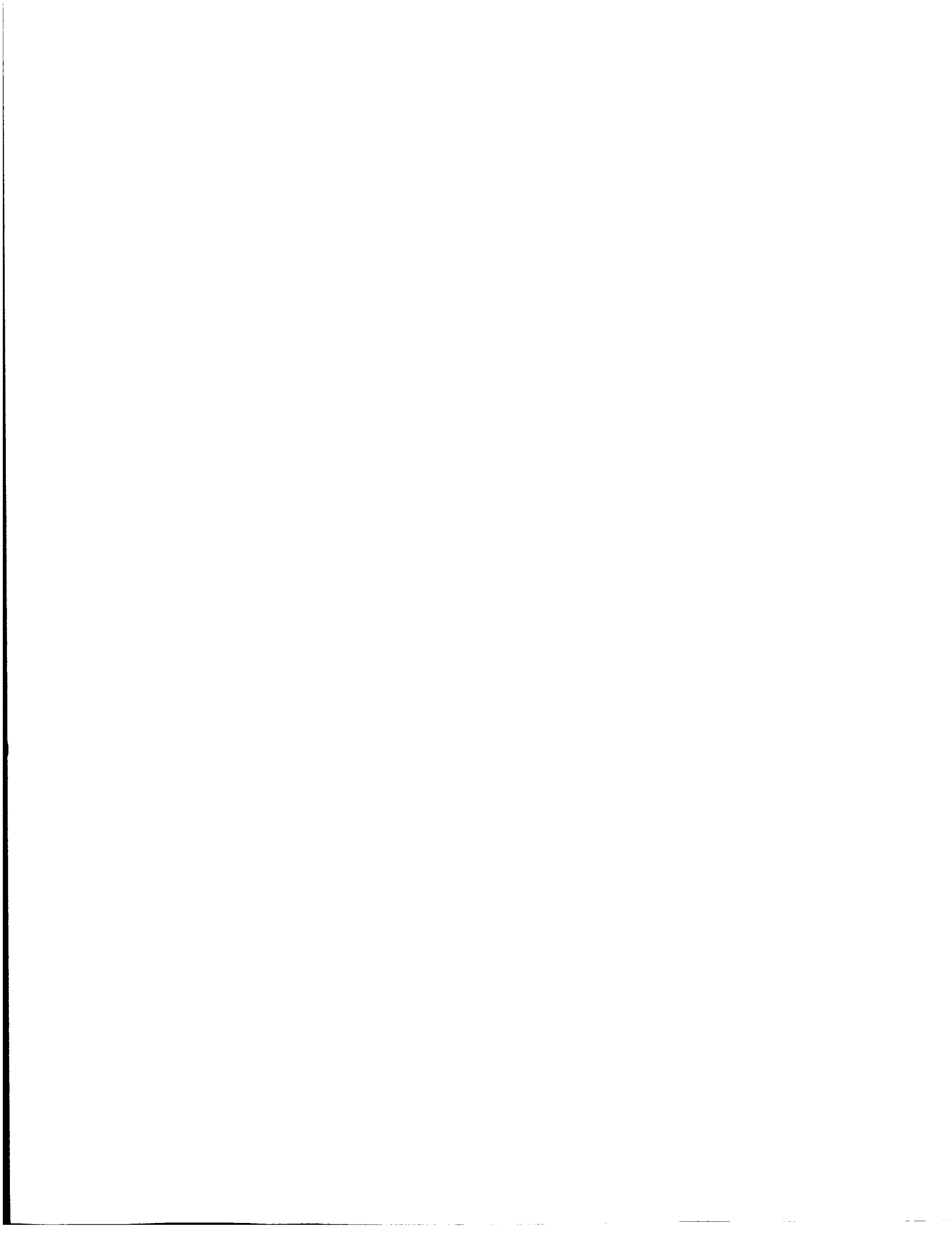
```

ERROR[JSC02]: exceeds plastic collapse load!
a=0.216E+00, c=0.361E+00
p=0.197E+03, pmax=0.195E+03

```

Pri. Load	a_init	a_crit	a_inst	da(tear)	P/P0_init	P/P0_crit
P/P0_inst	c_init	c_crit	c_inst	dc(tear)		
0.100E+01	0.319E-01	0.216E+00	0.359E+00	0.142E+00	0.113E+01	0.116E+01
0.120E+01						





ELASTIC-PLASTIC PROOF LOAD ANALYSIS FOR SC04

 DATE: 17-SEP-03 TIME: 16:10:41
 (computed: NASA/FLAGRO Version 3.00, October 1995.)
 Elastic-Plastic Fracture Module (EPFM) V.x.xx, Aug. 2002
 SI units [mm, MPa, MPa sqrt(mm)]

Input Filename = exam6.inp
 Output Filename = Exam6.out

Cylinder Thickness, t = 0.0840
 Outer Diameter, D = 1.1830

Crack Type = EXTERNAL

Material Yield Stress = 556.00

Material Ultimate Stress = 900.00

Data for the Nonlinear Material Behavior:

Sig0 = 0.5560E+03
 E = 0.2100E+06
 nu = 0.3000E+00
 alpha = 0.1677E+01
 n = 0.1770E+02

Data for the Elastic Plastic Failure Analysis

DUCTILE ANALYSIS is performed
 Ultimate Tensile Stress (Su) = 0.9000E+03
 Jmat = 0.4330E+00
 Kmat(c) = 0.3015E+03, Kmat(a) = 0.3161E+03
 Search for *CRITICAL CRACK LENGTH*

Constant aspect ratio = 0.6100E+00

Fracture resistance curve(quadratic form):

$J_r = (0.3610E+00) + (0.5033E+03) * x + (-.2325E+04) * x^2$
 $da(max) = 0.5000E-02$

Model Code= SC04

Internal Pressure 80.450

PRIMARY LOAD DISTRIBUTION 1:

Norm. x Stress

Stresses at 10 points

Distance x/t (from inner wall)	Stress due to Int. Pressure	Total Stress
0.0000	529.3516	529.3516
0.1111	518.4388	518.4388
0.2222	508.1016	508.1016
0.3333	498.3002	498.3002
0.4444	488.9981	488.9981

0.5556	480.1621	480.1621
0.6667	471.7615	471.7615
0.7778	463.7681	463.7681
0.8889	456.1561	456.1561
1.0000	448.9016	448.9016

NO SECONDARY LOAD SPECIFIED!

TABLE OUTPUT (Fixed a/c=0.610E+00):

```

*****
*****
*                IMPORTANT NOTE                *
*****
*****

```

The flaw size for Ductile Materials that will just survive the Proof Load is the calculated instability crack size and equals the critical crack size plus ductile tearing. A crack with an initial size greater than the size to initial ductile tearing but less than the critical size will tear under the Proof Load but not fail

Pri. Load	a_init	a_crit	a_inst	da(tear)	P/P0_init	P/P0_crit
0.100E+01	0.562E-01	0.610E-01	0.634E-01	0.241E-02	0.723E+01	0.757E+01
0.781E+01						
	0.921E-01	0.100E+00	0.104E+00	0.352E-02		

EXAMPLE 7

INPUT FILE: Exam7.inp

```

ex7.out      Output file name*12
  1      1=US units; 2=SI units
  2      Proof Test Procedure
  1      Proof Test - Proof Test Analysis
ec      Crack Model Type
  2      Crack Model Number
  0.500E+00  Thickness
  0.600E+01  Width
  0.3000E+05  Elastic Young's modulus
  0.300      Poisson's ratio
  1.000      Alpha
  0.8000E+02  Sigma0
  25.000     n
  0.8000E+02  material yield stress
  0.1200E+03  material ultimate stress

```

```

0.2500E+00    constant aspect ratio
2      1: brittle, 2: ductile
0.2000E+00    mat1 toughness
2      1: quad. 2: power
0.5000E+01    dj1 -- power law
0.5000E+00    dj2 -- power law
0.10000E+00    da(max) -- power law
1      1: with 2nd load, 0: w/o 2nd load
0.0000000000000000E+000    Nondim position
60.000000000000000    Stress value
0.2000000000000000    Nondim position
55.000000000000000    Stress value
0.4000000000000000    Nondim position
52.000000000000000    Stress value
0.6000000000000000    Nondim position
50.000000000000000    Stress value
0.8000000000000000    Nondim position
49.000000000000000    Stress value
1.0000000000000000    Nondim position
49.000000000000000    Stress value
-1.0000000000000000    Nondim position
0.0000E+00    Non-Dimensional position
0.9000E+02    Stress value
0.1000E+01    Non-Dimensional position
0.0000E+00    Stress value
-.1000E+01    Non-Dimensional position
1      1= interactively input, 2=create a table
0.2500E-01    a( 1)
0.3000E-01    a( 2)

0.3500E-01    a( 3)
0.4000E-01    a( 4)
0.4500E-01    a( 5)
0.5000E-01    a( 6)
-.1000E+01    end of input
P      P(1st col.): to print
0      1:to resume, 0: stop

```

OUTPUT FILE: Exam7.out

```

*****
*                PROOF TEST ANALYSIS                *
*****

```

PROOF LOAD ANALYSIS

Elastic-Plastic fracture mechanics will be used to determine the proof load necessary to screen against the presence of specified initial crack sizes



DATE: 18-SEP-03 TIME: 22:58:27
(computed: NASA/FLAGRO Version 3.00, October 1995.)
Elastic-Plastic Fracture Module (EPFM) V.x.xx, Aug. 2002
U.S. customary units [inches, ksi, ksi sqrt(in)]

Input Filename = ex7.inp
Output Filename = ex7.out

Thickness, t = 0.5000
Width, W = 6.0000
X Offset, XD = 0.0000

[Note: Solution accurate if $2c/W < \text{or} = 0.5$]

Material Yield Stress = 80.00

Material Ultimate Stress = 120.00

Data for the Nonlinear Material Behavior:

Sig0 = 0.8000E+02
E = 0.3000E+05
nu = 0.3000E+00
alpha = 0.1000E+01
n = 0.2500E+02

Data for the Elastic Plastic Failure Analysis

DUCTILE ANALYSIS is performed

Ultimate Tensile Stress (Su) = 0.1200E+03

Jmat = 0.2000E+00

Kmat(c) = 0.8120E+02, Kmat(a) = 0.8120E+02

Search for *CRITICAL LOAD*

Constant aspect ratio = 0.2500E+00

Fracture resistance curve (power law):

$J_r = (0.5000E+01) * x^{(0.5000E+00)}$

da(max) = 0.1000E+00

Model Code= EC02

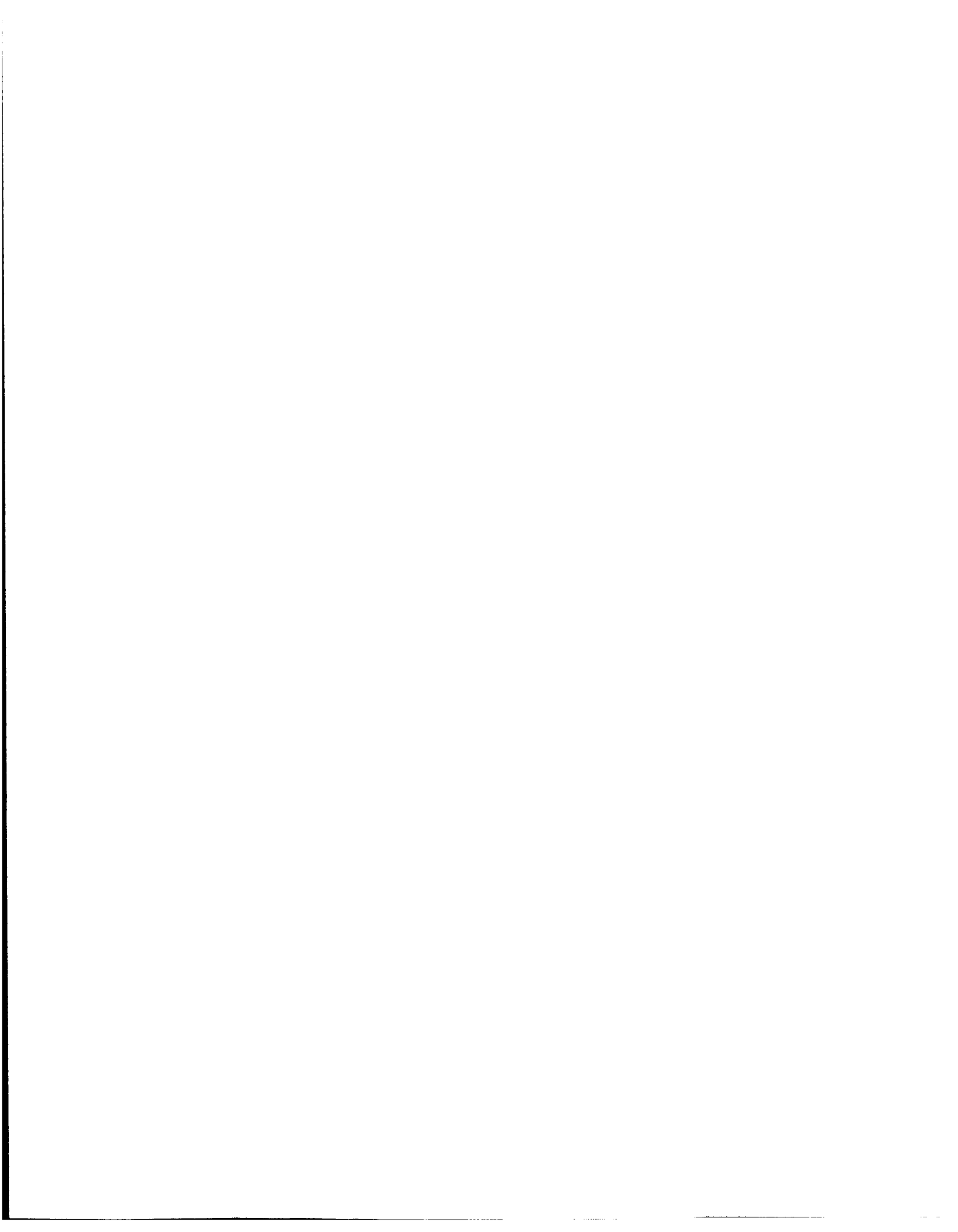
PRIMARY LOAD DISTRIBUTION 1:

Norm. x	Stress
0.00	0.6000E+02
0.20	0.5500E+02
0.40	0.5200E+02
0.60	0.5000E+02
0.80	0.4900E+02
1.00	0.4900E+02

SECONDARY LOAD DISTRIBUTION:

Norm. x	Stress
0.00	0.9000E+02
1.00	0.0000E+00

* IMPORTANT NOTE *



The Proof Load Factor for a Ductile Material containing a given initial crack size is equal to the instability load factor. A proof load that exceeds the load to initiate tearing but is less than the instability load will cause a crack to tear but not fail.

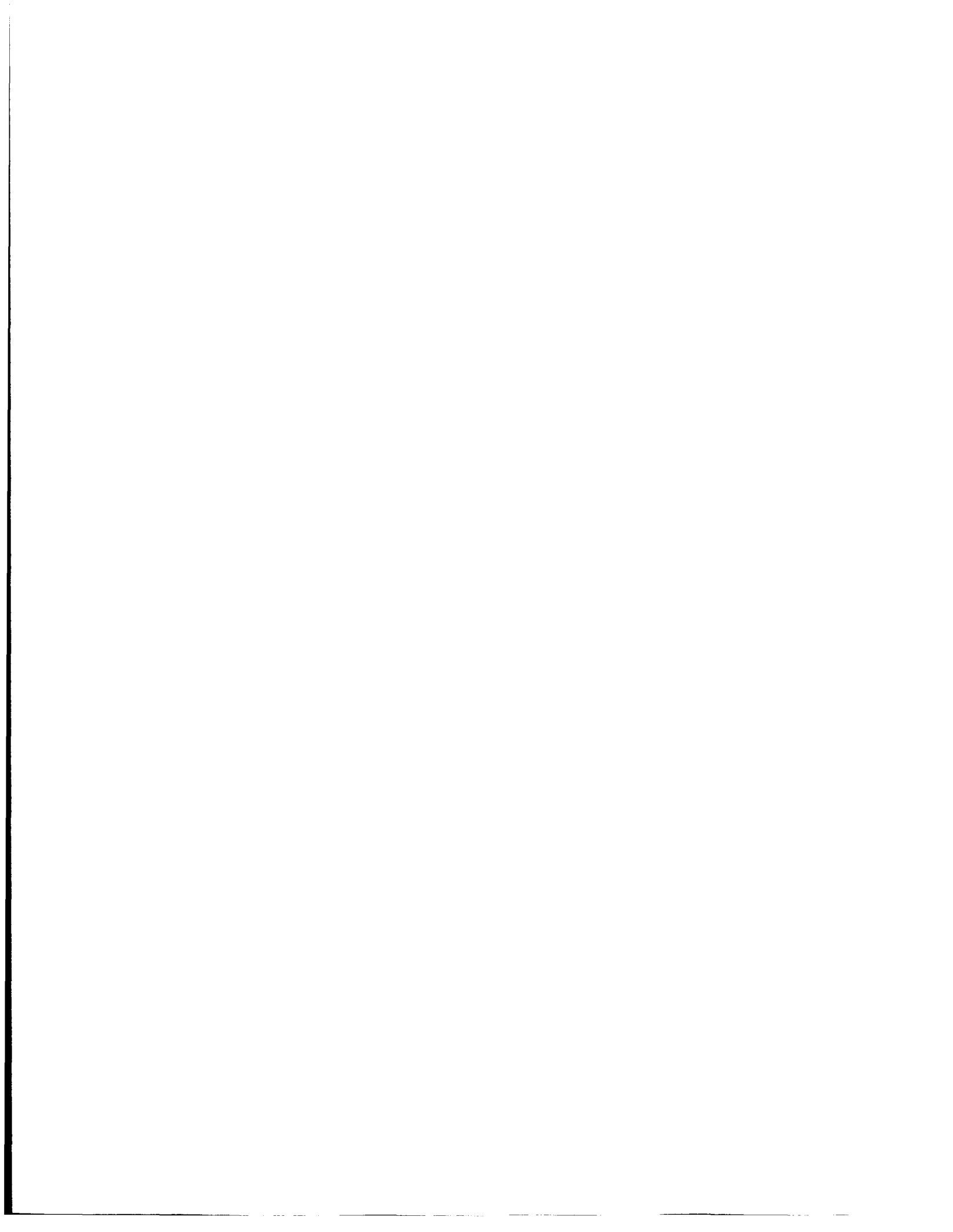
TABLE OUTPUT (Fixed a/c=0.250E+00):

	a	P_init	P_inst	da(tear)	dc(tear)	P_init/P0
P_inst/P0	0.250E-01	0.260E+03	0.270E+03	0.353E-01	0.943E-02	0.109E+01
0.113E+01	0.300E-01	0.257E+03	0.267E+03	0.349E-01	0.791E-02	0.107E+01
0.112E+01	0.350E-01	0.254E+03	0.265E+03	0.340E-01	0.659E-02	0.106E+01
0.111E+01	0.400E-01	0.251E+03	0.262E+03	0.328E-01	0.555E-02	0.105E+01
0.110E+01	0.450E-01	0.249E+03	0.260E+03	0.317E-01	0.473E-02	0.104E+01
0.109E+01	0.500E-01	0.246E+03	0.258E+03	0.306E-01	0.410E-02	0.104E+01
0.108E+01						

EXAMPLE81

INPUT FILE: Exam8.inp

Exam8.out Output file name*12
1 1=US units; 2=SI units
2 Proof Test Procedure
3 Proof Test - Proof Test Analysis
cc Crack Model Type
1 Crack Model Number
2 1=tension, 2=bending
0.2000E+01 Thickness
0.2000E+01 Width
0.3000E+05 Elastic Young's modulus
0.300 Poisson's ratio
1.200 Alpha
0.1500E+03 Sigma0
20.000 n
0.1500E+03 material yield stress
0.2000E+03 material ultimate stress
0.5000E+00 Initial Proof Crack Length
0.1000E+01 Init Proof a/c
0 proof secondary (0-no 1=yes)
0.2200E+03 loading stress



```

1      1: quad. 2: power
0.1450E+00    dj0 -- quadratic
0.3000E+02    dj1 -- quadratic
-.5000E+02    dj2 -- quadratic
0.3000E+00    da(max) -- quadratic
0.1500E+00    Jmat
P      P(1st col.): to print
0      1:to resume, 0: stop

```

OUTPUT FILE: Exam8.out

```

*****
*                PROOF TEST ANALYSIS                *
*****

```

FINAL FLAW SIZE ANALYSIS

Elastic-Plastic fracture mechanics is used to determine the final
flaw size after the application of the specified proof load

ELASTIC-PLASTIC PROOF LOAD ANALYSIS FOR CC01

DATE: 17-SEP-03 TIME: 16:14:11
(computed: NASA/FLAGRO Version 3.00, October 1995.)
Elastic-Plastic Fracture Module (EPFM) V.x.xx, Aug. 2002
U.S. customary units [inches, ksi, ksi sqrt(in)]

Input Filename = exam8.inp
Output Filename = Exam8.out

Plate Thickness, t = 2.0000
Plate Width, W = 2.0000

Material Yield Stress = 150.00

Material Ultimate Stress = 200.00

Data for the Nonlinear Material Behavior:

Sig0 = 0.1500E+03
E = 0.3000E+05
nu = 0.3000E+00
alpha = 0.1200E+01
n = 0.2000E+02

PRIMARY LOAD DISTRIBUTION

0.0000 S0: Tensile Stress
220.0000 S1: Bending Stress

0.0000 S2: Bending Stress

Fracture resistance curve(quadratic form):

$$J_r = (0.1450E+00) + (0.3000E+02) * x + (-.5000E+02) * x^2$$

da(max) = 0.3000E+00

. Toughness = 0.1500E+00

END OF PROOF TEST - FINAL FLAW SIZE ANALYSIS:

a	c	da	dc
0.5694E+00	0.6555E+00	0.6947E-01	0.1557E+00

EXAMPLE 9

INPUT FILE: Exam9.inp

```
Exam9.out      Output file name*12
 1      1=US units; 2=SI units
sc      Crack Model Type
4      Crack Model Number
0.500000E+00   T
0.400000E+02   Outer Diameter
e
0.3000E+05     Elastic Young"s modulus
0.300         Poisson"s ratio
1.000         Alpha
0.1000E+03     Sigma0
10.000        n
0.1000E+03     material yield stress
0.1500E+03     material ultimate stress
0.2500E+00     Initial Proof Crack Length
0.5000E+00     Init Proof a/c
              100   Number of Service Cycles
1      secondary (0-no 1=yes)
n
0.0000000000000000E+000   Nondim position
90.0000000000000000       Stress value
1.0000000000000000       Nondim position
80.0000000000000000       Stress value
-1.0000000000000000       Nondim position
0.0000E+00   Non-Dimensional position
-0.100E+03   Stress value
0.1000E+01   Non-Dimensional position
0.1000E+03   Stress value
-.1000E+01   Non-Dimensional position
n
0.0000000000000000E+000   Nondim position
0.0000000000000000E+000   Stress value
1.0000000000000000       Nondim position
0.0000000000000000E+000   Stress value
-1.0000000000000000       Nondim position
0.0000E+00   Non-Dimensional position
-0.100E+03   Stress value
0.1000E+01   Non-Dimensional position
0.1000E+03   Stress value
-.1000E+01   Non-Dimensional position
1      1: quad. 2: power
0.2000E+00   dj0 -- quadratic
0.3000E+02   dj1 -- quadratic
0.0000E+00   dj2 -- quadratic
0.2000E+00   da(max) -- quadratic
0.2100E+00   Jmat
0.1000E+01   baseline U0
0.1000E+01   alp_bury
0.1000E+01   alp_surf
```

0.1000E-09 C in Paris Law (Serv)
0.4000E+01 m in Paris Law (Serv)
P P(1st col.): to print
0 1:to resume, 0: stop

OUTPUT FILE: Exam9.out

TEAR-FATIGUE ANALYSIS FOR SC04

DATE: 19-SEP-03 TIME: 13:53:44
(computed: NASA/FLAGRO Version 3.00, October 1995.)
Elastic-Plastic Fracture Module (EPFM) V.x.xx, Jan. 2003
U.S. customary units [inches, ksi, ksi sqrt(in)]

Input Filename = exam9.inp
Output Filename = Exam9.out

Cylinder Thickness, t = 0.5000
Outer Diameter, D = 40.0000

Crack Type = EXTERNAL

Material Yield Stress = 100.00

Material Ultimate Stress = 150.00

Data for the Nonlinear Material Behavior:

Sig0 = 0.1000E+03
E = 0.3000E+05
nu = 0.3000E+00
alpha = 0.1000E+01
n = 0.1000E+02

SERVICE SPECTRUM

LOAD STEP 1

CYCLIC MAXIMUM DISTRIBUTION

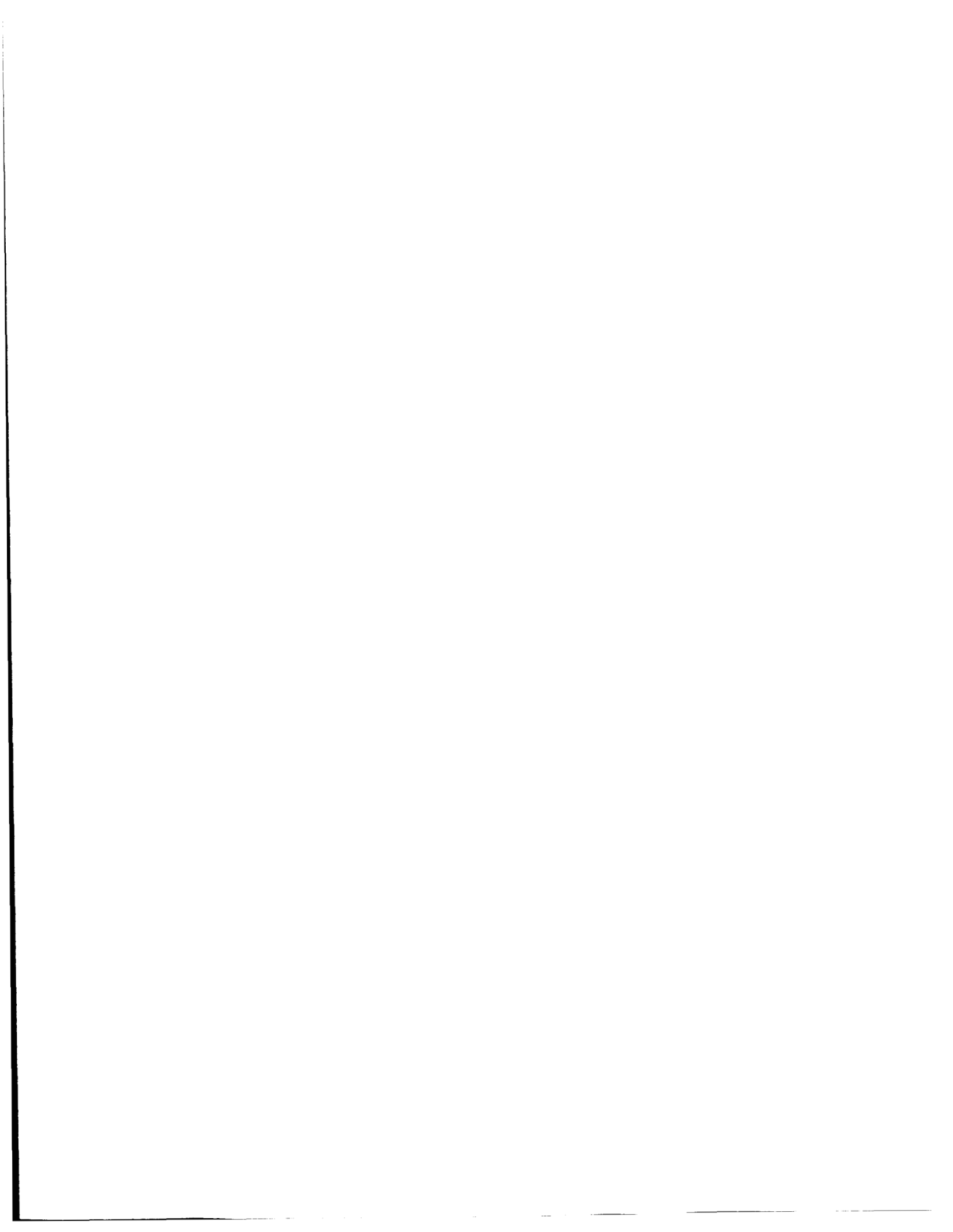
PRIMARY LOAD DISTRIBUTION 1:

Norm. x Stress
Stresses at 2 points

Distance x/t (from inner wall)	Stress due to Int. Pressure	Total Stress
0.00	0.9000E+02	
1.00	0.8000E+02	

SECONDARY LOAD DISTRIBUTION:

Norm. x Stress



0.00 0.1000E+03
 1.00 -.1000E+03

CYCLIC MINIMUM DISTRIBUTION

PRIMARY LOAD DISTRIBUTION 1:

Norm. x Stress
 Stresses at 2 points

Distance x/t Stress due to Total Stress
 (from inner wall) Int. Pressure

0.00 0.0000E+00
 1.00 0.0000E+00

SECONDARY LOAD DISTRIBUTION:

Norm. x Stress
 0.00 0.1000E+03
 1.00 -.1000E+03

Fracture resistance curve (quadratic form):

$$J_r = (0.2000E+00) + (0.3000E+02) * x + (0.0000E+00) * x^2$$

$$da(max) = 0.2000E+00$$

FATIGUE DATA ($da/dN = C * dK^m$):

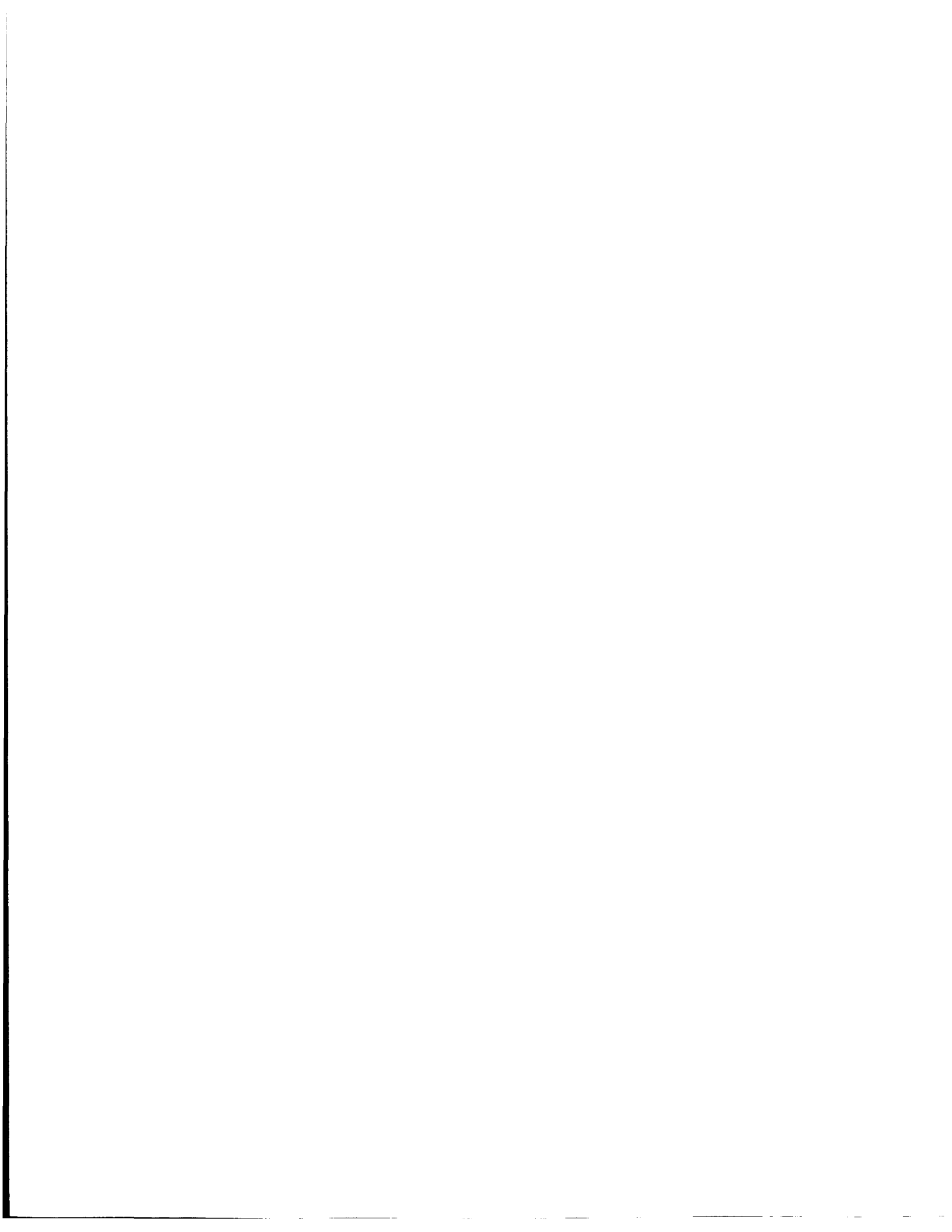
J(mat) = 0.2100E+00
 C = 0.1000E-09
 m = 0.4000E+01
 U0 = 0.1000E+01
 alp (c) = 0.1000E+01
 alp (a) = 0.1000E+01

a(init) = 0.2500E+00
 c(init) = 0.5000E+00

RESULTS OF TEAR-FATIGUE ANALYSIS:

Cycle	a	c	da	dc
0	0.2500E+00	0.5000E+00		
0	0.2578E+00	0.5133E+00	0.7968E-02	0.1365E-01
1	0.2729E+00	0.5310E+00	0.1509E-01	0.1767E-01
2	0.2879E+00	0.5514E+00	0.1502E-01	0.2045E-01
3	0.3029E+00	0.5750E+00	0.1499E-01	0.2356E-01
4	0.3179E+00	0.6021E+00	0.1502E-01	0.2706E-01
5	0.3330E+00	0.6331E+00	0.1513E-01	0.3102E-01
6	0.3484E+00	0.6686E+00	0.1533E-01	0.3557E-01
7	0.3640E+00	0.7095E+00	0.1566E-01	0.4086E-01
8	0.3802E+00	0.7566E+00	0.1615E-01	0.4713E-01
9	0.3971E+00	0.8114E+00	0.1693E-01	0.5481E-01
10	0.4156E+00	0.8764E+00	0.1845E-01	0.6493E-01
11	0.4390E+00	0.9585E+00	0.2344E-01	0.8210E-01
Failed on cycle		12		

END OF TEAR-FATIGUE ANALYSIS:



Cycle	a	c
11	0.4390E+00	0.9585E+00

EXAMPLE 10

MULTI-CYCLE PROOF TEST ANALYSIS FOR SC02

 DATE: 23-SEP-03 TIME: 15:51:23
 (computed: NASA/FLAGRO Version 3.00, October 1995.)
 Elastic-Plastic Fracture Module (EPFM) V.x.xx, Jan. 2003
 U.S. customary units [inches, ksi, ksi sqrt(in)]

Input Filename = exam10.inp
 Output Filename = Exam10.out

Plate Thickness, t = 1.0000
 " Width, W = 10.0000

Material Yield Stress = 100.00

Material Ultimate Stress = 200.00

Data for the Nonlinear Material Behavior:

Sig0	=	0.1000E+03
E	=	0.3000E+05
nu	=	0.3000E+00
alpha	=	0.1000E+01
n	=	0.5000E+01

PROOF LOAD

 Number of Proof Cycles..... 4

CYCLIC MAXIMUM DISTRIBUTION

PRIMARY LOAD DISTRIBUTION 1:

Norm. x	Stress
0.00	0.1200E+03
1.00	0.1200E+03

CYCLIC MINIMUM DISTRIBUTION

PRIMARY LOAD DISTRIBUTION 1:

Norm. x	Stress
0.00	0.0000E+00
1.00	0.0000E+00

SERVICE SPECTRUM

Number of Service Cycles..... 50

LOAD STEP 1

Load Step 1 applied 2 cycles per service spectrum

CYCLIC MAXIMUM DISTRIBUTION

PRIMARY LOAD DISTRIBUTION 1:

Norm. x	Stress
0.00	0.8000E+02
1.00	0.8000E+02

CYCLIC MINIMUM DISTRIBUTION

PRIMARY LOAD DISTRIBUTION 1:

Norm. x	Stress
0.00	0.0000E+00
1.00	0.0000E+00

Fracture resistance curve (quadratic form):

$$J_r = (0.2000E+00) + (0.2000E+02) * x + (0.0000E+00) * x^2$$

$$da(max) = 0.2000E+00$$

PROOF CYCLE FATIGUE DATA

FATIGUE DATA (da/dN=C*dK^m):

J(mat) = 0.2100E+00
 C = 0.1000E-08
 m = 0.4000E+01
 U0 = 0.1000E+01
 alp (c) = 0.1000E+01
 alp (a) = 0.1000E+01

a(init) = 0.0000E+00
 c(init) = 0.0000E+00

SERVICE CYCLE FATIGUE DATA

FATIGUE DATA (da/dN=C*dK^m):

J(mat) = 0.2100E+00
 C = 0.2000E-08
 m = 0.4000E+01

U0 = 0.1000E+01
alp (c)= 0.1000E+01
alp (a)= 0.1000E+01

a(init)= 0.0000E+00
c(init)= 0.0000E+00

The MCPT module employs a root-finding algorithm to determine the initial crack lengths:

Proof Load Only : maximum initial crack length which survives prescribed number of Proof Load applications.

Service Load : minimum initial crack length which survives prescribed number of Proof Load and Service Load applications.

During the initial crack length searches various error and warning messages may be displayed. These messages do not affect the probability calculation.

ERROR[JSC02]: exceeds plastic collapse load!
a=0.103E+01, c=0.133E+01
p=0.120E+03, pmax=0.118E+03

ERROR[JSC02]: exceeds plastic collapse load!
a=0.102E+01, c=0.131E+01
p=0.120E+03, pmax=0.119E+03

MCPT ANALYSIS COMPLETE

Mean of Exponential Dist 0.150000000000000
Conditional Probability of Failure 0.254858919567750
Probability of Proof Failure 0.806209301940743
Probability of Proof and Service Failure... 0.600739670302655
Initial crack size to just survive proof test
0.246146486746147
Initial crack size to just survive proof test and service
0.137721242920040



APPENDIX 4: VALIDATION AND CONSISTENCY CHECKS

This appendix lists in tabular form the results of part of the exercise performed to validate the NASGRO EPFM and Proof Test Analysis Modules (hereafter referred to as the Modules). Except for the Option 5 (J estimation), all the analyses used in the validation involved 2-DOF, and except for Option 5 and Option 7 (fatigue lifetime), all the validation analyses addressed ductile fracture behavior.

Ri	2.75	2.75	2.75	2.75	2.75	2.75
t	0.25	0.25	0.25	0.25	0.25	0.25
P	10	10	10	10	10	10
a	0.05	0.05	0.05	0.1	0.1	0.15
c	0.05	0.1	0.15	0.1	0.15	0.15
M	1.000365	1.00146	1.003282	1.002917	1.006552	1.009813
V	1	1	1	1	1	1
Rm	2.875	2.875	2.875	2.875	2.875	2.875
yield	100	100	100	100	100	100
n	10	10	10	10	10	10
mu	0.82416	0.82416	0.82416	0.82416	0.82416	0.82416
Po	9.09008	9.087597	9.083481	9.073313	9.051626	8.960303
Je(a)	0.0304	0.0563	0.0695	0.0621	0.0957	0.0954
Je(c)	0.0431	0.0399	0.0347	0.0931	0.0987	0.156
Jp(a) (manual)	0.0591	0.1098	0.1361	0.1228	0.1934	0.2112
Jp(a) (NASGRO SC04)	0.0591	0.1100	0.1360	0.1230	0.1930	0.2110
Jp(c) (manual)	0.1017	0.0944	0.0824	0.2234	0.2420	0.4190
Jp(c) (NASGRO SC04)	0.1020	0.0943	0.0825	0.2230	0.2420	0.4180

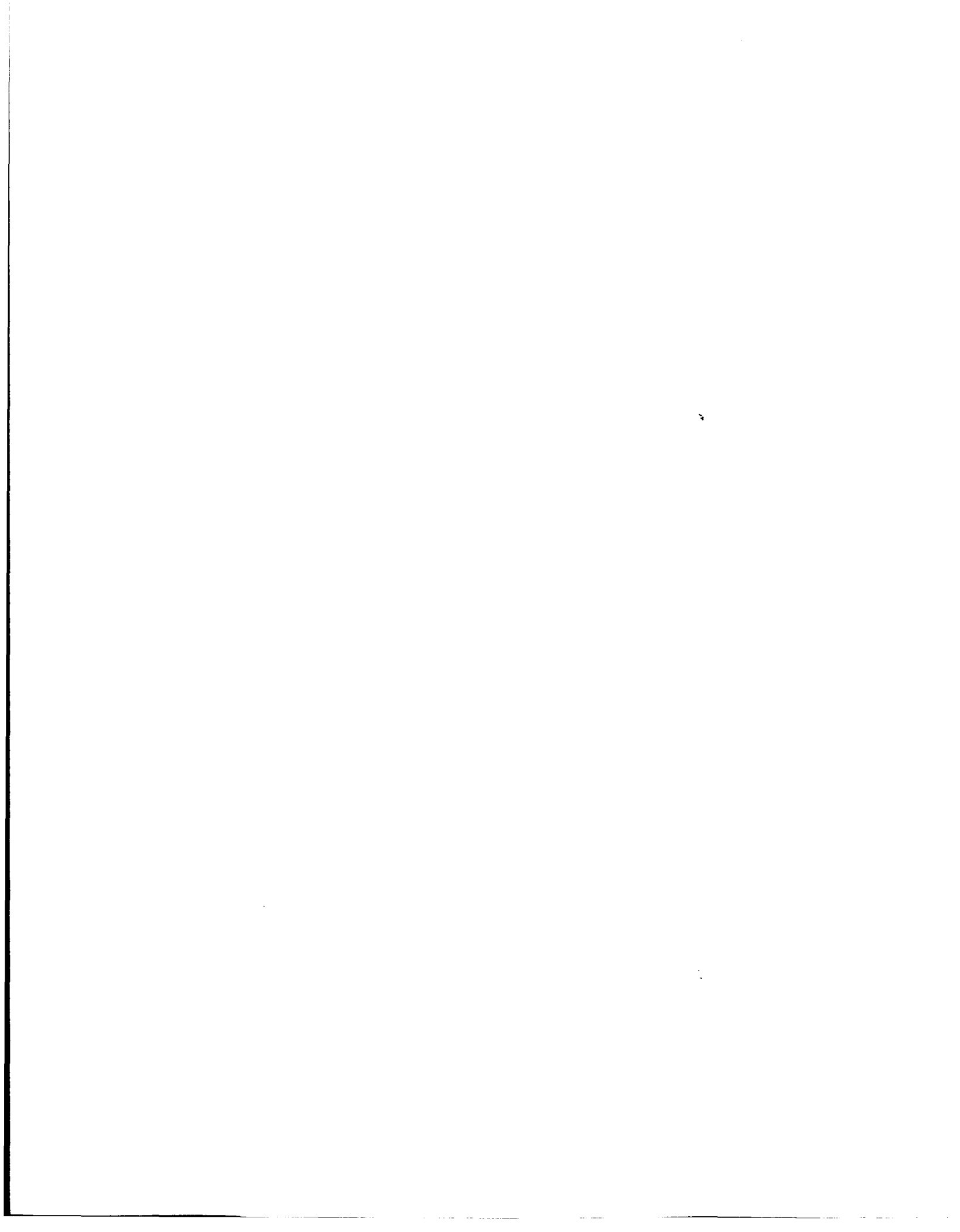


Table A4.2: Validation: J_p Solutions for SC02: Option 5 (Force, P)

W	4	4	4	4	4	4
t	1	1	1	1	1	1
Force, P, corresponding to primary quadratic stress $120-240(x/t)+240(x/t)^2$ Secondary stress $60-60(x/t)$	320	320	320	320	320	320
a	0.2	0.2	0.2	0.4	0.4	0.8
c	0.2	0.4	0.8	0.4	0.8	0.8
V_a	1.8164	1.8164	1.8164	1.8164	1.8164	1.8164
V_c	1.256	1.256	1.256	1.256	1.256	1.256
yield	80	80	80	80	80	80
alpha	1.5	1.5	1.5	1.5	1.5	1.5
n	15	15	15	15	15	15
mu	0.82416	0.82416	0.82416	0.82416	0.82416	0.82416
Po	314.970	309.95	299.89	299.89	279.79	239.58
Je(a, primary only)	0.0685	0.1360	0.1940	0.0970	0.2290	0.2050
Je(c, primary only)	0.1420	0.1320	0.1070	0.2780	0.3187	0.7180
Jp(a) (manual)	0.192	0.478	1.08	0.540	3.37	26.5
Jp(a) (NASGRO SC04)	0.192	0.476	1.08	0.540	3.37	26.5
Jp(c) (manual)	0.334	0.389	0.500	1.30	3.93	77.8
Jp(c) (NASGRO SC04)	0.333	0.388	0.502	1.30	3.92	77.8

Table A4.3: Validation: J_p Solutions for SC02: Option 5 (Force, P, and Moment, M)						
W	4	4	4	4	4	4
t	1	1	1	1	1	1
Force, P, and moment, M corresponding to the primary linear stress $120-120(x/t) = 60+60(1-2(x/t))$	P=240 M=40	P=240 M=40	P=240 M=40	P=240 M=40	P=240 M=40	P=240 M=40
$\lambda=M/Pt$	0.1667	0.1667	0.1667	0.1667	0.1667	0.1667
a	0.2	0.2	0.2	0.4	0.4	0.8
c	0.2	0.4	0.8	0.4	0.8	0.8
$V_a(\lambda)$	1.8164	1.8164	1.8164	1.8164	1.8164	1.8164
$V_c(\lambda)$	1.256	1.256	1.256	1.256	1.256	1.256
yield	80	80	80	80	80	80
alpha	1.5	1.5	1.5	1.5	1.5	1.5
n	15	15	15	15	15	15
Mu (a-tip)	0.82416	0.82416	0.82416	0.82416	0.82416	0.82416
Mu (c-tip)	1	1	1	1	1	1
Po	314.970	309.95	299.89	299.89	279.79	239.58
Je(a)	0.0868	0.1680	0.2400	0.1300	0.3010	0.1120
Je(c)	0.1520	0.1410	0.1140	0.3130	0.3560	0.8210
Jp(a) (manual)	0.430	1.11	2.89	1.488	11.7	41.0
Jp(a) (NASGRO SC04)	0.430	1.11	2.89	1.470	11.7	40.8
Jp(c) (manual)	0.646	0.799	1.18	3.06	11.9	258
Jp(c) (NASGRO SC04)	0.645	0.799	1.17	3.05	11.9	258

Table A4.4: Validation: J_p Solutions for CC01 Option 5 (Moment, M)						
W	2	2	2	2	2	2
t	2	2	2	2	2	2
Moment, M, corresponding to primary bending stress 160	320	320	320	320	320	320
a	0.2	0.2	0.2	0.4	0.4	0.8
c	0.2	0.4	0.8	0.4	0.8	0.8
V_a	0.8089	0.8089	0.8089	0.8089	0.8089	0.8089
V_c	0.8089	0.8089	0.8089	0.8089	0.8089	0.8089
yield	80	80	80	80	80	80
alpha	1.5	1.5	1.5	1.5	1.5	1.5
n	15	15	15	15	15	15
mu	1	1	1	1	1	1
M_o	314.970	309.95	299.89	299.89	279.79	239.58
Je(a)	0.127	0.208	0.269	0.187	0.353	0.223
Je(c)	0.160	0.147	0.115	0.310	0.302	0.667
Jp(a) (manual)	0.167	0.340	0.683	0.358	1.631	3.07
Jp(a) (NASGRO SC04)	0.167	0.339	0.682	0.357	1.63	3.07
Jp(c) (manual)	0.211	0.240	0.292	0.593	1.40	9.19
Jp(c) (NASGRO SC04)	0.210	0.240	0.291	0.593	1.40	9.19

Table A4.5: Validation: J_p Solutions for EC02: Option 5						
W	4	4	4	4	4	4
t	2	2	2	2	2	2
Force, P, corresponding to primary quadratic stress $120-240(x/t)+240(x/t)^2$ Secondary stress $60-60(x/t)$	320	320	320	320	320	320
a	0.2	0.2	0.2	0.4	0.4	0.8
c	0.2	0.4	0.8	0.4	0.8	0.8
V_a	1.6575	1.6575	1.6575	1.6575	1.6575	1.6575
V_c	1.6575	1.6575	1.6575	1.6575	1.6575	1.6575
yield	80	80	80	80	80	80
alpha	1.5	1.5	1.5	1.5	1.5	1.5
n	15	15	15	15	15	15
mu	0.82416	0.82416	0.82416	0.82416	0.82416	0.82416
Po	625.81	600.94	554.78	565.20	482.91	371.33
Je(+a, primary only)	0.0307	0.0507	0.0648	0.0719	0.1200	0.2820
Je(c, primary only)	0.0280	0.0237	0.0153	0.0576	0.0496	0.1300
Je(-a, primary only)	0.0307	0.0507	0.0648	0.0719	0.1200	0.2820
Jp(+a) (manual)	0.0861	0.251	0.982	0.839	12.7	1179
Jp(+a) (NASGRO SC04)	0.0861	0.251	0.981	0.839	12.7	1180
Jp(c) (manual)	0.0785	0.117	0.232	0.672	5.24	544
Jp(c) (NASGRO SC04)	0.0786	0.117	0.232	0.672	5.24	543
Jp(-a) (manual)	0.0861	0.251	0.982	0.839	12.7	1179
Jp(-a) (NASGRO SC04)	0.0861	0.251	0.981	0.839	12.7	1180

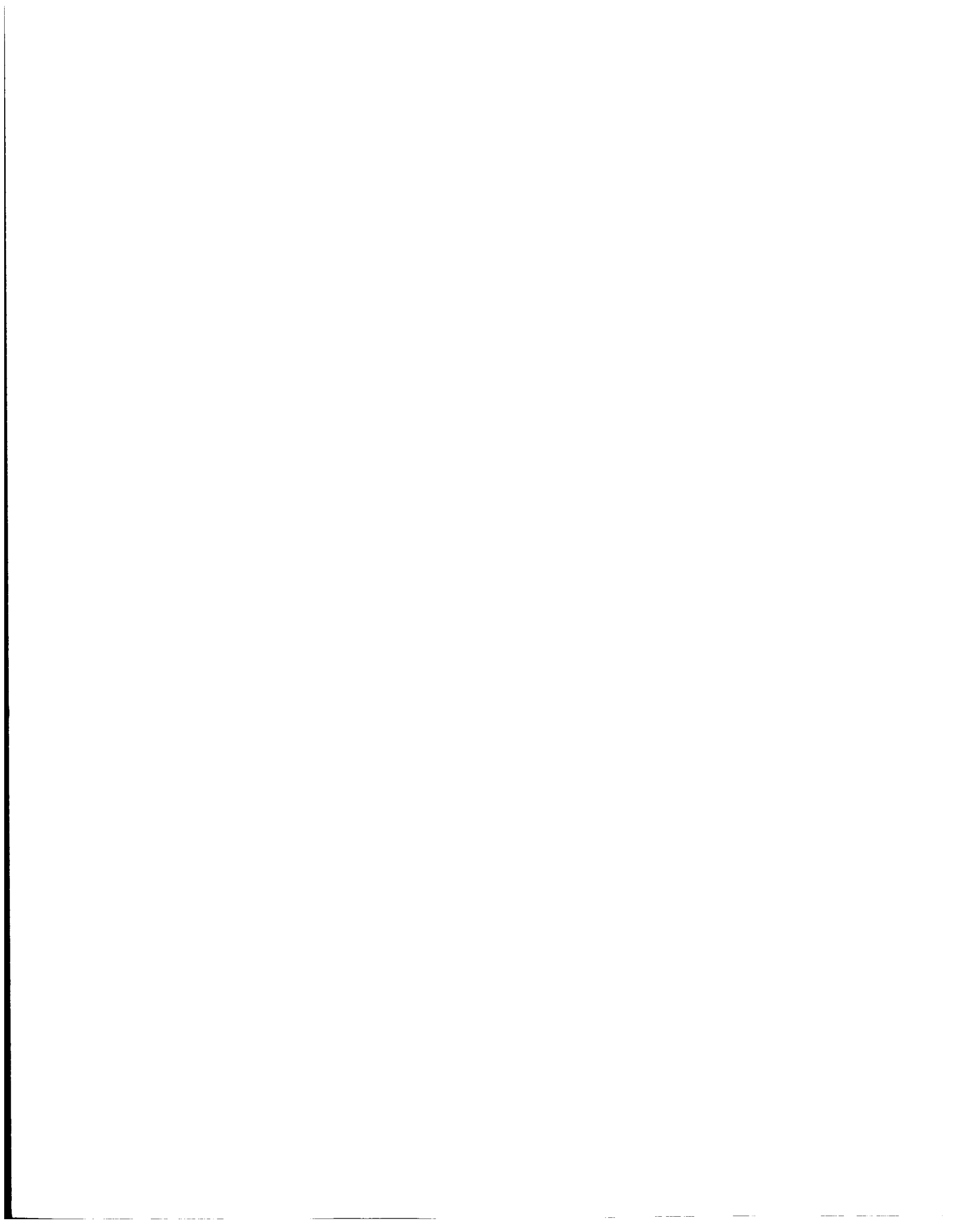


Table A4.6: Validation of Example 2: Critical Crack Failure Analysis									
Instability Predictions for 2-DOF Cracks for SC02: Option 6									
Resistance Curve: $0.245+30 \Delta a - 50 (\Delta a)^2$									
Instability Conditions:									
$J(a) = JR(\Delta a)$ and $J(c) = JR(\Delta c)$									
$(X-A)(Y-D) - BC = 0$									
a	c	J(a)	J(c)	Derivatives**		Δa	Δc	JR(Δa)	JR(Δc)
0.3342	0.641	3.56	2.56	$A=[dJ(a)/da]_c$	$B=[dJ(c)/da]_c$				
0.341	0.641	3.62	2.66	9.531	14.663	0.151	0.096	3.63	2.66
0.3478	0.641	3.69	2.76						
0.3342	0.6282	3.53	2.63	$C=[dJ(a)/dc]_a$	$D=[dJ(c)/dc]_a$			$X=dJR/d(\Delta a)$	$Y=dJR/d(\Delta c)$
0.3342	0.641	3.62	2.66	7.020	1.950				
0.3342	0.6538	3.71	2.68					14.9	20.4
				** The accuracy of the derivatives					
				is limited by the fact that NASGRO				(X-A)(Y-D)	BC
				outputs are only printed to three				99.06	102.94
				significant figures.				(X-A)(Y-D) - BC = -3.88	

Table A4.7: Validation of Example 2: Consistency Check: SC02					
Critical Crack Failure Analysis: Option 6					
Predicted Critical crack size, a-tip	Predicted Critical crack size, c-tip	Predicted tear at instability, a-tip	Predicted tear at instability, c-tip	Applied primary load	Applied secondary load
0.191	0.545	0.151	0.0960	110	100-50(x/t)
Check: Critical Load Failure Analysis: Option 6					
Initial crack size, a-tip	Initial crack size, c-tip	Predicted tear at instability, a-tip	Predicted tear at instability, c-tip	Predicted instability primary load	Applied secondary load
0.191	0.545	0.151	0.0961	114	100-50(x/t)



Table A4.8: Validation of Example 3: Consistency Check: EC02**Critical Load Failure Analysis: Option 6**

Initial crack size, a-tip	Initial aspect ratio, a/c	Predicted tear at instability, a-tip	Predicted tear at instability, c-tip	Predicted instability primary load	Applied secondary load
0.003	0.25	0.00168	0.000237	448	0
0.004	0.25	0.0015	0.000167	428	0
0.005	0.25	0.00135	0.000128	408	0

Check: Critical Crack Failure Analysis: Option 6

Predicted Critical crack size, a-tip	Initial aspect ratio, a/c	Predicted tear at instability, a-tip	Predicted tear at instability, c-tip	Applied primary load	Applied secondary load
0.00298	0.25	0.00169	0.000239	448	0
0.00399	0.25	0.0015	0.000168	428	0
0.00497	0.25	0.00135	0.000129	408	0

Table A4.9: Validation of Example 4: Consistency Check: CC01 (tension)					
Fatigue Life Analysis: Option 7			Check: Safe Life Pre-Proof Test Fatigue Life Analysis: Option 8		
Schedule	Predicted Crack size, a-tip	Predicted Crack size, c-tip	Schedule	Predicted Crack size, a-tip	Predicted Crack size, c-tip
0	0.05	0.1	0	0.05	0.1
10	0.06651	0.1037	10	0.06651	0.1037
20	0.08660	0.1113	20	0.08660	0.1113
30	0.1115	0.1259	30	0.1115	0.1259
40	0.1454	0.1524	40	0.1454	0.1524
50	0.1999	0.2025	50	0.1999	0.2025
58 (Failure)	0.2978	0.2985	58 (Failure)	0.2978	0.2985

Table A4.10: Validation of Example 5: Consistency Check: SC02					
Safe Life Pre-Proof Test Critical Crack Analysis: Option 8					
Predicted Critical crack size, a-tip	Predicted Critical crack size, c-tip	Predicted tear at instability, a-tip	Predicted tear at instability, c-tip	Applied primary load	Applied secondary load
0.215	0.359	0.142	0.129	110+10(x/t) (tensile force = 575)	100-50(x/t)
Check: Critical Load Failure Analysis: Option 6					
Initial crack size, a-tip	Initial crack size, c-tip	Predicted tear at instability, a-tip	Predicted tear at instability, c-tip	Predicted instability primary load	Applied secondary load
0.215	0.359	0.142	0.129	575 (tensile force)	100-50(x/t)

Table A4.11: Validation of Example 6^{}: Consistency Check: SC04**

Proof Test Analysis: Flaw Screening: Option 8					
Predicted Maximum Flaw Size Screened (crack size at incipient instability, includes tearing), a-tip	Predicted Maximum Flaw Size Screened (crack size at incipient instability, includes tearing), c-tip	Predicted tear at end of proof test, a-tip	Predicted tear at end of proof test, c-tip	Applied proof primary load	Secondary load present during proof test
0.0634	0.104	0.00241	0.00352	80.45 (pressure)	0
Check: Proof Test Analysis: Proof Load: Option 8					
Initial crack size, a-tip (no tearing included)	Initial aspect ratio, a/c	Predicted tear at instability, a-tip	Predicted tear at instability, c-tip	Predicted Proof Primary Load Needed to Screen Initial Flaw	Applied secondary load
0.061	0.61	0.00241	0.00352	80.5 (pressure)	0
Check: Critical Load Failure Analysis: Option 6					
Initial crack size, a-tip (no tearing included)	Initial crack size, c-tip (no tearing included)	Predicted tear at instability, a-tip	Predicted tear at instability, c-tip	Predicted instability primary load	Applied secondary load
0.061	0.100	0.00241	0.00352	80.5 (pressure)	0
Critical Crack Failure Analysis: Option 6					
Predicted Critical crack size, a-tip (no tearing included)	Initial aspect ratio, a/c	Predicted tear at instability, a-tip	Predicted tear at instability, c-tip	Applied primary load	Applied secondary load
0.061	0.61	0.00241	0.00352	80.45 (pressure)	0
<p>^{**} This example is based on a full-scale pressure vessel test. The material properties are those measured on the pressure vessel steel. In the test, an axial crack was machined into the outer surface of the vessel with a depth of 61mm and a total surface length of 200mm. This crack extended by ductile tearing under increasing hydraulic pressure until the crack failed (caused a leak) at a pressure of 80.45 MPa.</p>					

Table A4.12: Validation of Example 7: Consistency Check: EC02					
Proof Test Analysis: Proof Load: Option 8					
Initial crack size, a-tip	Initial aspect ratio, a/c	Predicted tear at instability, a-tip	Predicted tear at instability, c-tip	Predicted proof primary load	Applied secondary load
0.025	0.25	0.0353	0.00943	270	90-90(x/t)
0.035	0.25	0.0340	0.00659	265	90-90(x/t)
0.045	0.25	0.0316	0.00473	260	90-90(x/t)
Check: Proof Test Analysis: Flaw Screening: Option 8					
Predicted Critical crack size, a-tip	Initial aspect ratio, a/c	Predicted tear at instability, a-tip	Predicted tear at instability, c-tip	Applied primary load	Applied secondary load
0.0250	0.25	0.0353	0.00944	270	90-90(x/t)
0.0353	0.25	0.0339	0.00652	265	90-90(x/t)
0.0453	0.25	0.0316	0.00469	260	90-90(x/t)

Table A4.13: Validation of Example 8: Consistency Check: CC01 (bend)					
Proof Test Analysis: Final Crack Size: Option 8					
Initial crack size, a-tip	Initial aspect ratio, a/c	Predicted crack size after proof load applied, a-tip	Predicted crack size after proof load applied, c-tip	Proof primary load (bend)	Applied secondary load
0.5	0.5	0.5694	0.6555	220	0
Check: Tear-Fatigue Analysis: Option 9 (predicted crack extension on first load application)					
Initial crack size, a-tip	Initial aspect ratio, a/c	Predicted crack size after service load applied, a-tip	Predicted crack size after service load applied, c-tip	Service primary load (bend): maximum, minimum	Applied secondary load
0.5	0.5	0.5694	0.6555	220, 0	0

Table A4.14: Validation of Example 9: Consistency Check: SC04					
Tear-Fatigue Analysis: Option 9					
Initial crack size, a-tip	Initial aspect ratio, a/c	Predicted crack size after service load applied, a-tip	Predicted crack size after service load applied, c-tip	Service primary load: maximum, minimum (stress origin with respect to inner surface)	Applied secondary load
0.25	0.5	0.2578	0.5133	90-10(x/t), 0	100-200(x/t)
Check: Proof Test Analysis: Final Crack Size: Option 8 (predicted crack extension on first load application)					
Initial crack size, a-tip	Initial aspect ratio, a/c	Predicted crack size after proof load applied, a-tip	Predicted crack size after proof load applied, c-tip	Proof primary load (stress origin with respect to inner surface)	Applied secondary load
0.25	0.5	0.2578	0.5133	90-10(x/t)	100-200(x/t)

Table A4.15: Validation of Example 10: SC02				
Multiple Cycle Proof Test: Option 10				
Crack size, a_p , to just survive the proof test predicted by NASGRO Option 10 Analysis	Crack size, a_{ps} , to just survive the proof test and service predicted by NASGRO Option 10 Analysis	Probability of failing during the proof test: $P_p = 1 - e^{-\left(\frac{a_p}{0.15}\right)}$	Probability of failing during the proof test and service: $P_{ps} = 1 - e^{-\left(\frac{a_{ps}}{0.15}\right)}$	Conditional probability of failure for specified service lifetime given survival of MCPT $P_{cond} = \frac{(P_p - P_{ps})}{P_p}$
0.26104	0.13763			
Manual		0.8245	0.6005	0.2717
NASGRO SC02		0.8245	0.6005	0.2717

Table A4.16: Validation: SC02	
Multiple Cycle Proof Test: Option 10: (No Proof Test)	Check: Fatigue Life Analysis: Option 7
Predicted Crack size, a-tip, to just survive service lifetime of 50 cycles	Predicted service lifetime (cycles) for initial crack size of 0.21214
0.21214	49

Table A4.17: Validation: SC02	
Multiple Cycle Proof Test: Option 10: (No Service)	Check: Tear-Fatigue Analysis: Option 9
Predicted Crack size, a-tip, to just survive 4 proof cycles	Predicted lifetime (cycles) for initial crack size of 0.26104
0.26104	4

REPORT DOCUMENTATION PAGE

Form Approved
OMB No. 0704-0188

Public reporting burden for this collection of information is estimated to average 1 hour per response, including the time for reviewing instructions, searching data sources, gathering and maintaining the data needed, and completing and reviewing the collection of information. Send comments regarding this burden estimate or any other aspect of this collection of information, including suggestions for reducing this burden to Washington Headquarters Service, Directorate for Information Operations and Reports, 1215 Jefferson Davis Highway, Suite 1204, Arlington, VA 22202-4302, and to the Office of Management and Budget, Paperwork Reduction Project (0704-0188) Washington, DC 20503.

PLEASE DO NOT RETURN YOUR FORM TO THE ABOVE ADDRESS.

1. REPORT DATE (DD-MM-YYYY) 23-00-2003		2. REPORT DATE Final Report		3. DATES COVERED (From - To) Jun 2002 - Sept 2003	
4. TITLE AND SUBTITLE Addendum to the User Manual for NASGRO Elastic-Plastic Fracture Mechanics Software Module				5a. CONTRACT NUMBER NAS8-02051	
				5b. GRANT NUMBER	
				5c. PROGRAM ELEMENT NUMBER	
				5d. PROJECT NUMBER	
				5e. TASK NUMBER	
				5f. WORK UNIT NUMBER	
6. AUTHOR(S) Chell, Graham and Gardner, Brian					
7. PERFORMING ORGANIZATION NAME(S) AND ADDRESS(ES) Southwest Research Institute 6220 Culebra Road San Antonio, TX 78238				8. PERFORMING ORGANIZATION REPORT NUMBER 18-05756	
9. SPONSORING/MONITORING AGENCY NAME(S) AND ADDRESS(ES) National Aeronautics and Space Administration, Marshall Space Flight Center AL 35812				10. SPONSOR/MONITOR'S ACRONYM(S) NASA MSFC	
				11. SPONSORING/MONITORING AGENCY REPORT NUMBER	
12. DISTRIBUTION AVAILABILITY STATEMENT Unclassified-Unlimited; Subject Category: 39; Standard Distribution					
13. SUPPLEMENTARY NOTES Prepared for Structures & Dynamics Laboratory, Science and Engineering Directorate Technical Monitor, M. Wayne Gregg					
14. ABSTRACT The elastic-plastic fracture mechanics modules in NASGRO have been enhanced by the addition of the following: new J-integral solutions based on the reference stress method and finite element solutions; the extension of the critical crack and critical load modules for cracks with two degrees of freedom that tear and failure by ductile instability; the addition of a proof test analysis module that includes safe life analysis, calculates proof loads, and determines the flaw screening capability for a given proof load; the addition of a tear-fatigue module for ductile materials that simultaneously tear and extend by fatigue; and a multiple cycle proof test module for estimating service reliability following a proof test.					
15. SUBJECT TERMS NASGRO software, elastic-plastic fracture mechanics, fully plastic fatigue crack growth, proof test, multiple cycle proof test, tear-fatigue, ductile tearing, J-integral, reference stress method					
16. SECURITY CLASSIFICATION OF:			17. LIMITATION OF ABSTRACT UU	18. NUMBER OF PAGES 120	19a. NAME OF RESPONSIBLE PERSON Graham Chell
a. REPORT U	b. ABSTRACT U	c. THIS PAGE U			19b. TELEPHONE NUMBER (Include area code) 210-522-5427